# PHASE SWEEPING TRANSMIT DIVERSITY WITH FADING RESISTANT CONSTELLATIONS

by

Edward Mah

A thesis submitted in conformity with the requirements
for the degree of Master of Applied Science
Graduate Department of Electrical and Computer Engineering
University of Toronto

# Abstract

**Phase Sweeping Transmit Diversity with Fading Resistant Constellations**
by Edward Mah
Master of Applied Science, 1998
Department of Electrical and Computer Engineering, University of Toronto

The problem of slow fading in the forward link of a mobile radio system is addressed in this thesis. Transmit diversity at the base station is investigated as a solution to mitigating the long term impairment. A diversity system is proposed in which multiple antennas spaced far apart transmit simultaneously the same signal to the mobile terminal. The objective is to create artificial fast fading in an otherwise static environment. A channel coding scheme is devised which exploits the autocorrelation properties of the resulting fading envelope. By matching the frequency offset of the carriers to the interleaving depth of the channel coder, it is possible to realize antenna diversity gain at low mobile velocities and coding gain at high velocities. Simulations demonstrate the feasibility of increasing the diversity order of the forward link under slow fading conditions without having to maintain a condition of orthogonality between the multiple transmissions.

# Acknowledgment

I wish to thank my supervisor, Professor E. Sousa, for the guidance and support through my research. Much appreciation goes to my family and friends for their moral encouragement. My graduate studies was made possible through the financial assistance provided by the Natural Sciences and Engineering Research Council.

# Contents

# List of Tables

# List of Figures

# Chapter 1

# Introduction

## 1.1 Mobile Communications

The mobile communications industry has experienced phenomenal growth over the last decade. The ability to establish communications with others at anytime anywhere has improved individual productivity and mobility. The introduction of personal communication services provide mobile users with ubiquitous access to voice as well as data services. In 1995, the FCC regulatory body auctioned off radio spectrum in the C band to selected telecommunications companies for a total of $10.2 billion. The price paid by the successful bidders is an attestation of the profit potential of the new services as foreseen by the industry.

With the advent of miniaturization of the mobile station came an increase in the proportion of hand-held mobile stations in a conventional cellular system. Since pedestrian users tend to remain stationary for an extended period of time, they are susceptible to slow fading. Slow fading can cause temporary outages in service, lost messages, and dropped calls when the received power falls below an acceptable level. In order to mitigate this impairment, some form of diversity is required.

The issue of coverage and quality of service requires dwelling into the properties of the radio channel and methods of improving the reliability of communications through this medium.

## 1.2 Radio Channel

Consider a radio link between a base station transmitter and a mobile receiver. Typically, there exist a multitude of paths that radio waves may follow in traveling from one antenna to the other. Multipath propagation is attributed to the presence of scatterers in the environment which act as reflectors of electro-magnetic radiation. The resultant signal that the receiver actually receives is the sum of all these reflected radio waves. Depending on the relative phase of these constituent components, either constructive or destructive interference occurs at the receiving antenna. Fluctuations in the received signal strength is termed *fading* [1]. In general, the receiver is mobile relative to the transmitter and/or scattering bodies. Hence, fading of the received signal is both time and spatially varying.

In addition to multipath interference, the attenuation of the received power can be attributed to a number of phenomena. If a large structure is situated along a direct path between the transmitter and the receiver then shadowing results. The radio waves must travel an indirect route to reach the receiver. Standing wave interference occurs when the receiver lies in between the transmitter and an almost perfect reflector. Since the standing wave pattern that arises is frequency dependent, this induces spectral nulls and peaks in the channel at certain frequencies. This is an example of frequency selective fading in which the amount of fading is variable over the bandwidth of the channel.

Slowly moving or pseudo-stationary terminals are sensitive to nulls in the received signal due to multipath propagation. Long term fading caused by shadowing also poses a problem for pedestrian users because a person in an affected area tends to remain there for prolonged periods of time. It is this group of mobile terminals that benefit the most from antenna diversity schemes.

## 1.3 Diversity Techniques

Various diversity schemes are used to combat the effects of fading. For instance, data symbols may be transmitted repeatedly over distinct channels so that the receiver will ideally have multiple independent estimates of which symbol was sent. These channels

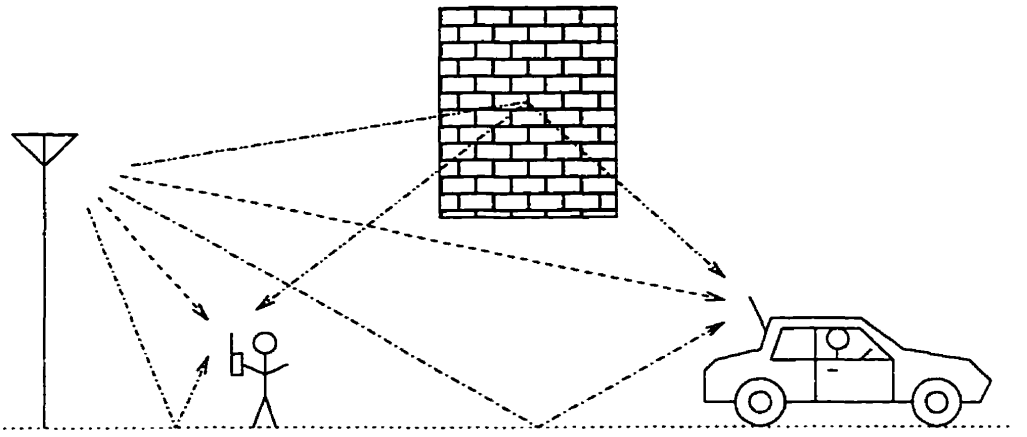

Figure 1.1: Illustration of Multipath and Scattering Phenomena

may be separated by intervals of time, frequency, or space. In time diversity, if the period in which a data symbol is repeated is greater than the *coherence time* of the system then the amount of fading affecting the different estimates are uncorrelated [2]. Similarly, radio channels that are apart in frequency by an amount larger than the *coherence bandwidth* of the system also undergo independent fading conditions. In space diversity, multiple antennas separated by a physical distance are located at the transmitter and/or receiver to achieve the same purpose.

In periods of deep fade, the received SNR is low which causes a high bit error rate to occur. However, the dynamics of the channel may change leading to a sudden rise in SNR and substantial improvement in the probability of error. Consequently, transmission errors are prone to be bursty in nature over a fading channel. This characteristic defeats the gains offered by error correction coding unless interleaving of the data symbols is performed. The purpose of interleaving is to ensure that adjacent data symbols are transmitted at different times which subjects them ideally to independent fading amplitudes. The net result is a more uniform spreading of the bit errors over the entire data stream which is more desirable from an error correction coding point of view. The limitation of this approach is the amount of delay incurred during transmission. If the coherence time of the channel is very large then the interleaver depth will also have to be large to compensate for this. A significant length of delay may be intolerable for a real time voice application. One of the drawbacks of using time diversity is that it assumes that the mobile station

is in motion relative to its environment. Since coherence time is inversely related to Doppler spread, a perfectly stationary system exhibits an infinite coherence time. Consequently, no time diversity is obtained in a fixed environment.

## 1.4 Antenna Diversity

Antenna diversity techniques are classified by their use of multiple transmit and/or receive antennas separated in space for the purpose of realizing alternate radio channels with different fading conditions. Performance gains are achieved by exploiting the de-correlation property of fading with increasing antenna separation distance. Antenna diversity techniques are advantageous over other forms of diversity in that they do not incur a bandwidth penalty to implement. A receiver which performs diversity combining from multiple antennas can be made compatible with any mobile radio communication standard. Receive antenna diversity is typically employed at the base station to improve the reception of signals originating from mobile stations which have relatively low transmit power.

Although receive antenna diversity may be feasible for vehicular based receivers, it is usually not an option in hand-held units as the required spacing for multiple antennas would make the device quite bulky. Assuming that a large number of scatterers are uniformly distributed around the mobile station, the antenna spacing needed to achieve a correlation factor of 0.2 is in the order of 0.5 to 1.0 wavelengths [3]. This corresponds to a separation distance of 17 cm at a carrier frequency of 900 MHz. The reciprocity of the channel between the transmitter and the receiver ensures that the propagation conditions in both directions are fairly identical. However, the spatial distribution of received multipath signals is often uniform at the mobile but directional at the base station. This is because the receiver experiences local multipath due to the presence of scatterers all around the mobile whereas the base station antenna is usually located at an elevated position clear of most obstructions. A consequence of the narrow angular spread of the multipath rays at the base station is that the spatial correlation of fading is much higher than in the case of the mobile station. The required spacing between antennas may be upwards of tens of wavelengths in order to achieve a correlation factor of 0.2 at the base station [3].

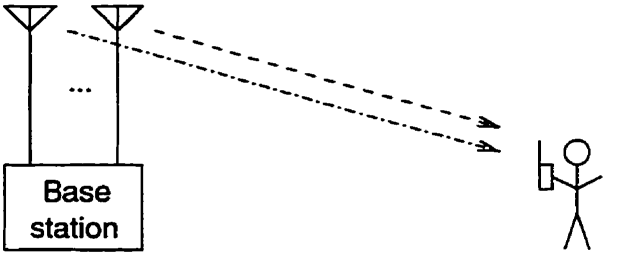


Figure 1.2: Base Station Antenna Diversity

## 1.5 Transmit Diversity

### 1.5.1 Considerations

Transmit antenna diversity involves coordinating the transmissions from multiple antennas to obtain spatial diversity in the system. The different antennas might be excited selectively one at a time or they may transmit together simultaneously. In practice, the large separation distance between transmit antennas makes transmit diversity schemes feasible only at the base station (ie. the forward link) where space is readily available. Although they introduce more complexity to the system in comparison to receive diversity, the centralized role of the base station means that all mobile receivers benefit from their application. Transmit antenna diversity schemes are most effective in mitigating slow fading and/or long term fading in the forward link because of their ability to effect change on the propagation paths thereby altering drastically channel conditions. If feedback information regarding the receiver's performance is unavailable to the transmitter then only diversity techniques operating under open loop control are possible.

### 1.5.2 Non-Overlapping Transmissions

In selection diversity, the base station cycles through all the antennas by exciting each one individually while the mobile station notes the fading amplitude that arises from its use at each step. The mobile station then notifies the base station via a control channel as to which antenna yielded the best channel response. Subsequent communications originate from the selected antenna until either a fixed period of

time has elapsed or the performance of the link deteriorates below a preset threshold. At that point, the selection process is initiated once again. A drawback of selection diversity is the amount of time consumed in searching for the best antenna. The selection process incurs a search time which is proportional to the number of available antennas. The overhead can be significant when frequent switching is required because it reduces the overall throughput of the link. The decision time can be reduced by restricting the number of antennas that must be searched at each iteration. Another concern is the round trip propagation delay which causes the moment when the selected antenna is activated to lag behind the point in time when the optimum decision was made. Under fast fading conditions, selection diversity can not keep up with the rapid fluctuations in the fading envelope. Figure 1.3 illustrates the resultant fading envelope for two branch selection diversity over a Rayleigh fading channel.

If time division duplexing (TDD) is employed in the system then the selection process is greatly simplified. The mobile station and the base station alternate turns transmitting to each other over a common frequency band or over two bands which are separated in frequency by no more than the coherence bandwidth of the system. During the period when the radio channel is operating in the reverse direction, the base station monitors the signal from the mobile station as it is received by each antenna. Assuming that the coherence time is sufficiently long, the task of channel probing is realized here for free transparent to the transmitter and receiver pair. When the link flow changes to the forward direction, the base station transmits from the one antenna that yielded the best reception for the up-link signal. The reciprocity of the radio channel makes the selection of the optimum antenna the same for both link directions. Hence, there is no need to perform a systematic search among the candidate antennas.

Another technique that circumvents the search procedure is switched diversity [4]. When the fading envelope affecting the forward link falls below some minimum level, the mobile station instructs the base station to switch antennas. The choice of alternate antenna is predetermined in either a random manner or a cyclic fashion. The decision process is quick and simple but it is not optimum. There is no provision that the newly selected antenna results in a radio channel which is better than the previous one. The likelihood of switching to a better antenna is increased with a lower

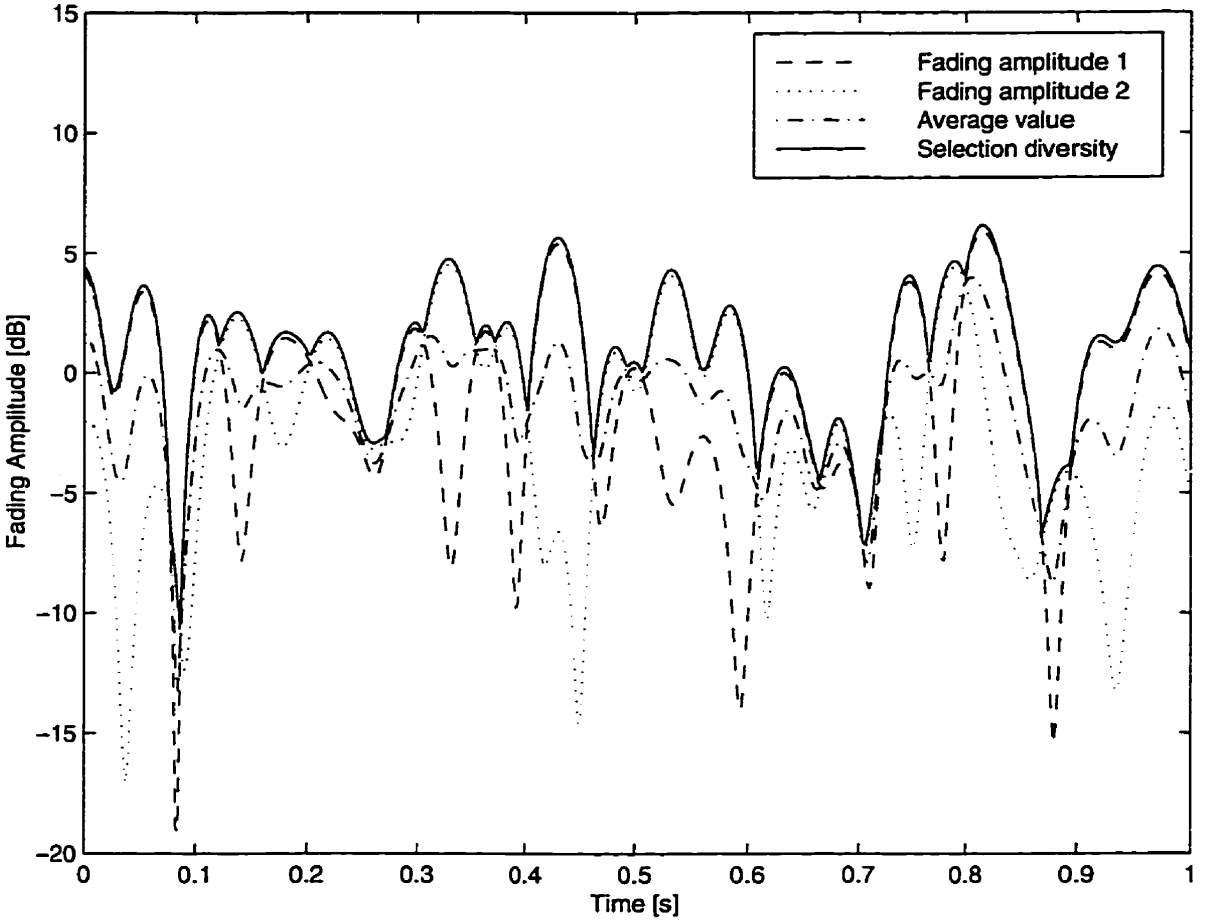


Figure 1.3: Resultant Fading Envelope for Two Branch Selection Diversity over a Rayleigh Fading Channel, $f = 1$ GHz, $v = 10$ km/h

threshold setting. However, a threshold value which is too low results in the system dwelling in a sub-optimum state for unnecessarily long durations. Consequently, the challenge of switched diversity is to determine the threshold level which yields the best performance.

Rather than switching when directed by the mobile station, the base station can simply transmit from a different antenna at regular intervals. In pre-switched diversity [5], alternate transmit antennas are selected for use just prior to the transmission of a new frame of data. Forward error correction coding is applied jointly across the multiple antennas in order to guard against data loss. When one antenna is affected by fading, ideally another one can still provide sufficient signal to the receiver so that it can recover the transmitted data. The net result is an average link performance which is neither the best nor the worst that can be acheived from using only a single transmit antenna out of the group. Pre-switched diversity is suitable for combating slow fading channels and applications where feedback control from the mobile station is unavailable. This technique can be viewed as a low frequency on-off gating of the antennas which purpose is to create time varying channel conditions. A drawback of pre-switched diversity is that it is not optimum for mitigating shadow fading. For example, it would be spectrally inefficient to reserve different time slots for transmit antennas which cover disjoint areas in the service region (to overcome shadow fading) [6]. It is better to simply place a transmitter in the problem area and re-transmit the blocked signal.

### 1.5.3 Overlapping Transmissions

Several authors have proposed transmit diversity techniques that exploit the properties of the channel equalizer in the mobile receiver [7][8][9][10][11]. For instance, delay signal transmission in the forward link can be used to create artificial time dispersion in the radio channel. If the equalizer window is wide enough to accommodate large delays typical of large cells then the equalizer might not be utilized to its full potential in smaller cells where the propagation delays are much less. Therefore, in a small cell environment it may be possible to transmit the same signal twice but delayed in time. The second transmission would originate from a spatially separate antenna such that the fading envelope exhibited by the two antennas are uncorrelated. The equalizer

can compensate the received signal for the artificially introduced multipath distortion. Performance gain is obtained through diversity combining of the received signal energy provided that the differential delay between the transmissions is sufficiently long. With most equalization algorithms, it is necessary for the differential delay to be greater than about a quarter of the symbol period before any diversity benefit is realized [12].

If the base station employs a phased array for both reception and transmission then a time division duplex system can utilize adaptive retransmission to improve signal reception at the mobile station. Time division duplexing exploits the reciprocity of the transmission channel to implement open loop selection diversity and/or power control. During the up-link cycle, the base station observes the signals received at each antenna and measures the relative phase difference separating them. When the direction of the link changes, the base station uses the antenna array to transmit in the forward direction by feeding each element with a delayed signal which phase is determined by the complex conjugate of the previously observed phase difference. Effectively, this steers the main lobe of the array in the direction of the general vicinity of the mobile unit. For a sufficiently slow varying channel, this also causes the various signal paths to add constructively at the mobile receiver. Antenna arrays are capable of concentrating the transmitted signal energy through a thin beam width which illuminates a narrowly defined region. A consequence of the directivity in transmission is that interference to other users outside the coverage of the main lobe is reduced in comparison to a system which employs only a single antenna.

In jitter diversity [13][14], the main lobe of the transmit antenna is subject to constant movement in space with the purpose of creating artificial fast fading at the mobile station. The displacement in the direction of illumination about its mean position is only a few degrees. Angular shifting of the main lobe is accomplished by either rotary motion of the transmit antenna or the introduction of a time varying differential phase in the signals feeding the various elements of a phased array. Jitter is normally something to be avoided in communication systems as it complicates the process of synchronization and impairs symbol detection. However, forcing the fading envelope to vary over time can actually improve the coding gain provided by forward error correction codes. An interleaver with finite memory is able to better randomize

the position of the faded symbols when the fading amplitude is changing rapidly. In turn, this leads to more effective use of time diversity.

In phase sweeping diversity [15], multiple antennas transmit the same signal simultaneously except that the RF carrier of each antenna is phase modulated slightly by different functions of time. Note that the transmissions do not necessarily originate from co-located sources. The transmit antennas are spaced sufficiently far apart such that they experience independent fading conditions. Phase sweeping prevents the incidence of multiple carriers from the different antennas canceling each other's signal at a fixed location in space. Fast fading is induced in the overlapping areas of coverage which benefits pseudo-stationary mobile receivers. Non-overlapping areas gain by the fact that multiple transmit antennas can provide more thorough coverage of a service region than a single antenna.

The introduction of artificial fast fading to an indoor environment has been proposed in [16].

## 1.6 Simulcasting

The term simulcast is a derived from the words simultaneous and broadcast. In a simulcast system, a common RF signal is transmitted simultaneously from multiple antennas distributed over a wide geographical area [17]. The ubiquitous nature of these transmissions ensures greater service coverage than would otherwise be possible from using a single transmitting antenna. Applications where simulcasting is employed include paging, dispatch, digital radio, etc.

Simulcasting is a form of transmit diversity in that the mobile terminal may receive its signal from more than one radiating source [18] [19]. However, it is usual to distinguish simulcasting from transmit diversity in that latter classification usually denotes the schemes which involve several transmit antennas common to one base station. Transmit diversity may or may not operate under closed loop control whereas simulcasting is open loop by design.

Inherent to a simulcast signal is the problem of intersymbol interference in which the mobile terminal receives multiple time delayed versions of the same signal. These signals can originate from different transmitting antennas or from even the same

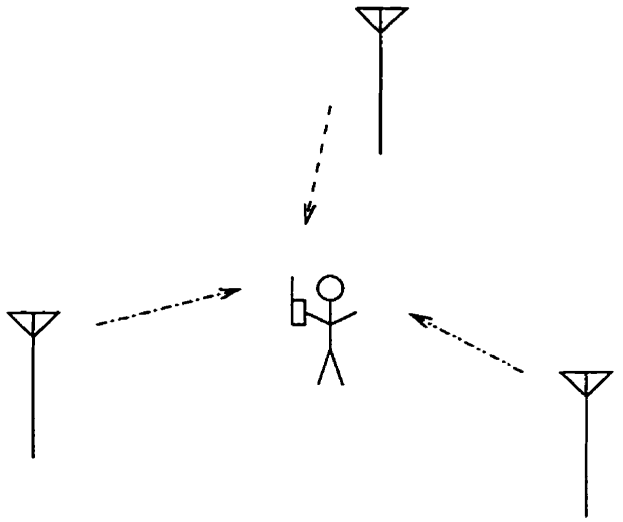

Figure 1.4: Illustration of Simulcast System with 3 Transmitters

source due to multipath propagation. The receiver observes the superposition of these time shifted signals which, in a narrowband scheme, can not be resolved individually. When the delays are small compared to the symbol duration, the received signal behaves as if it were originating as a single ray subject to a time varying multiplicative distortion [20][21].

Simulcasting is inferior in performance to selection transmit diversity for a given amount of transmitted power. Redundant transmissions throughout a service region inevitably results in signals being radiated in areas in which the intended recipient is not present. This may seem wasteful of system bandwidth considering that frequency spectrum is a scarce resource. For a given amount of spectrum, frequency reuse enables a cellular system to support simultaneously more users thereby increasing overall throughput. However, simulcasting is necessary for applications in which only one way communications is available. The lack of a reverse channel means that the system has no way of knowing where the mobile terminal is located.

## 1.7 Research Objectives

The use of multiple transmit antennas to mitigate slow fading is the objective of this research. The emphasis is on transmit antenna diversity for the forward channel of

a mobile radio system characterized by short delay spreads (eg. indoor radio). It is assumed is that the base station can always implement receive diversity/adaptive antenna arrays to mitigate fading/interference in the reverse link making it straightforward to improve upon. These mitigation techniques are usually not feasible at the mobile station though due to practical considerations. It is a challenge to add antenna diversity to the forward link as an after thought, once a particular signaling format has been standardized or when no feedback control channel is available. In order to resolve these issues, there are four self imposed requirements that must be satisfied in the following research.

- The slow fading problem needs to be addressed.
- Multiple transmit antennas are used to achieve space diversity.
- The proposed diversity scheme should operate under open loop control.
- The design of the diversity receiver should be compatible with a non-transmit diversity scheme.

The last criterion allows for the installation of a single transmitter to cover a service area with the option of adding later additional antennas as needed. In other words, the operation of the mobile receiver should be transparent to the invocation of transmit antenna diversity at the base station.

A phase sweeping technique combined with fading resistant constellations is researched in this thesis. It is proposed that artificial fast fading be introduced to an otherwise slow fading environment to realize an increase in coding gain. The possibility of applying transmit diversity at the base station as well as in a simulcast network is investigated.

## 1.8 Outline of Thesis

The simultaneous transmission of a signal from multiple antennas in the forward link is studied in Chapter 2. The performance of orthogonal, co-phased, and non co-phased carriers is compared. Phase sweeping is investigated as a method of simulating fast fading for a static environment. The autocorrelation of frequency offset carriers

is derived to characterize the artificially induced fading. A novel transmit antenna diversity technique is proposed in Chapter 3. The architecture of the transmitter and receiver pair, choice of coding and modulation are outlined. The merits of simulcasting are explored for its ability to provide redundant coverage to a given service area. The performance of phase sweeping transmit diversity, obtained through computer simulations, is presented in Chapter 4. A complete transceiver pair is simulated for different values of mobile velocity, differential delay, number of antennas, choice of constellation, etc. Lastly, conclusions drawn from the research and suggested future work are summarized in Chapter 5.

# Chapter 2

# Simultaneous Narrowband Transmissions from Multiple Antennas

## 2.1 Coverage and Capture Zones

Consider the case of a forward link consisting of a single transmitter with no co-channel interference. Associated with the transmit antenna is a region in space in which it can generally provide adequate illumination for a given level of radiated power. If contour lines could be mapped tracing out points with identical average received power, the terrain features and the presence of scatterers would determine their geometry while the transmit power would affect their size. When a second transmitter is introduced to the system, the joint region which is serviceable by at least one of the two antennas would ideally be the union of their individual areas of coverage. This is true provided that their transmissions are disjoint somehow, that is, they do not interfere with each other. For narrowband radio, the signals from the two antennas could be made separate in time or in frequency but this would be spectrally inefficient. With cross-polar discrimination, the signals from two co-channel sources can be made separable if they are transmitted on different polarizations. This allows for better utilization of the frequency spectrum. Figure 2.1 illustrates the use of simulcasting to increase coverage and to overcome shadow fading. The regions of

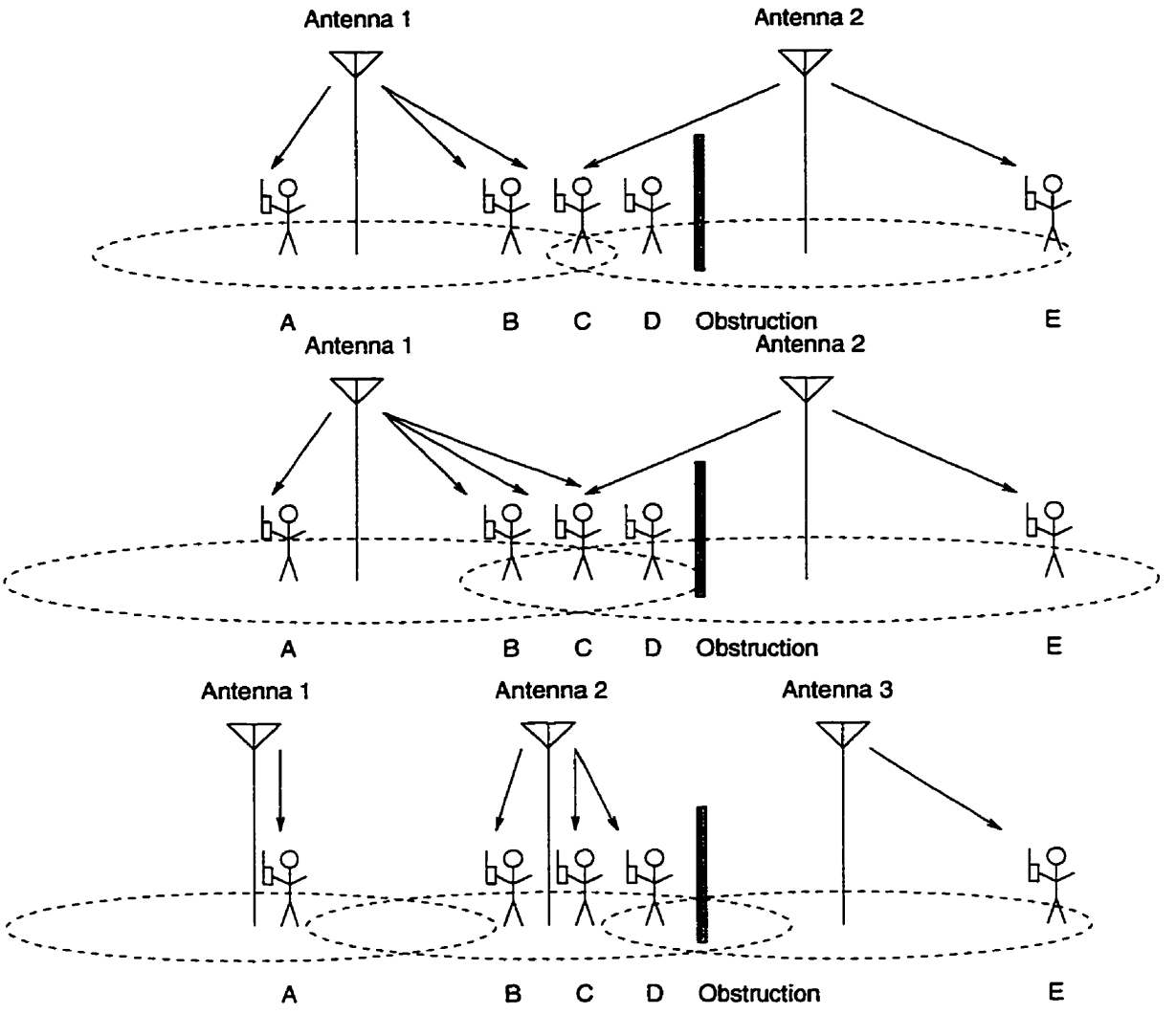


Figure 2.1: Illustration of Larger Overlapping Coverage in a Simulcast System (top) with Increased Transmit Power (middle) or More Transmit Antennas (bottom)

overlapping coverage can be either beneficial or detrimental to the mobile receiver depending on the method of transmission and modulation used.

In general, determining the total coverage area in a simulcast network of transmitters is not as simple as in the example illustrated previously. Assuming that the receiver is not capable of diversity combining, the simultaneous reception of two or more comparable strength transmissions at a common radio frequency results in simulcast interference. Simulcast interference causes non-capture zones to appear in a conventional digital FM simulcast system where the receiver is unable to adequately lock on to one particular carrier. A capture zone is a geographical region where the

signal received from one antenna is strong enough to overcome the simulcast interference from other antennas thereby permitting proper signal detection to occur. In determining whether a given location coincides with a capture or non-capture zone, it is necessary to compare the relative strengths and differential delays of the received signals. There are three distinct scenarios to consider.

- *Single dominant ray*: The mobile station receives most of its signal energy from one radiating element. This usually happens when the receiver is close to one transmitting antenna. Any simulcast or intersymbol interference that may be present is small enough so that its degradation on receiver performance is minimal. Multipath fading and shadow fading are the primary channel impairment which affect communications, as in the case in which the forward link comprises of only a single transmitter. Reliable communications is possible in this region.

- *Comparable strength rays, small differential delay*: Multiple carriers of similar magnitude impinge the receiver from different sources. The differential delay separating the various transmissions is small relative to a symbol duration. Hence, intersymbol interference is not a significant problem. Such a situation would likely occur when the mobile station is located approximately equidistant to two or more transmitters. The simulcast interference can be either constructive or destructive in nature resulting in fluctuations in the received signal envelope. Communications is feasible in this region provided that certain issues are addressed. For example, a good forward error correction scheme can overcome the simulcast interference present in the channel (provided that the fading is not flat). Also, strict tolerances on the exact transmit frequency must be maintained.

- *Comparable strength rays, large differential delay*: As before, the path gains from two or more transmit antennas to the mobile station are similar in strength. However, the path delays incurred along the various propagation paths differ by a duration comparable to a symbol period. Severe intersymbol interference occurs which complicates and degrades the process of symbol detection. A scenario like this would happen if shadow fading attenuates the transmission coming from the closest antenna. Hence, the signal energy originating from

more distant sources become significant in comparison. Communications is generally difficult, if not impossible, in this region without the help of channel equalization and coding. Note that with equalization, the link performance can actually actually be better here than in the previous case. An equalizer can perform diversity combining of the received signal energy when a large differential delay exists between the paths.

The first situation described above can be classified as a capture zone. The latter two cases exemplify the properties of a non-capture zone.

## 2.2 Important Simulcast Parameters

The composite signal that the receiver observes is a superposition of multiple carrier wavefronts from different transmitters. Assuming that the differential delay for the various propagation paths is negligibly small, the received signal for a simulcast system employing phase modulation may be expressed as

$$r(t) = \sum_{i=1}^{L} A_i e^{j(\omega_i t + \phi_i(t) + \theta_i)} \tag{2.1}$$

$$\phi_i(t) = \delta_i \cos(\alpha_i t + \beta_i) \tag{2.2}$$

where

- $A_i$ is the amplitude of the signal from the $i^{th}$ transmitter,
- $\omega_i$ is the carrier frequency,
- $\phi_i(t)$ is the information bearing phase,
- $\theta_i$ is the carrier phase,
- $\delta_i$ is the peak deviation of the phase modulation,
- $\alpha_i$ is the frequency of the baseband signal, and
- $\beta_i$ is the phase of the baseband signal.

The subscript $i$ enumerates the $L$ radiating elements that are transmitting simultaneously to the mobile station. In the ideal case, $\omega_i$, $\phi_i$, and $\theta_i$ would be the same for all of the transmitters. This condition would result in all the signals adding coherently at the receiver. The carrier phase $\theta_i$ that is observed at the mobile station is dependent

| Parameter Mismatch | Effect on Simulcast Channel |
|---|---|
| $\omega_1 \neq \omega_2$ | A frequency offset $\Delta\omega$ exists between the two carriers which induces a beat frequency component on the received signal envelope. If $A_0 \approx A_1$ then periods of deep fade will occur whenever the two signals add destructively. Artificial fast fading is superimposed on top of the slow fading envelope for large $\Delta\omega$. |
| $\theta_1 \neq \theta_2$ | A phase offset $\Delta\theta$ exists between the two carriers which gives rise to standing wave interference patterns in regions where there is overlapping coverage. The standing wave patterns remains fixed in space provided that the scattering environment is static, $\omega_1 = \omega_2$, and $\phi_1 = \phi_2$. It is possible for a stationary mobile station to be situated in a null region for an extended period of time. |
| $\delta_1 \neq \delta_2$ | An imbalance in the amplitudes $\Delta\delta$ of the modulating waveform translates into a mismatch in the modulation indices for the different transmitters. A small value for $\Delta\delta$ causes distortion in the received baseband signal. A moderate value of $\Delta\delta$ can actually be beneficial when the $A_i$'s are unequal because it enables the receiver to be captured by the strongest signal. |
| $\alpha_1 \neq \alpha_2$ | A frequency offset $\Delta\alpha$ exists between the two modulating waveforms which results in spectral spreading of the received baseband signal. Severe distortion can occur if $\Delta\alpha$ is relatively large. |
| $\beta_1 \neq \beta_2$ | A phase offset $\Delta\beta$ exists between the two modulating waveforms. Attenuation occurs in the detected signal if $\Delta\beta \neq 0$. If all else remains equal, maximum signal loss occurs when $\Delta\beta = \pi$. |

Table 2.1: Effect of Parameter Mismatch on a Simulcast Channel

on the complex manner in which multipath components add together making it not a determinant quantity prior to transmission. Consequently, the base station has no control over this quantity in a simulcast application. Suppose that $L = 2$ and there is a mismatch in one of the above parameters. The effect of the mismatch on the simulcast channel is summarized in Table 2.1.

## 2.3 Frequency Tolerance

It is critical to the operation of a simulcast network to maintain the carrier frequency of the transmitters within a prescribed tolerance. Consider the case where a line of sight condition exists between the mobile station and two transmitting base stations.

Hence, the receiver is situated geographically in an area where there is overlapping coverage from two transmitters. If the transmit frequencies of the two antennas are derived from a common reference then the superposition of their carrier waves will add either constructively or destructively at the receiver depending on their relative path difference. Consequently, there will be static regions of standing wave interference in the overlap area. This can lead to the undesirable situation in which either one of the two base stations operating alone could have adequately served the mobile station but when both antennas are transmitting simultaneously, the radio channel is in a faded condition.

If the carriers for the two different transmitters originate from independent oscillators then they generally will be running at frequencies slightly offset from each other. A small displacement in frequency generates artificial fast fading at the mobile station due to the superposition of the carriers cycling between a co-phase and anti-phase condition. The frequency offset should not be so large as to cause the fading envelope to change appreciably over a two symbol periods.

## 2.4 Average Energy of Simulcast Signals

### 2.4.1 Slow Fading Channel Model

Since the velocity of the mobile station follows directly from the user, its value can range from zero (ie. stationary mobile) to walking speeds and then up to vehicular speeds. Pedestrian behavior is often characterized by stop and go movement. Consequently, the velocity of the mobile station is assumed to take on a limited number of discrete values. In the simplest case, velocity is generalized as being in either a zero or non-zero state. When the mobile station is at rest, the channel is said to exhibit *pseudo-stationary* fading. The static nature of the environment fixes the amplitude and phase relationships between individual multipath components. This causes the overall fading amplitude to remain constant over an extended period of time.

Let the channel between a given base station transmit antenna and the mobile terminal be modeled as a single ray Rayleigh fading channel. It is assumed that $L$ such transmit antennas are available and that they are situated sufficiently far apart

to experience independent fading conditions. Furthermore, the fading process varies slow enough that the envelope can be deemed constant over one signaling interval. Consider the simultaneous transmission of a single pulse through this system of $L$ antennas. The composite signal is received via one omni-directional antenna at the mobile station. After down conversion to baseband the received signal is fed to a correlator, the output of which is used for symbol detection. In the following sections, the received signal energy $\mathcal{E}_s$ is defined as the magnitude squared output of the correlator in a noiseless system.

### 2.4.2 Orthogonal Carriers

If the channels corresponding to the $L$ transmit antennas are orthogonal (eg. via time or frequency division multiplexing) then the transmissions do not interfere with each other. Let $a_i$ denote the complex valued fading amplitude associated with the $i^{th}$ antenna. It is assumed that the fading processes affecting each channel are independent. The signal energy from the $L$ diversity branches can be combined using the maximal ratio combining technique [1] which yields

$$\mathcal{E}_s = \sum_{i=1}^{L} |a_i|^2 \tag{2.3}$$

$$\overline{\mathcal{E}}_s = \sum_{i=1}^{L} \sigma_i^2 \tag{2.4}$$

The $a_i$'s are modeled as independent complex, zero-mean, Gaussian random variables, each with a variance $\sigma_i^2$. Thus, $\mathcal{E}_s$ is a sum of $L$ independent $\chi^2$ distributed random variables. In general, the $\sigma_i$'s will not be equal in a simulcast system where the propagation paths and/or conditions among the $L$ transmit antennas and the mobile terminal may differ considerably. The probability density function of $\mathcal{E}_s$ is

$$p(\mathcal{E}_s) = \sum_{i=1}^{L} \frac{k_i}{\sigma_i^2} e^{-\frac{\mathcal{E}_s}{\sigma_i^2}} \tag{2.5}$$

$$k_i = \prod_{\substack{j=1 \\ j \neq i}}^{L} \left(1 - \frac{\sigma_j^2}{\sigma_i^2}\right)^{-1} \tag{2.6}$$

For transmit antenna diversity at a base station, the $\sigma_i$'s are taken to be equal due to the relative proximity of the antennas. In this case, the probability density function of $\mathcal{E}_s$ is

$$p(\mathcal{E}_s) = \frac{1}{(L-1)!\sigma_i^{2L}} \mathcal{E}_s^{L-1} e^{-\frac{\mathcal{E}_s}{\sigma_i^2}} \tag{2.7}$$

Note that for a system with $L$ orthogonal channels, there are $L$ correlator outputs to consider. Consequently, there will be $L$ sources of noise in the decision statistic.

### 2.4.3 Co-Phased Carriers

In an ideal system, multiple transmissions originating from spatially separate antennas could be coordinated such that their signals all add constructively at the receiver. The coherent addition of RF signals requires that the phase of the carriers be the same. Also, the differential delay separating the transmissions must be small compared to the symbol period. The antenna gain that would arise from evenly distributing a given transmit power among $L$ antennas equidistant to the receiver which then co-phase the $L$ equal strength carriers at the receive antenna is equal to $\sqrt{L}$, assuming a free space environment.

Given a slow fading channel, the signal energy received at the mobile station from $L$ co-phased transmissions is equal to

$$\mathcal{E}_s = \sum_{i=1}^{L} |a_i|^2 + \sum_{i=1}^{L} \sum_{\substack{j=1 \\ j \neq i}}^{L} |a_i||a_j| \tag{2.8}$$

The first summation term is analogous to Eq. (2.3) and the second summation term is always non-negative. The probability density function of $\mathcal{E}_s$ can be evaluated iteratively as

$$p(\mathcal{E}_s) = \frac{1}{2\sqrt{\mathcal{E}_s}} f_{y_L}\left(\sqrt{\mathcal{E}_s}\right) \tag{2.9}$$

where

$$f_{y_i}(y_i) = \int_0^\infty f_{y_{i-1}}(y_i - x_i) f_{x_i}(x_i) dx_i \tag{2.10}$$

$$f_{y_1}(y_1) = f_{x_1}(x_1) \tag{2.11}$$

$$f_{x_i}(x_i) = \frac{2x_i}{\sigma_i^2} e^{-\frac{x_i^2}{\sigma_i^2}} \tag{2.12}$$

It is worthwhile to note that the mean value $\overline{\mathcal{E}}_s$ is larger here than in the case of orthogonal carriers.

$$\overline{\mathcal{E}}_s = \sum_{i=1}^{L} \sigma_i^2 + \frac{\pi}{4} \sum_{i=1}^{L} \sum_{\substack{j=1 \\ j \neq i}}^{L} \sigma_i \sigma_j \tag{2.13}$$

An antenna array would be an example of co-phased transmission of signals except that the $a_i$ are correlated. Also, the spacing between antenna elements is kept small, on the order of half a wavelength, to ensure that the signals add coherently at the receiver. Such a small separation does not provide adequate spatial diversity to mitigate shadow fading. In a non-stationary environment, the co-phasing of carriers from geographically disperse transmitters is not feasible due to the rapid changes in carrier phase caused by the displacement of scatterers relative to the receiver.

### 2.4.4 Non Co-Phased Carriers

If the co-phasing of carriers is not performed then the impulse response of the channel as observed by the receiver can be modeled over a short period of time as

$$h(t) = \sum_{i=1}^{L} a_i \delta(t - \tau_i) \tag{2.14}$$

The equation for $h(t)$ is similar to that describing an $L$-path Rayleigh fading channel for a single transmit antenna system. The matched filter bound on the performance of binary (or 4-QAM) transmission over a multipath Rayleigh fading channel has been derived previously in the literature [22][23]. Since the simulcast channel model is similar to that of the time-discrete multipath fading channel, a similar approach to the derivation of $p(\mathcal{E}_s)$ is followed. The equation for the signal energy $\mathcal{E}_s$ is

$$\begin{aligned} \mathcal{E}_s &= \sum_{i=1}^{L} \sum_{j=1}^{L} a_i a_j^* R_g(\tau_i - \tau_j) \\ &= \mathbf{z}^H \mathbf{R} \mathbf{z} \end{aligned}$$

where $R_g(t)$ is the autocorrelation of the transmitted pulse, $\mathbf{z}$ is a column vector of complex, zero-mean, unit variance, Gaussian random variables of length $L$, and $\mathbf{R}$ is an $LxL$ matrix of elements defined by $r_{ij} = \sigma_i \sigma_j R_g(\tau_i - \tau_j)$. A singular value

decomposition of the Hermitian matrix $\mathbf{R}$ yields a diagonal matrix $\mathbf{\Lambda}$. The diagonal elements $\lambda_i$ are the eigenvalues of the system. If the eigenvalues are distinct then the probability density function of $\mathcal{E}_s$ is given by

$$p(\mathcal{E}_s) = \sum_{i=1}^{L} \frac{l_i}{\lambda_i} e^{-\frac{\mathcal{E}_s}{\lambda_i}} \tag{2.15}$$

$$l_i = \prod_{\substack{j=1 \\ j \neq i}}^{L} \left(1 - \frac{\lambda_j^2}{\lambda_i^2}\right)^{-1} \tag{2.16}$$

The case of non-distinct eigenvalues is treated in [22]. Typically for a simulcast arrangement of transmitters, $\lambda_i \neq \lambda_j$ for $i \neq j$ because the individual propagation paths that comprise a simulcast channel are inherently dissimilar.

### 2.4.5 Performance of BPSK Signaling

The matched filter bound on the performance of BPSK signaling over the channels described in Sections 2.4.2-2.4.4 is determined by averaging the probability of error over the range of $\mathcal{E}_s$.

$$P_e = \int_0^\infty \frac{1}{2} \text{erfc}\left(\sqrt{\frac{\mathcal{E}_s}{\overline{\mathcal{E}}_s} \frac{E_b}{N_0}}\right) p(\mathcal{E}_s) d\mathcal{E}_s \tag{2.17}$$

In order to compare the performance of BPSK for the three channels in the case of transmit antenna diversity at the base station, the following assumptions are taken.

- The $L$ transmit antennas undergo independent Rayleigh fading.
- The average received power from each of the $L$ antennas is the same.
- The differential delays are small relative to the symbol period.
- The total transmit power is held constant across all schemes.

Given these conditions, the case of $L$ non co-phased transmissions reduces to that of single ray Rayleigh fading. That is, the sum of $L$ complex valued fading amplitudes (each of which is complex Gaussian distributed) yields a complex Gaussian random process, the magnitude of which is Rayleigh distributed. Consequently, the baseline

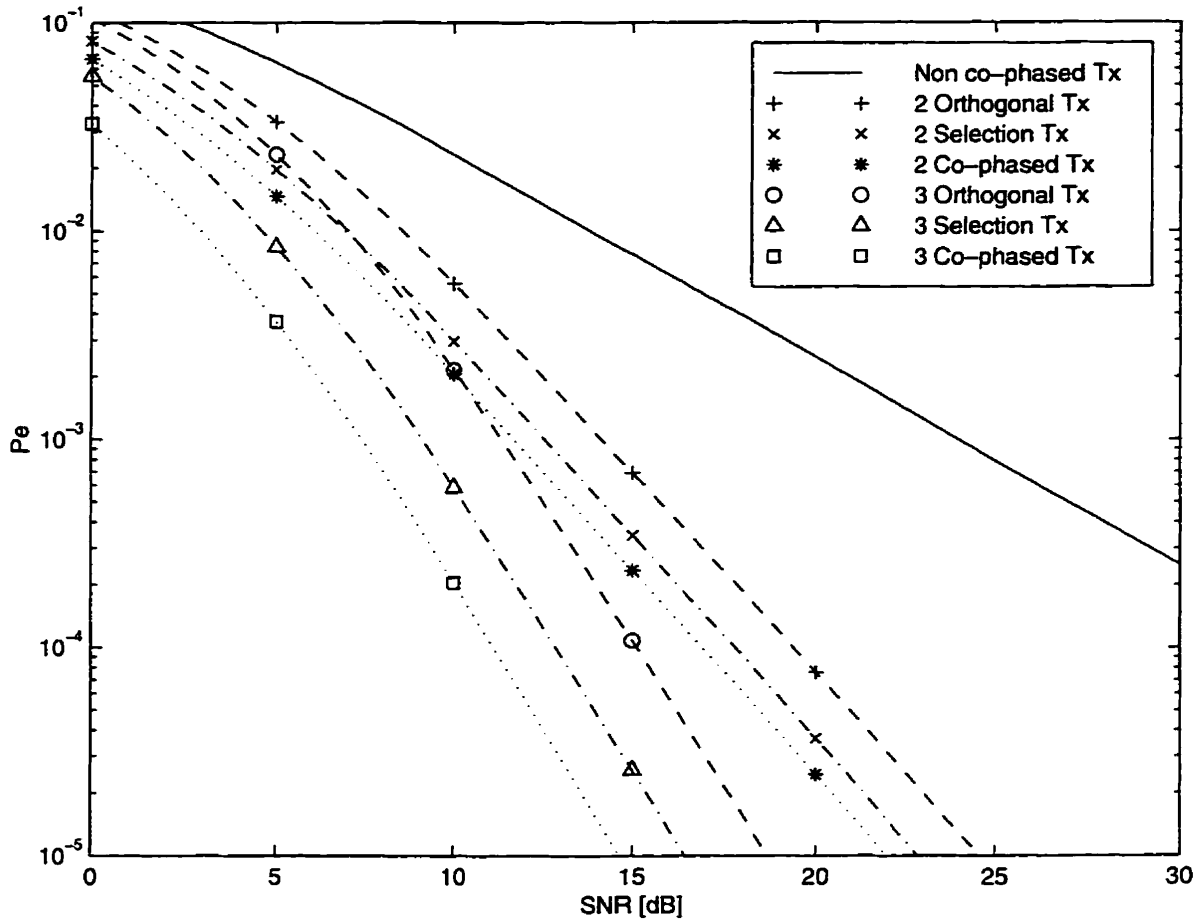


Figure 2.2: Performance of BPSK for Multiple Transmit Antenna Configurations

scheme is that of BPSK signaling via a single diversity branch. The performance of selection transmit diversity, transmission over $L$ orthogonal carriers, and co-phased transmission is plotted in Figure 2.2. The majority of schemes exhibit a probability of error curve that varies asymptotically as $\frac{1}{\text{SNR}^L}$. The notable exception is the error rate for non co-phased transmission which falls only as $\frac{1}{\text{SNR}}$. Although the performance of 3 orthogonal transmissions is inferior to that of selection transmit diversity by 2.2 dB, it is superior to co-phased transmission with 2 antennas at a probability of error better than 0.002. The benefit of the $L$ orthogonal transmissions scheme is that it operates without any feedback control. The diversity gain of the four schemes over a single antenna system at a bit error rate of $P_e = 10^{-4}$ is summarized in Table 2.2 for $L = 2$ and $L = 3$.

| Scheme | Gain [dB] | |
|---|---|---|
| | $L=2$ | $L=3$ |
| Selection Tx | 16.2 | 21.1 |
| Orthogonal Tx | 14.6 | 18.9 |
| Co-phased Tx | 17.1 | 22.8 |
| Non Co-phased Tx | 0 | 0 |

Table 2.2: Performance Gain of Simultaneous Transmission over Baseline Scheme, $P_e = 10^{-4}$

## 2.5 Phase Sweeping

Since the co-phasing of carriers is not feasible without some elaborate control mechanism, the alternative is to design a transmission scheme in which the receiver can somehow capture the mean signal level provided jointly by the $L$ transmit antennas. The objective of phase sweeping is to create an averaging effect over the fading amplitudes corresponding to the $L$ antennas rather than seeking constantly the optimum transmit antenna configuration via feedback control. The application of phase sweeping creates an artificial fast fading environment which finds use in the mitigation of slow fading environments.

Let $x_i(t)$ denote the passband PAM signal transmitted via the $i^{th}$ antenna, centered at a carrier frequency of $\omega_c = 2\pi f_c$.

$$x_i(t) = \sum_{k=-\infty}^{\infty} A_k g(t - kT) e^{j(\omega_c t + \phi_i(t))} \tag{2.18}$$

The time-varying phase $\phi_i(t)$ in the complex exponential is defined as the phase sweeping function for the $i^{th}$ transmitter. Any drift or offset component in the carrier frequency is assumed to be absorbed by the term $\phi_i(t)$. The channel impulse response can be modeled to include the effect of phase sweeping on the channel.

$$h(t, \tau) = \sum_{i=1}^{L} a_i b_i(t) \delta(\tau - \tau_i) \tag{2.19}$$

where $b_i(t) = e^{j\phi_i(t)}$ is the complex exponential which is superimposed on the transmitted signal from the $i^{th}$ antenna. Two time indices, $t$ and $\tau$, are required to model

the time varying nature of the impulse response. The phase sweeping functions are chosen such that

- $\phi_i(t) \neq \phi_j(t) + C$ for $i \neq j$ and any constant $C$.
- The phase difference $\phi_i(t) - \phi_j(t)$ has close to a uniform distribution over the interval $[0, 2\pi)$.
- The variation of $\phi_i(t)$ over two successive symbol durations is small enough to permit differential detection at the receiver.
- The effect of phase modulation on the carrier is small so as not to cause appreciable spectral widening of the passband signal.

The first point ensures that any interference pattern that arises between the $L$ simultaneous transmissions does not remain fixed in space. The second point attempts to equalize the likelihood of occurrence of constructive and destructive interference over a given observation interval. If the set of phase sweeping functions $\phi_i(t)$ is jointly periodic then the period over which this occurs is defined as one phase swept cycle. Examples of phase sweeping functions are sine waves and triangle waves [15]. The simplest of phase sweeping functions that satisfies all of the above properties is a linear ramp $\phi_i(t) = \alpha_i t$ which is equivalent to having a frequency offset between the $L$ carriers. The only restriction on the choice of frequency offsets is that they all be unique.

## 2.6 Autocorrelation of Frequency Offset Carriers

Consider a phase sweeping transmit diversity system with dual transmit antennas (ie. $L = 2$) employing a frequency offset strategy. The transmission of an unmodulated carrier wave is investigated here but the result can also be applied to a modulated carrier as long as the overall fading envelope can be considered constant over one signaling interval. Let $x(t)$ and $y(t)$ represent the time varying fading amplitudes associated with the two antennas. It is assumed that $x(t)$ and $y(t)$ are complex valued (ie. comprising of magnitude and phase) and that the fading processes are independent. Let $\omega_o$ denote the frequency offset between the two carriers. The autocorrelation

of the received signal $r(t)$ is

$$\begin{aligned} R_{rr}(t_0,t_1) &= E\left[\left(x^*(t_0)e^{-j\left(\omega_c+\frac{\omega_o}{2}\right)t_0}+y^*(t_0)e^{-j\left(\omega_c-\frac{\omega_o}{2}\right)t_0}\right)\cdot \right. \\ &\quad \left.\left(x(t_1)e^{j\left(\omega_c+\frac{\omega_o}{2}\right)t_1}+y(t_1)e^{j\left(\omega_c-\frac{\omega_o}{2}\right)t_1}\right)\right] \qquad (2.20) \\ &= R_{xx}(t_0,t_1)e^{j\frac{\omega_o}{2}(t_1-t_0)}+R_{xy}(t_0,t_1)e^{-j\frac{\omega_o}{2}(t_0+t_1)}+ \\ &\quad R_{yx}(t_0,t_1)e^{j\frac{\omega_o}{2}(t_0+t_1)}+R_{yy}(t_0,t_1)e^{-j\frac{\omega_o}{2}(t_1-t_0)} \qquad (2.21) \\ R_{rr}(\tau) &= R_{xx}(\tau)e^{j\frac{\omega_o}{2}\tau}+R_{yy}(\tau)e^{-j\frac{\omega_o}{2}\tau} \qquad (2.22) \end{aligned}$$

where $R_{xy}(t_0,t_1)=0$ and $R_{yx}(t_0,t_1)=0$ given that $x(t)$ and $y(t)$ are independent. Note that the autocorrelation of $r(t)$ depends only on the difference of the time indices $t_0$ and $t_1$. In the case of transmit antenna diversity, the two antennas are co-located at a common base station. The proximity of the antennas causes their fading statistics to be the same even though their corresponding fading amplitudes are uncorrelated due to multipath propagation (assuming a non-zero mobile velocity). Hence, the autocorrelation of $x(t)$ tends to equal that of $y(t)$ which yields

$$R_{rr}(\tau)=2R_{xx}(\tau)\cos\left(\frac{\omega_o}{2}\tau\right) \qquad (2.23)$$

Without phase sweeping the autocorrelation of $r(t)$ is simply

$$R_{rr}(\tau)=2R_{xx}(\tau) \qquad (2.24)$$

The quantity $R_{xx}(\tau)$ depends on the mobile velocity, the spatial distribution of scatterers around the mobile station, and whether or not line of sight propagation is available. If the magnitude of the fading process follows a Rayleigh distribution and there exists a uniform circular distribution of scatterers around the mobile station (see Jakes method [2]) then Eq. (2.23) becomes

$$R_{rr}(\tau)=2PJ_0(\omega_m\tau)\cos\left(\frac{\omega_o}{2}\tau\right) \qquad (2.25)$$

The significance of invoking phase sweeping is that by controlling the frequency offset parameter $\omega_o$, it is possible to force the autocorrelation function $R_{rr}(\tau)$ to zero at

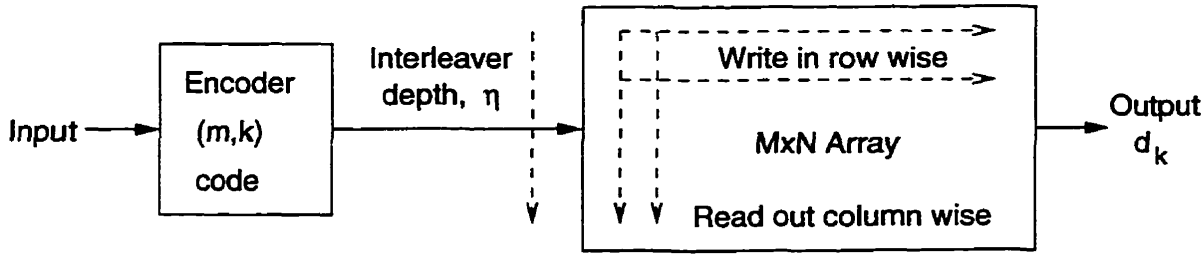


Figure 2.3: Encoder followed by MxN Block Interleaver

regular intervals of $\tau$.

$$R_{rr}(\tau) = 0,\ \tau = \frac{(2n+1)\pi}{\omega_o},\ n \in I \tag{2.26}$$

The set of time lags satisfying Eq. (2.26) also includes those which correspond to the zeros of $R_{xx}(\tau)$. However, $R_{xx}(\tau) = 0$ has no fixed solution given that it depends on the mobile velocity and the propagation conditions. The zero forcing of $R_{rr}(\tau)$ at known values of $\tau$ can be advantageous in forward error correction coding for slow fading channels (depending on the coding strategy employed). Figure 2.3 illustrates a conventional channel coding scheme in which the encoded bits are passed through a block interleaver. By matching the interleaving degree $\eta$ of the channel coder to one of $\left\{\frac{(2n+1)\pi}{\omega_o}\right\}$, it is possible to engineer uncorrelated fading amplitudes for adjacent coded symbols independent of the mobile velocity provided that

$$\omega_o = \frac{(2n+1)\pi}{\eta T_s} \tag{2.27}$$

where $T_s$ is the symbol period. For a slow fading channel, this technique causes adjacent coded symbols to undergo uncorrelated fading but coded symbols positioned two intervals apart experience similar fading amplitudes unless the interleaving degree is sufficiently large. Consequently, two branch diversity is feasible even under pseudo-stationary fading conditions. A plot of Eq. (2.25) is shown in Figure 2.4 for a carrier frequency $f = 1$ GHz and a frequency offset $f_o = 25$ Hz. In a conventional system with a single transmit antenna, the rate at which the autocorrelation of the fading envelope decreases with time lag $\tau$ and the location of the zero crossings are closely related to

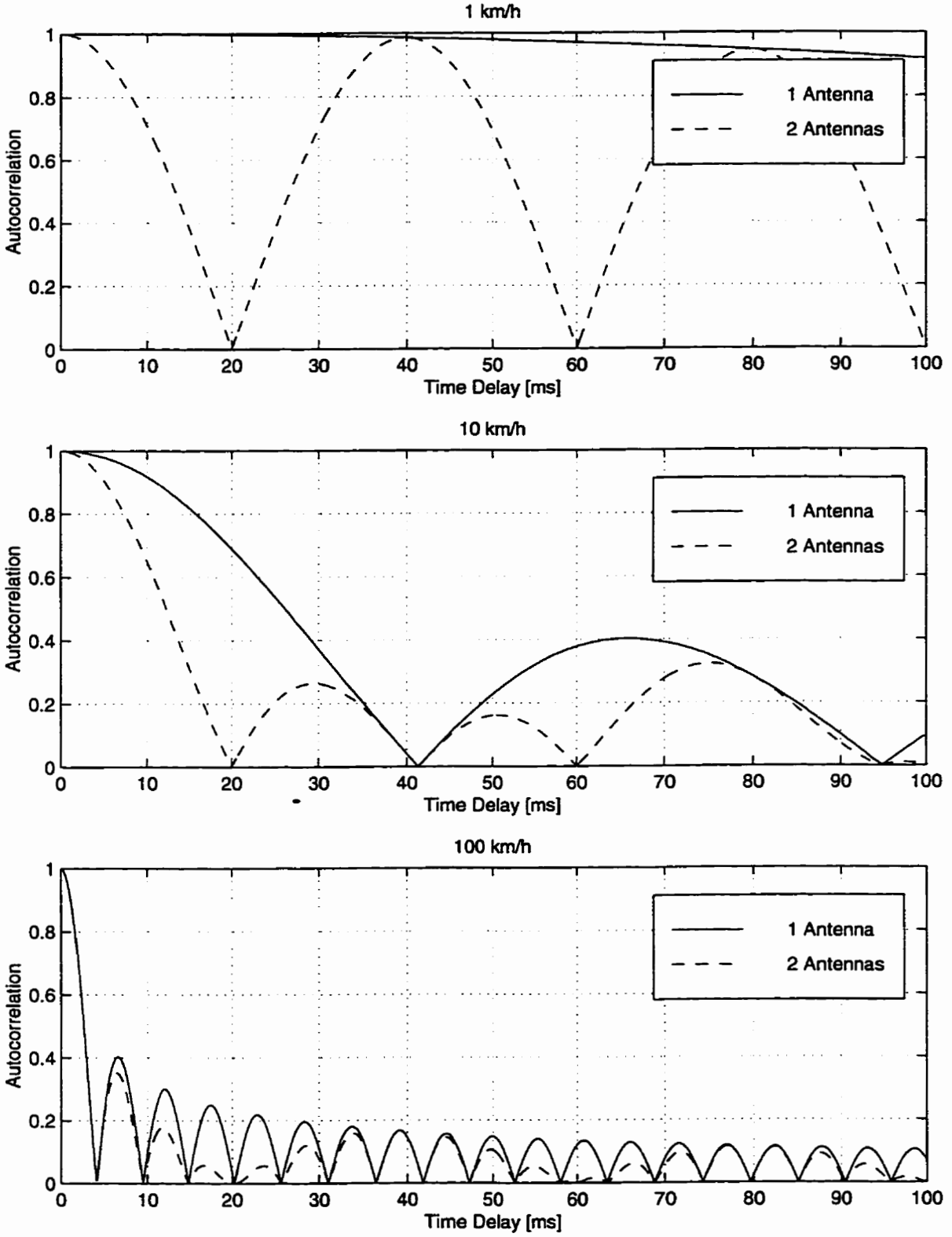


Figure 2.4: Autocorrelation of Rayleigh Fading Envelope with Simulcasting, $f = 1$ GHz, $f_o = 25$ Hz

the mobile velocity. Given that mobile velocity is an uncontrollable parameter and that the interleaving depth of a channel coder is often fixed and finite in extent, a conventional system with a single transmit antenna is vulnerable to slow fading. In the limit, interleaving becomes ineffective and the diversity order of the system tends to unity in a pseudo-stationary fading channel.

Similarly, consider a phase sweeping transmit diversity system employing three antennas (ie. $L = 3$). Let $x(t)$, $y(t)$, and $z(t)$ represent the independent complex fading amplitudes for antennas 1, 2, and 3 respectively. The difference in carrier frequency between antennas 1 and 2 is the same as that between antennas 2 and 3 and is denoted by $\omega_o$. The autocorrelation of the fading envelope is derived in a manner analogous to the previous example.

$$R_{rr}(\tau) = R_{xx}(\tau)e^{j\omega_o\tau} + R_{yy}(\tau) + R_{zz}(\tau)e^{-j\omega_o\tau} \tag{2.28}$$

where $R_{xy}(t_0, t_1) = R_{yx}(t_0, t_1) = R_{xz}(t_0, t_1) = R_{zx}(t_0, t_1) = R_{yz}(t_0, t_1) = R_{zy}(t_0, t_1) = 0$. If the fading statistics of the three antennas are identical then it follows that

$$R_{rr}(\tau) = R_{xx}(\tau)\left(2\cos(\omega_o\tau) + 1\right) \tag{2.29}$$

Without phase sweeping the autocorrelation of $r(t)$ is simply

$$R_{rr}(\tau) = 3R_{xx}(\tau) \tag{2.30}$$

It is possible to force the autocorrelation function $R_{rr}(\tau)$ to zero for at regular intervals of $\tau$.

$$R_{rr}(\tau) = 0, \ \tau \in \left\{\frac{2\pi}{3\omega_o}, \frac{4\pi}{3\omega_o}, \frac{8\pi}{3\omega_o}, \frac{10\pi}{3\omega_o}, \ldots\right\} \tag{2.31}$$

The set of time lags satisfying Eq. (2.31) also includes those which correspond to the zeros of $R_{xx}(\tau)$. Note that the solutions for $\tau$ are not evenly spaced apart. It is possible to engineer uncorrelated fading amplitudes for adjacent coded symbols, independent of the mobile velocity, when the block interleaving scheme of Figure 2.3

is used provided that

$$\omega_o \in \left\{ \frac{2\pi}{3\eta T_s}, \frac{4\pi}{3\eta T_s}, \frac{8\pi}{3\eta T_s}, \frac{10\pi}{3\eta T_s}, \ldots \right\} \tag{2.32}$$

If $\omega_o = \frac{2\pi}{3\eta T_s}$ then coded symbols positioned one and two intervals apart undergo mutually uncorrelated fading whereas the fading amplitude affecting every third coded symbol can be highly correlated in a slow fading channel. Thus, three branch diversity is feasible even under pseudo-stationary fading conditions.

## 2.7 Average Symbol Energy

An alternative argument for choosing the combination of frequency offset $\omega_o$ and the interleaving depth $\eta T_s$ is to maintain constant symbol energy over a slow fading channel. A symbol is defined here as a point in signal space drawn from an $L$-dimensional constellation. The application of phase sweeping transmit diversity over a fading channel can actually deteriorate the performance of uncoded transmission due to the simulcast like interference it creates. This is especially true when the signal received from multiple antennas exhibits a strong coherent component. It is desirable to pair a faded signal with a non-faded signal so that the information they bear together may be recovered via some means of joint detection. Hence, the transceiver pair should be designed to exploit any anti-correlation properties in the received signal envelope.

Consider a phase sweeping transmit diversity system with two antennas. Let $a_1$ and $a_2$ denote the complex valued fading amplitudes corresponding to the two antennas and assume a slow fading channel. Over many phase swept cycles, the fading envelope as observed at the receiver resembles that of standing wave interference. The instantaneous received signal energy is given by

$$|r(t)|^2 = |a_1|^2 + |a_2|^2 + 2|a_1||a_2|\cos(\omega_o t + \theta_{12}) \tag{2.33}$$

$$\theta_{12} = \mathrm{Tan}^{-1}\left(\frac{\mathrm{Im}[a_1 a_2^*]}{\mathrm{Re}[a_1 a_2^*]}\right) \tag{2.34}$$

where $\theta_{12}$ is a random quantity uniformly distributed over $[0, 2\pi)$. Note that the

average of the instantaneous received signal energy at the peak and at the null of the fading envelope happens to equal to the average signal energy $\overline{\mathcal{E}_s}$ defined as

$$\overline{\mathcal{E}_s} = \sum_{i=1}^{L} |a_i|^2 \tag{2.35}$$

Since the fading envelope is pseudo-periodic with the period determined by the frequency offset, it is possible to match any fading amplitude observed over one phase swept interval with a dual $\tau$ seconds later such that their mean square is unaffected by the artificially induced fast fading.

$$\begin{aligned} & |r(t)|^2 + |r(t+\tau)|^2 \\ &= 2(|a_1|^2 + |a_2|^2) + 2|a_1||a_2|(\cos(\omega_o t + \theta_{12}) + \cos(\omega_o(t+\tau) + \theta_{12})) \quad (2.36) \\ &= 2(|a_1|^2 + |a_2|^2),\ \tau = \frac{(2n+1)\pi}{\omega_o},\ n \in I \quad (2.37) \end{aligned}$$

The result is analogous to combining the energy received from two antennas individually (ie. $|a_1|^2 + |a_2|^2$) over two signaling intervals. By transmitting one coordinate of a 2-dimensional symbol at time $t$ and then the other coordinate at time $t+\tau$, the average symbol energy remains constant given a pseudo-stationary fading channel. Observe that the solution for $\tau$ is the same here as in Eq. (2.27). A similar derivation for the case of phase sweeping transmit diversity with 3 antennas yields

$$\begin{aligned} & \sum_{k=0}^{2} |r(t+k\tau)|^2 \\ &= 3\sum_{k=1}^{3} |a_k|^2 + \sum_{l=0}^{2}\sum_{i=1}^{3}\sum_{\substack{j=1 \\ j\neq i}}^{3} |a_i||a_j| \cos((i-j)\omega_o(t+l\tau) + \theta_{ij}) \quad (2.38) \\ &= 3\sum_{k=1}^{3} |a_k|^2,\ \tau \in \left\{ \frac{2\pi}{3\omega_o}, \frac{4\pi}{3\omega_o}, \frac{8\pi}{3\omega_o}, \frac{10\pi}{3\omega_o}, \ldots \right\} \quad (2.39) \end{aligned}$$

Hence, it is possible to average $|r(t)|^2$ over three points in time $\tau$ seconds apart to yield an average symbol energy which is constant over one phase swept cycle (assuming that $a_i$ is constant over that interval). Note that the solution for $\tau$ is identical to that of Eq. (2.32).

The analysis can be generalized to $L$ antennas where $\tau = \frac{2\pi}{L\omega_o}$. In general for a non-

stationary system, the fading amplitudes will diverge both in magnitude and in phase by the time a full cycle of phase sweeping has occurred. Consequently, the average symbol energy will not be constant over one phase swept interval. Nevertheless, the de-correlation in the fading amplitudes along the different dimensions of a symbol still holds.

# Chapter 3

# Phase Sweeping Transmit Diversity

## 3.1 Fading Resistant Constellations

Rather than relying strictly on channel coding to mitigate the fades induced by phase sweeping, the use of $L$-dimensional fading resistant constellations is investigated. A constellation is deemed fading resistant if all the signal points remain distinct when projected along any one of the $L$ dimensions. This property introduces redundancy in the constellation as to which symbol is selected for transmission. The coordinates along each dimension are transmitted to the receiver ideally via $L$ independent fading channels which are realized by using time, frequency, or space diversity techniques. Up to $L-1$ channels may be subject to a faded condition simultaneously and the receiver can still uniquely decode the correct signal point provided that an estimate of the fading amplitude affecting each dimension is known.

A fading resistant constellation can be constructed by rotating an $L$-dimensional hypercube along $\binom{L}{2}$ axes [24]. An optimum rotated constellation in $L$ space can be found via a search procedure, the solution of which depends on the fading channel conditions and the method of signal detection used. Figure 3.1 illustrates the rotation procedure for a 4-QAM constellation. A characteristic of rotated constellations is that the transformation is an isometry, that is, the distance properties of the constellation are preserved. Consequently, there is no performance degradation in using this constellation over the AWGN channel. Also, the symbol energy is identical for all points in a rotated hypercube.

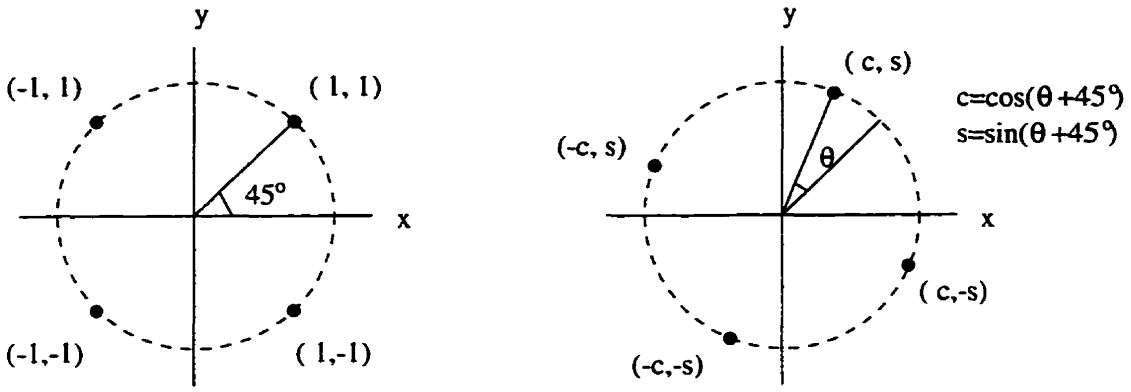


Figure 3.1: Rotated 4-QAM Constellation about the z-Axis

Another family of fading resistant constellations is that proposed by Kerpez [25]. Let $c_{ij}$ denote the coordinate of the $i^{th}$ symbol along the $j^{th}$ dimension of an $L$-dimensional constellation. A Kerpez constellation is given by

$$c_{ij} = -2\left(\left((i-1)M^{L-j+1}\right) \bmod M^L + M^{L-j+1} - \left\lceil \frac{i}{M^{j-1}} \right\rceil\right) + M^L - 1 \qquad (3.1)$$

where $1 < i < M^L$, $1 < j < L$, and $M = 2$. A characteristic of these constellations is that the signal points collapse into an equally spaced PAM constellation when projected onto any one dimension. The different symbols in this constellation do not all have the same energy except for the case of $L = 2$. Note that a Gray[1] coded fading resistant constellation does not generally yield a Gray coded PAM signal when a fade occurs along $L - 1$ dimensions.

The optimally rotated constellations of [26] and the Kerpez constellations of [25] for $L = 2$ and $L = 3$ are reproduced in the Appendix.

## 3.2 Architecture of Transmitter

Consider the forward link of a base station with $L$ transmit antennas employing the phase sweeping diversity scheme described in Section 2.6. It is emphasized that all

[1]Gray coding is the assignment of symbols to constellation points such that the symbols of neighbouring points differ in value by one bit, those of second nearest neighbours differ by two bits, and so forth.

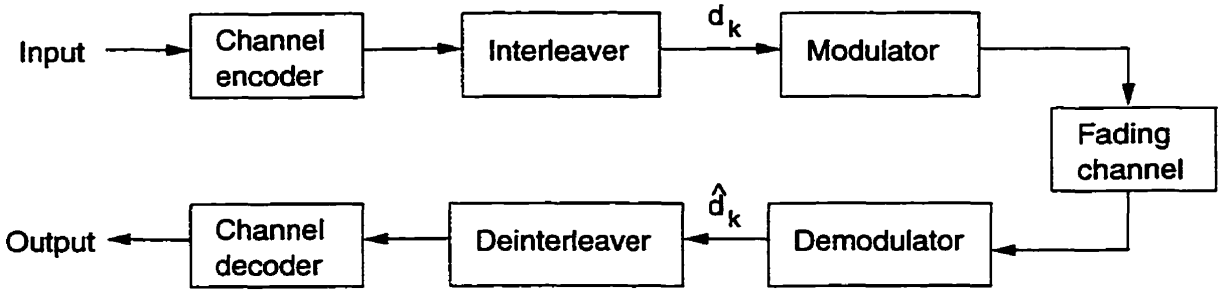


Figure 3.2: Block Diagram of Channel Coding for Transmission over a Fading Channel

the antennas transmit the same signal except that their carriers are slightly offset relative to each other. If the coordinates of an $L$-dimensional symbol are transmitted (simultaneously from each antenna) as $L$ 1-D PAM signals at times $\{t, t+\tau, \ldots, t+(L-1)\tau\}$ where $\tau = \frac{2\pi}{L\omega_o}$ then by the previous analysis:

- The coordinates along the $L$ dimensions are subjected to uncorrelated fading.
- Given a slow fading channel, the received symbol energy per dimension is approximately equal to the instantaneous mean signal level averaged over the $L$ antennas.

A novel transmitter architecture is proposed to implement phase sweeping transmit diversity. A detailed description of the system follows the block diagram representation outlined in Figure 3.2.

Error correction coding is applied to the source bits to protect data integrity. Either a block code or a convolutional code may be employed to introduce redundancy to the data stream. The sequence of encoded bits is re-ordered by interleaving which purpose is to guard against burst errors. In Figure 3.3, the input bit stream $d_k$ denotes the channel coded bits at the output of the block interleaver (see Figure 2.3). The interleaved bits are paired off in groups of $L$ bits which are then passed onto the symbol mapper. Each $L$-bit word is used to choose one point, from a signal space of $2^L$ points, drawn from an $L$-dimensional fading resistant constellation. The coordinates of each selected point are fed sequentially through a convolutional interleaver. The latter operation permits the construction of $L$ logical channels separated in time which undergo different degrees of fading. The parameter $T_d$ determines the depth of the

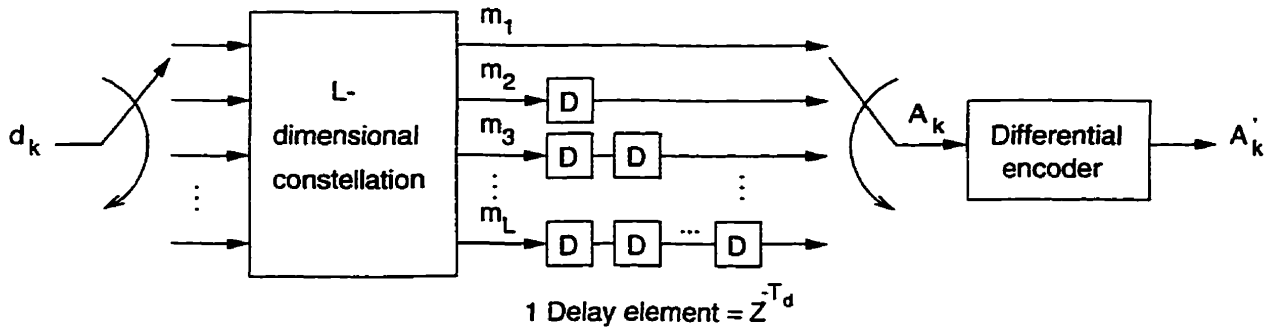


Figure 3.3: Convolutional Interleaving of Symbol Coordinates followed by Differential Encoding

convolutional interleaving and is given by

$$T_d = \frac{1}{L}\left(\frac{\tau}{T_s} - 1\right), \; T_d \in I \tag{3.2}$$

where $\tau$ is chosen according to Eq. (2.26) and $T_s$ is the signaling period. The individual interleaved coordinates are subsequently treated as a 1-D pulse amplitude modulated signal denoted as $A_k$ in Figure 3.3. The application of differential encoding to $A_k$ yields another sequence $A_k^{'}$ which is robust against phase ambiguity (see Section 3.3). The differential encoding is given by

$$A_k^{'} = A_k \mathrm{sgn}(A_{k-1}^{'}) \tag{3.3}$$

The pulse train $A_k^{'}$ is subsequently filtered by a square root raised cosine filter with a roll-off factor of 0.35. The choice of roll-off factor is a balance between spectral efficiency and having a rapidly decaying impulse response $g(t)$. Finally, the resultant signal $x(t)$ is up-converted to the carrier frequency $\omega_c$ and then transmitted from $L$ spatially separate antennas. The baseband representation of the transmitter is illustrated in left half of Figure 3.4. A fixed frequency offset is introduced to the $i^{th}$ branch by the phase sweeping function $b_i(t)$ given by

$$b_i(t) = e^{j\frac{2i-L-1}{2}\omega_o t} \tag{3.4}$$

where $\omega_o$ is set according to Eq. (2.27).

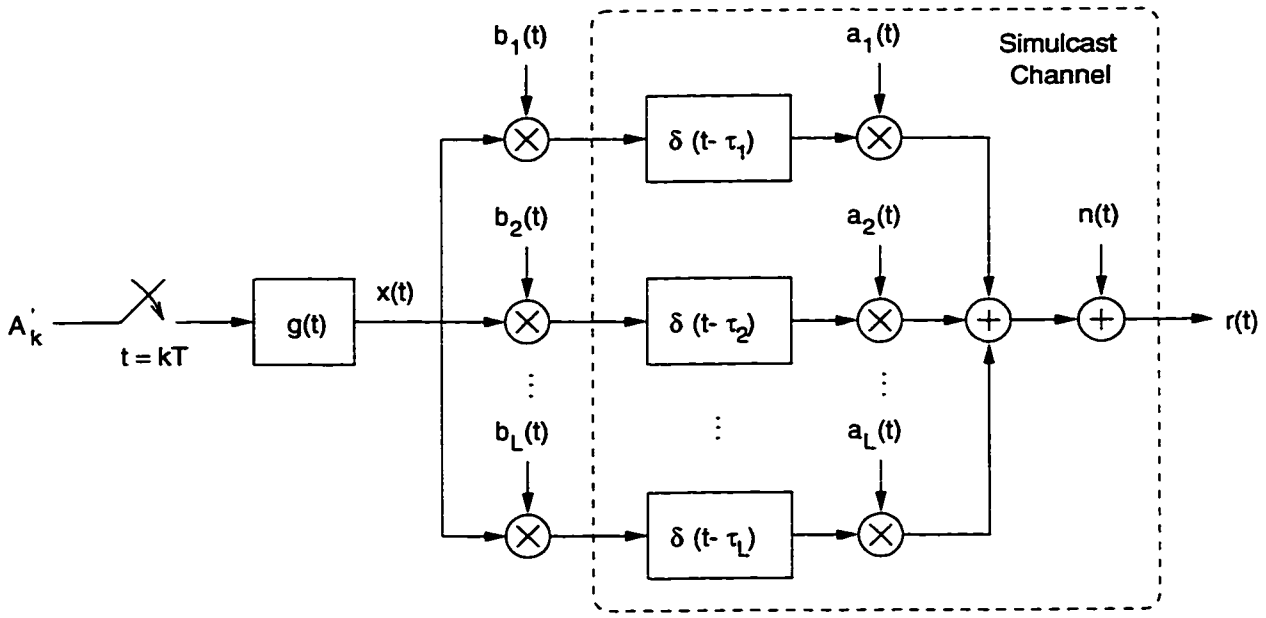


Figure 3.4: PAM Signaling via Multiple Phase Swept Transmit Antennas

## 3.3 Channel Model and Considerations

A mobile radio channel characterized by a very short delay spread is assumed such that the coherence bandwidth of the channel is larger than the bandwidth of the receiver. For example, these propagation conditions would exist in an indoor environment. A single ray model to Rayleigh and Rician fading is adopted as a result. Let the $L$ transmit antennas in Figure 3.4 be subject to independent fading processes $\{a_1, a_2, \ldots, a_L\}$ and the differential delays $|\tau_i - \tau_j|$ be a negligible small fraction of the symbol period. Consequently, the receiver perceives there being only one path overall which is impaired by multiplicative distortion. The $L$ separate transmissions sum together in the simulcast channel which is perturbed by additive white Gaussian noise denoted by $n(t)$.

The application of phase sweeping transmit diversity results in frequent nulls in the received signal envelope. The phase of the carrier may change abruptly after incurring a deep fade which renders carrier tracking difficult. A phase ambiguity can arise in the transmission of PAM signals where the sign of the received signal is inverted unexpectedly. Figure 3.5 illustrates the effect of simulcast interference on a rotated 4-QAM constellation over one phase swept interval for a transmit diversity

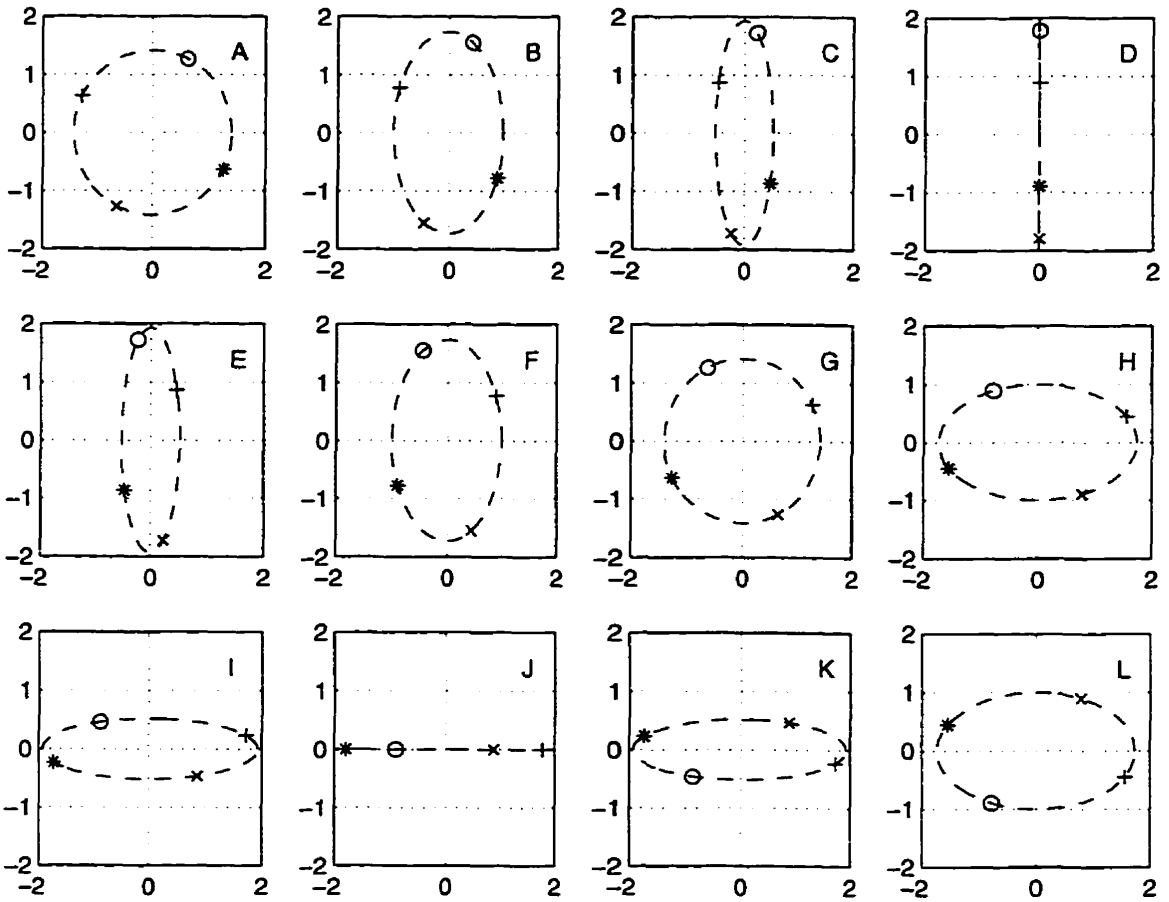


Figure 3.5: Effect of Phase Sweeping on Signal Constellation over Time for a Coherent Receiver, $L = 2$, $\theta = 18.4°$

system employing coherent detection. Note the zero crossing phenomenon for the signal points after the occurrence of a deep fade. Consequently, a differential encoding scheme is employed which enables differential detection at the receiver and simplifies the task of carrier tracking. Figure 3.6 corresponds to a differentially coherent system which is able to resolve the sign reversal problem.

## 3.4 Architecture of Receiver

The front end of a differentially coherent receiver is depicted in Figure 3.7. The received signal $r(t)$ is down-converted to baseband where the in phase and quadrature

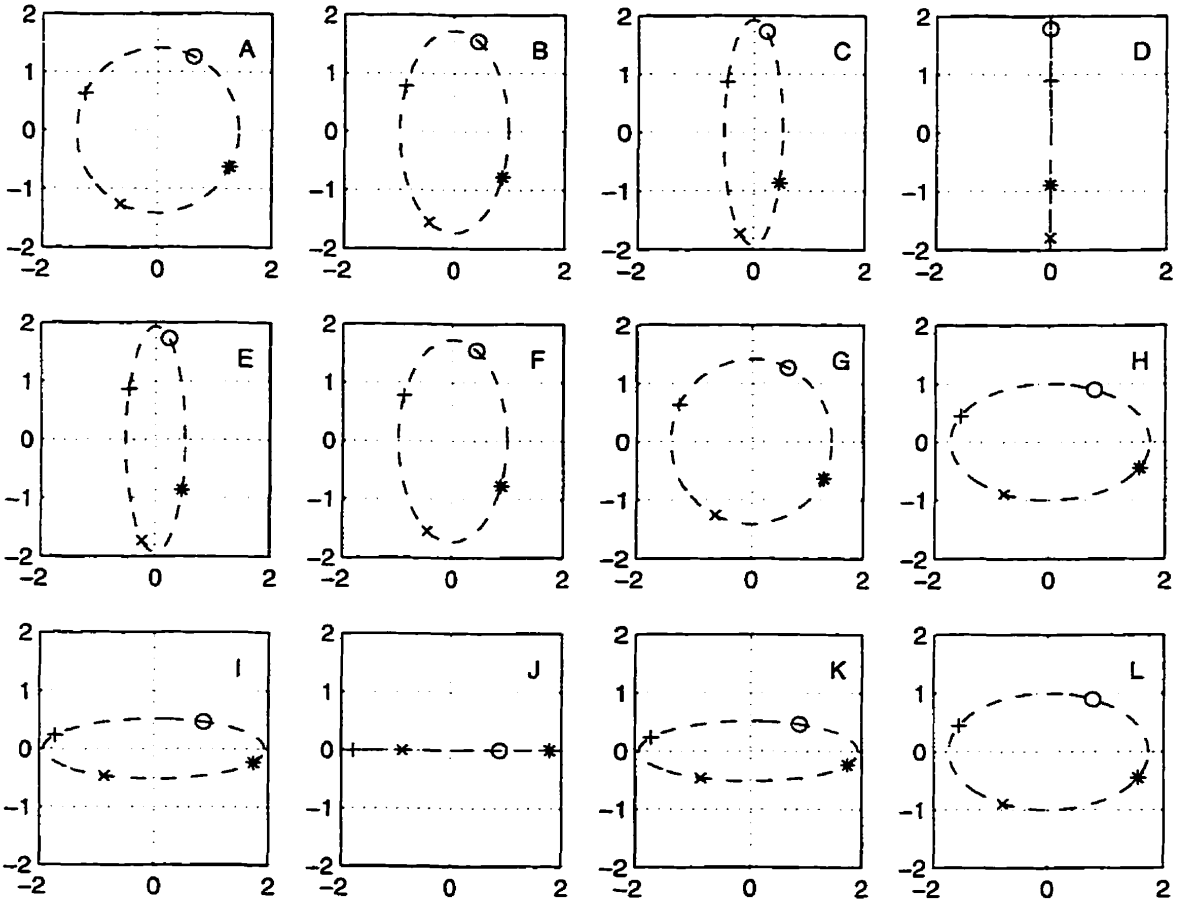


Figure 3.6: Effect of Phase Sweeping on Signal Constellation over Time for a Differentially Coherent Receiver, $L = 2$, $\theta = 18.4°$

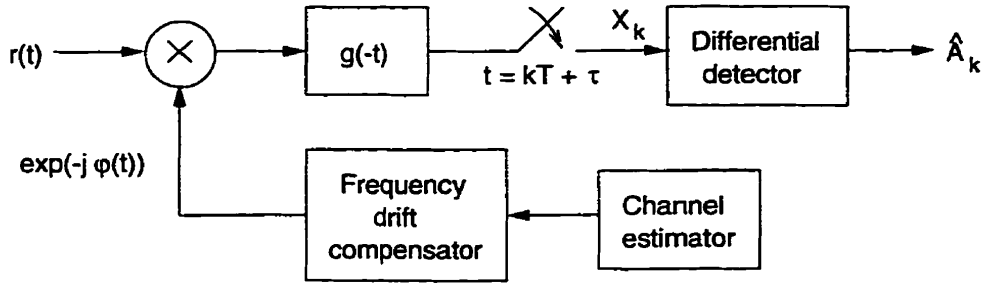


Figure 3.7: Baseband Representation of Matched Filter Receiver with Differential Detector

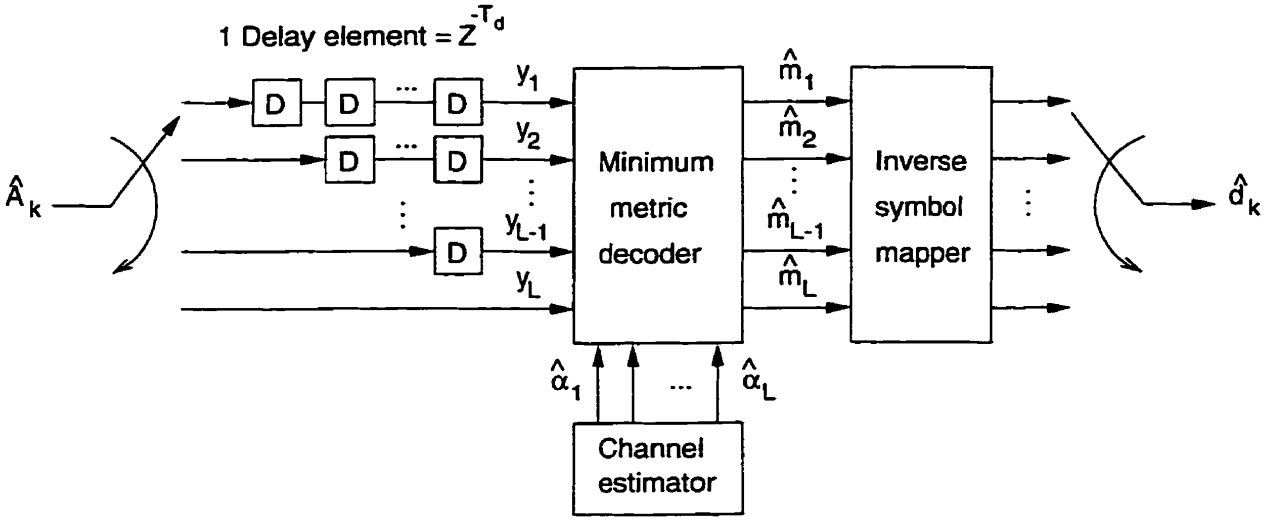


Figure 3.8: Convolutional De-interleaving of Coordinates Followed by Symbol Detection

components are correlated with the transmitted pulse $g(t)$. The complex valued output of the correlator, denoted by $X_k = X_k^c + jX_k^s$, is compared relative to the previous value $X_{k-1}$ to derive a decision variable $\hat{A}_k$ for use by the decision device.

$$\hat{A}_k = \frac{X_k^c X_{k-1}^c + X_k^s X_{k-1}^s}{\sqrt{(X_{k-1}^c)^2 + (X_{k-1}^s)^2}}$$

The sequence $\hat{A}_k$ must pass through a convolutional de-interleaver to restore the original sequence of 1-D PAM signals prior to symbol detection. The re-ordering of the input is illustrated in Figure 3.8. The $L$-dimensional vector $\mathbf{y} = (y_1, y_2, \ldots, y_L)$

represents a noisy estimate of the transmitted symbol subject to fading. Since the received signal $r(t)$ is formed by the superposition of $L$ transmissions, the resultant fading amplitude $\alpha$ observed at the receiver is the magnitude of the sum of $L$ complex valued fading processes.

$$\alpha = |a_1 + a_2 + \ldots + a_L| \tag{3.5}$$

Given an estimate of the fading amplitudes $\{\hat{\alpha}_1, \hat{\alpha}_2, \ldots, \hat{\alpha}_L, \}$ along each dimension, the vector $\mathbf{y}$ is compared with all possible points $\mathbf{m}$ in the constellation. The decision device chooses the symbol $\hat{\mathbf{m}}$ which minimizes the following metric (see [27]).

$$\sum_{i=1} L \frac{(y_{i,k} - \hat{\alpha}_i \hat{m}_i)^2}{\left(\frac{\hat{\alpha}_i \hat{m}_i}{y_{i,k-1}}\right)^2 + 1} \tag{3.6}$$

A parallel to serial conversion of the message bits corresponding to $\hat{\mathbf{m}}$ yields an estimate of the coded data stream $\hat{d}_k$. The $\hat{d}_k$ bits are block de-interleaved and then decoded. The $\hat{\alpha}_i$ are subject to the same re-ordering as $\hat{A}_k$ and $\hat{d}_k$ before being passed on to the decision device and channel decoder. If soft decision decoding is required then symbol detection and channel decoding are treated jointly.

## 3.5 Effect of Constellation on Performance

### 3.5.1 Choice of Constellation

In addition to carrier frequency offsets and channel coding, the other important aspect of phase sweeping transmit diversity is the choice of signal constellation. Constellations which are optimum for an AWGN or Rayleigh fading channel may or may not be optimum for a simulcast channel. The search for good constellations follows the approach outlined in [26] for the case of Rayleigh fading except that here the rotation is limited to one degree of freedom. For $L = 2$, a 4-QAM constellation is rotated incrementally clockwise about the positive $z$-axis. A union bound on the probability of symbol error is calculated for the resultant signal constellation. For $L = 3$, a 3-dimensional hypercube constellation is rotated clockwise about the vector $(1, 1, 1)$[2].

[2]The rotation of a 3-dimensional hypercube constellation about an arbitrary vector is formulated in the Appendix. See Section A.4.

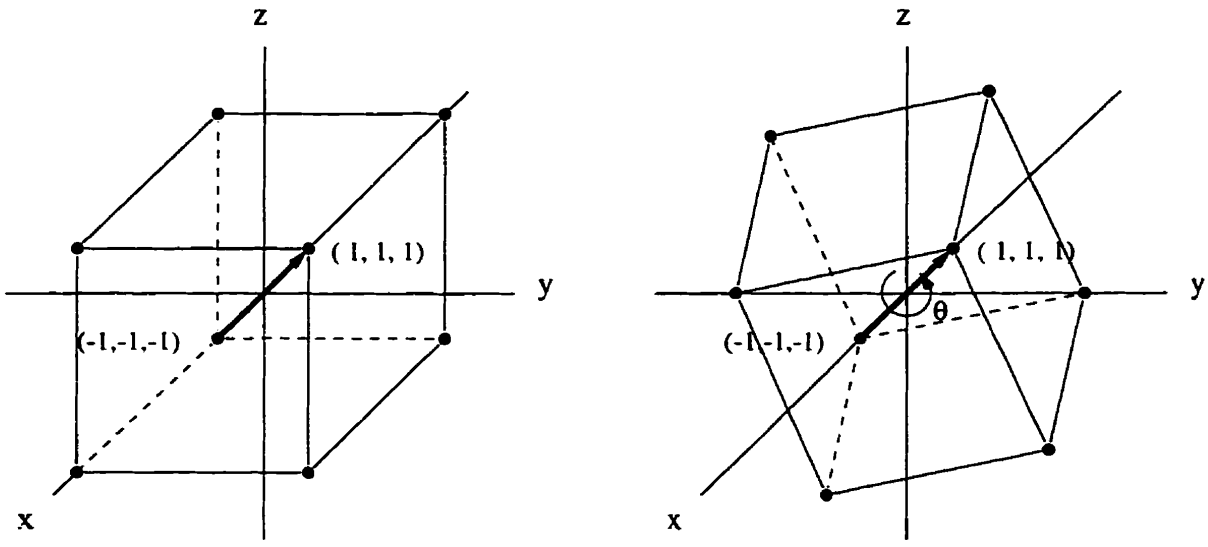


Figure 3.9: Rotated 3-D Hypercube Constellation about the Vector (1,1,1)

The Kerpez constellations described by Eq. (3.1) are also considered.

Note that the 2-D Kerpez constellation is equivalent to Figure 3.1 with $\theta = 26.6°$. Also, the 3-D rotated hypercube constellations optimized for a coherent and a differentially coherent receiver in [26] are equivalent to Figure 3.9 with $\theta = 28°$ and $\theta = 52°$ respectively. This symmetry is not surprising as one would expect the projections of the constellation on any one axis to yield the same 1-D PAM signal. Otherwise, the transmission along some channels/dimensions would be favored more than others.

A union bound on the probability of symbol error is calculated for the resultant signal constellation $C$.

$$P_{e,sym} \leq \frac{1}{|C|} \sum_{m} \sum_{\substack{\hat{m} \\ \hat{m} \neq m}} P(m \rightarrow \hat{m}) \tag{3.7}$$

Phase sweeping transmit diversity with dual antennas (ie. $L = 2$) and PAM signaling with coherent detection over a pseudo-stationary Rayleigh fading channel are assumed in the following sections.

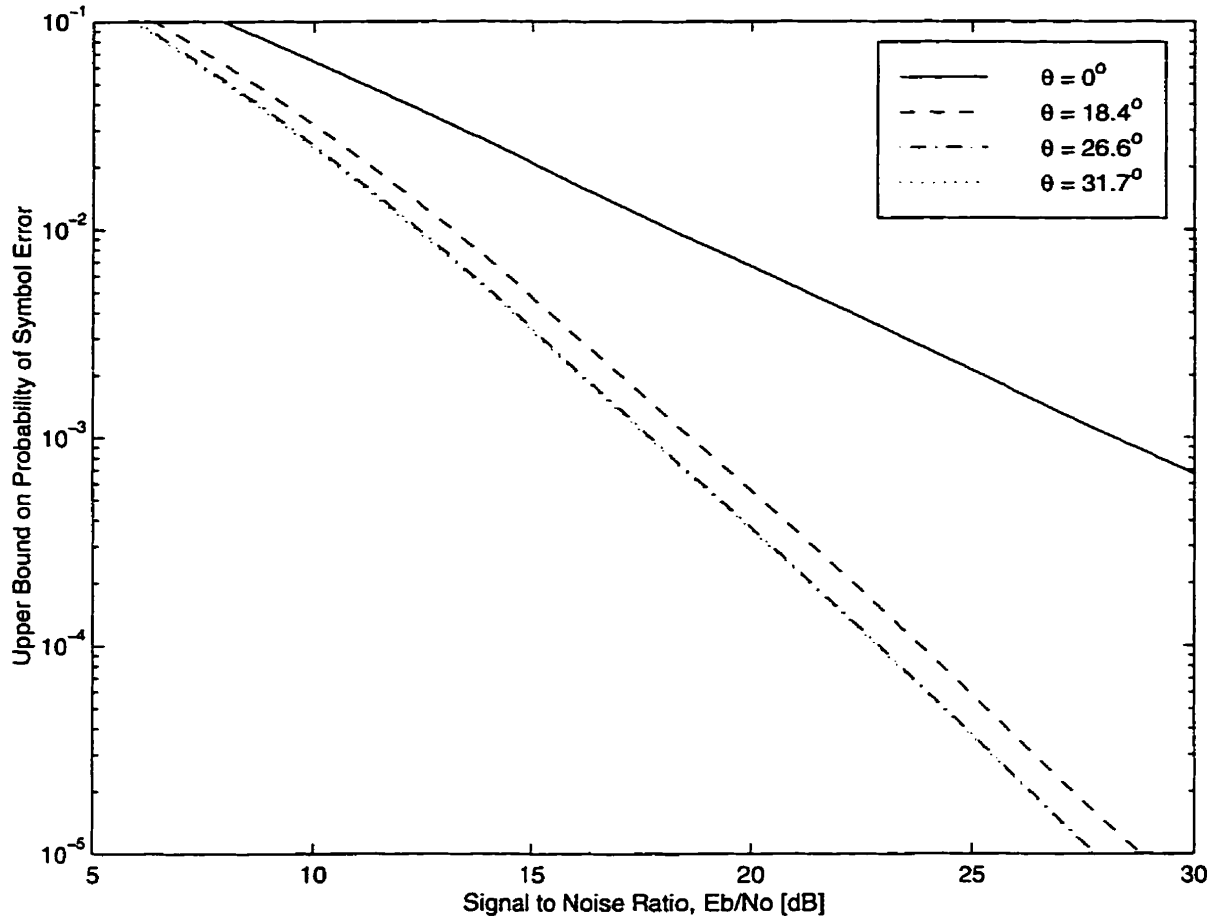


Figure 3.10: Upper Bound on Probability of Symbol Error for Various 2-D Constellations, $L = 2$

### 3.5.2 Rotation Angle

The performance of phase sweeping transmit diversity as a function of the 2-D rotation angle is shown in Figure 3.10. It is found that the optimum constellation is that of $\theta = 31.7°$. Note that the error curve is insensitive to small deviations from the optimum rotation angle. Observe that probability of error for the $\theta \in \{18.4°, 26.6°, 31.7°\}$ constellations vary as $\frac{1}{\text{SNR}^2}$.

### 3.5.3 Rician Parameter

If line of sight propagation is available then the fading envelope follows a Rician distribution. The performance of a phase sweeping transmit diversity scheme under a

| $\theta$ [deg] | $\gamma$ [dB] |
|---|---|
| 18.6 | 9.9 |
| 22.5 | 8.3 |
| 26.6 | 7.0 |
| 31.7 | 6.7 |

Table 3.1: Asymptotic Gain Penalty for Phase Sweeping Transmit Diversity over an AWGN Channel

Rician fading channel is plotted in Figure 3.11. The probability of error improves as the Rician parameter $K$ is increased. When the received signal comprises of only a coherent component (ie. $K = \infty$), then the radio channel approaches an AWGN channel. For an AWGN channel, the asymptotic uncoded bit error rate is determined solely by the minimum Euclidean distance separating constellation points in signal space. Since the presence of simulcast interference still causes the 4-QAM constellation to periodically collapse to a 1-D PAM signal, it is the minimum distance properties of the PAM constellation which ultimately characterizes the probability of error curve at high SNR. The performance of dual antenna phase sweeping transmit diversity over an AWGN like channel is no worst than uncoded BPSK by a maximum of $\gamma$ dB where $\gamma$ is given by Table 3.1. Therefore, the decision whether to invoke phase sweeping transmit diversity at the base station depends on the Rician parameter.

### 3.5.4 Random Interleaving

If the frequency offset $\omega_o$ and the interleaving depth $\eta$ are not matched or a random interleaver is assumed then the symbol energy will not be constant over one phase swept cycle. The performance of phase sweeping transmit diversity would then be less than ideal. A plot of Eq. (3.7) is shown in Figure 3.12. The diversity order of the system is reduced effectively from 2 to 1.7.

### 3.5.5 Relative Power

If the receiver is closer to one antenna than the other or if shadow fading affects the two links differently then the mean received power from the two antennas will not be the same. In general, the received power from two separate simulcast transmitters

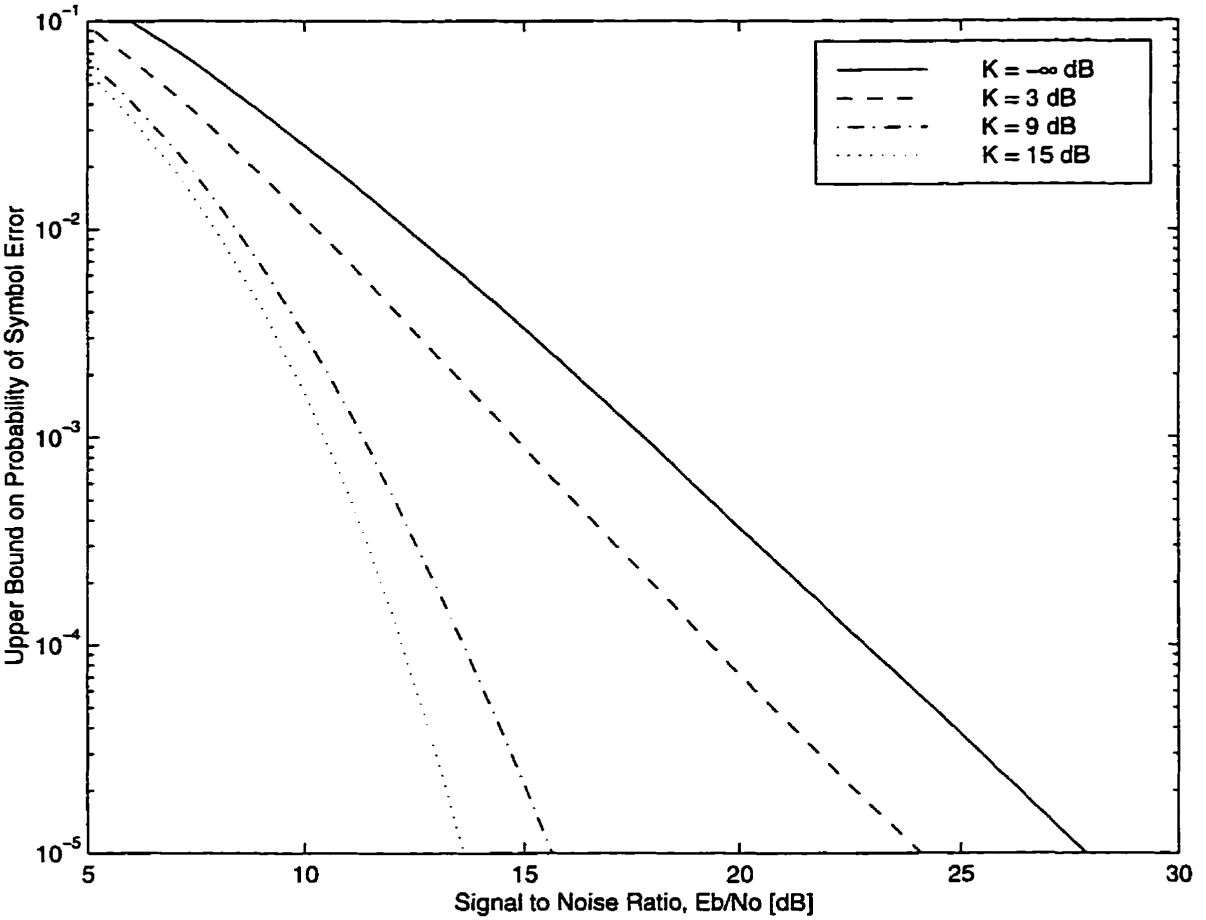


Figure 3.11: Upper Bound on Probability of Symbol Error versus Rician Parameter, $L = 2$, $\theta = 31.7°$

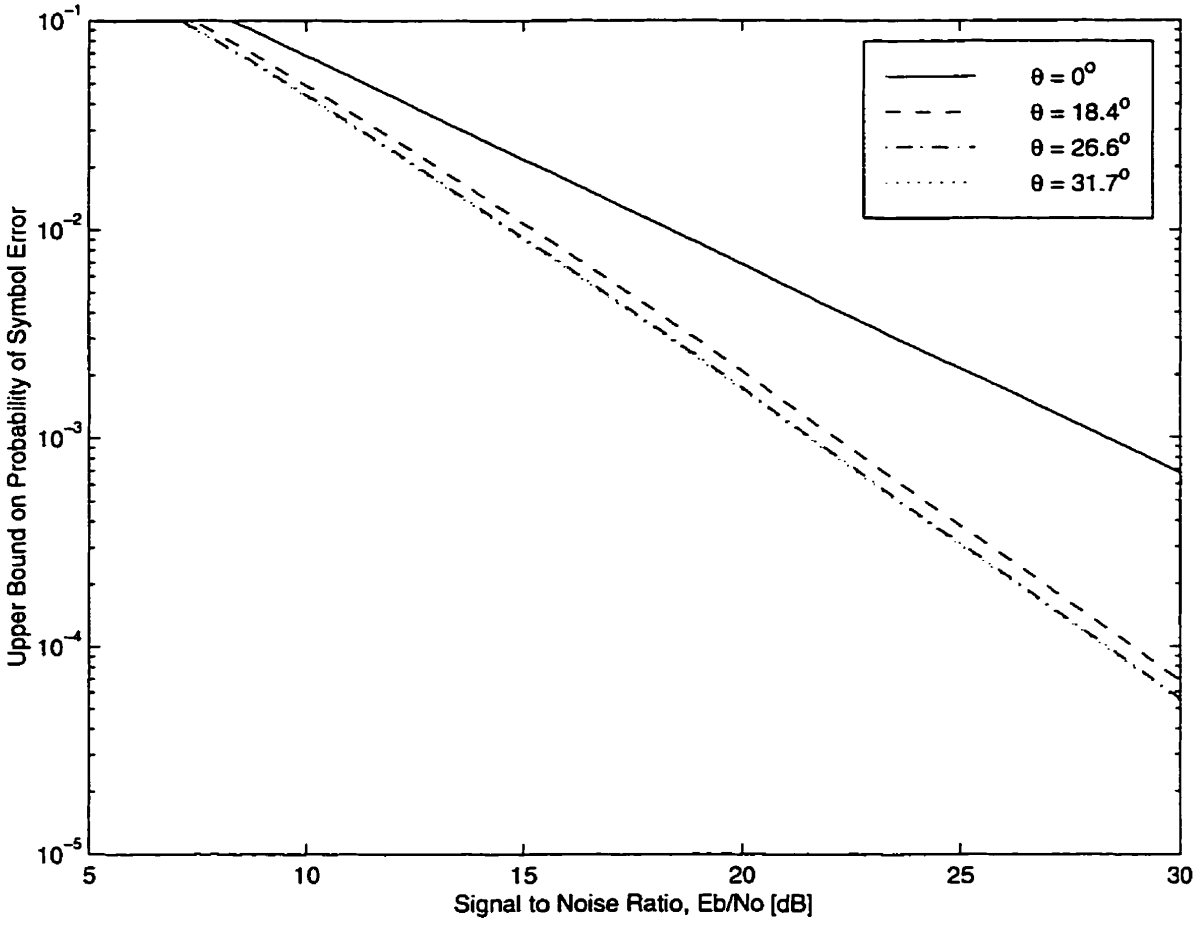


Figure 3.12: Upper Bound on Probability of Symbol Error with Random Interleaving, $L = 2$

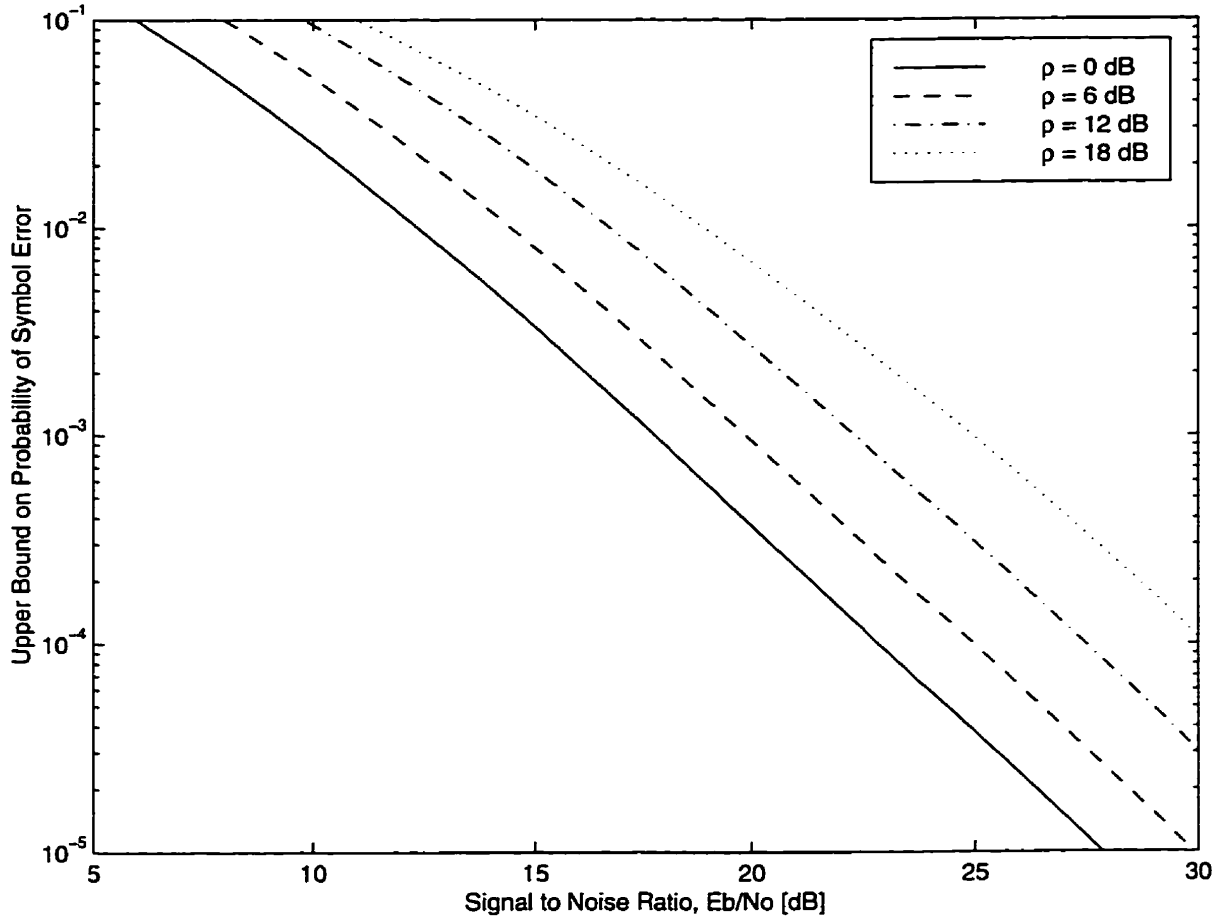


Figure 3.13: Upper Bound on Probability of Symbol Error versus Relative Power, $L = 2$, $\theta = 31.7°$

will not be identical due to shadow fading or propagation path loss with distance. However, it is not feasible though to average the bit error rate of phase sweeping transmit diversity under shadow fading through simulation because of the required computation time. Consequently, the BER performance is inferred by simulating the system with a relative imbalance $\rho$ in the average received power from the two transmit antennas. It is seen in Figure 3.13 that the BER for the case of Rayleigh fading worsens as the relative imbalance diverges from unity. The contribution of space diversity to the system is reduced when the received power of from one antenna dominates over the other. In contrast, the BER actually improves with increasing $\rho$ for the case of an AWGN channel because of lower simulcast interference.

## 3.6 PDF of Relative Received Power

In the search for optimum constellations for simulcast channels, it was assumed that the mean power received from each of $L$ antennas is identical. The assumption is generally true for antennas which are co-located at a common base station and for locations in space which are equidistant to all the antennas involved. However, the occurrence of shadowing and propagation path loss with distance will cause inevitably an imbalance in the received power from different transmitter locations. In order to determine the distribution of the relative received powers, a Monte Carlo simulation approach is taken.

Consider a system consisting of seven simulcast transmitters arranged in a hexagonal grid as illustrated in Figure 3.14. Define the region $R_0$ as being the collection of points in space which are closer to the transmitter in the center than to any other transmitter in the system. The region $R_0$ takes on the shape of a hexagon which is shaded in the diagram. A point $P_i$ is drawn randomly from the region $R_0$ in a uniformly distributed manner. The propagation path loss to point $P_i$ is calculated for each transmitter. In addition to the attenuation due to distance, independent shadow fading is added to each link. A path loss exponent of 3 and a log-normal standard deviation of 6 dB are assumed. The relative strengths of the seven transmissions are recorded. The whole procedure is repeated for 1 million iterations. A histogram of the relative received power (in dB) between the strongest rays is calculated using a bin size of 1 dB. After normalizing the result, it is interpreted as an approximation to the desired continuous valued probability density function. Figure 3.15 shows the pdf of the relative received power between the two strongest rays. It is evident that the situation in which the mobile station is receiving two approximately equal strength rays is the most probable. Figure 3.15 also shows the pdf of the relative received power between the first and third strongest rays and the first and fourth strongest rays. The plot reveals that the reception of three closely equal strength signals is not likely. That is, it happens with only 5.3 percent likelihood that their powers differ by no more than 3 dB. It was determined from the simulations the probability that the transmitter at the center yields the first, second, or third strongest signal among the group is 0.786, 0.132, and 0.049 respectively. Consequently, the probability that the

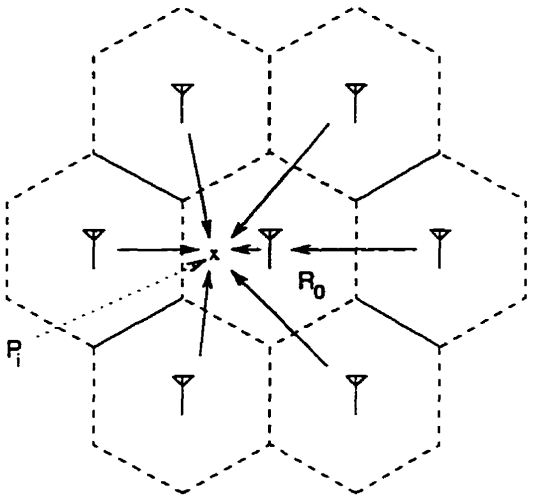


Figure 3.14: Hexagonal Placement of Simulcast Transmitters

closest transmitter in the given simulcast system is not among the top 2 or 3 strongest received signals is 0.082 and 0.033 respectively. Since 42 percent of the time the two strongest rays are within 6 dB of each other, it is important that the coding and/or modulation employed for transmission be robust against simulcast interference.

In the case of rectangular placement of simulcast transmitters, a system of nine transmitters arranged in a square grid as shown in Figure 3.16 is considered. Here the region $R_0$, as defined previously, is the square portion shaded in the diagram. Figure 3.17 shows the pdf of the relative received power between the two, three, four strongest rays. The probability that the transmitter at the center yields the first, second, or third strongest signal among the group is 0.689, 0.166, and 0.074 respectively. Consequently, the probability that the closest transmitter in the given simulcast system is not among the top 2 or 3 strongest received signals is 0.145 and 0.071 respectively. It is inferred from the pdf that 51 percent of the time the two strongest rays are within 6 dB of each other.

It is possible in the hexagonal scheme for the mobile station to lie at a point which is equidistant to two or three transmitters. In the square scenario, the mobile station may be situated midway between two or four transmitters. Consequently, the problem of simulcast interference is more severe in the case of a rectangular placement. The hexagonal arrangement of antennas is more efficient in that it maximizes the area

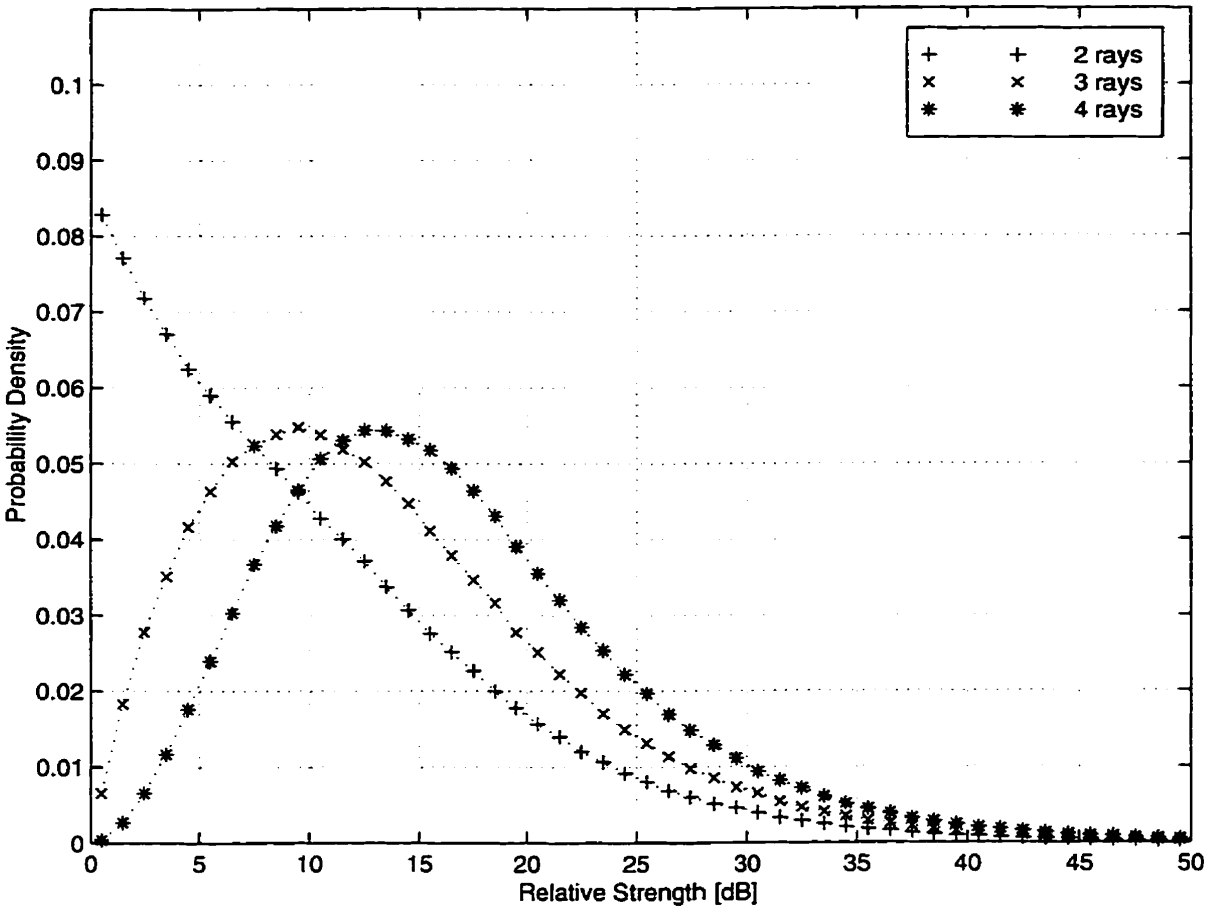


Figure 3.15: Simulated PDF of Relative Received Power Between Top 2, 3, and 4 Strongest Rays, Hexagonal Grid

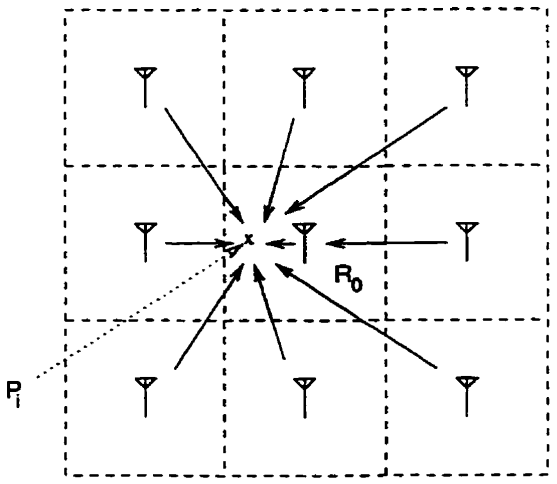


Figure 3.16: Square Placement of Simulcast Transmitters

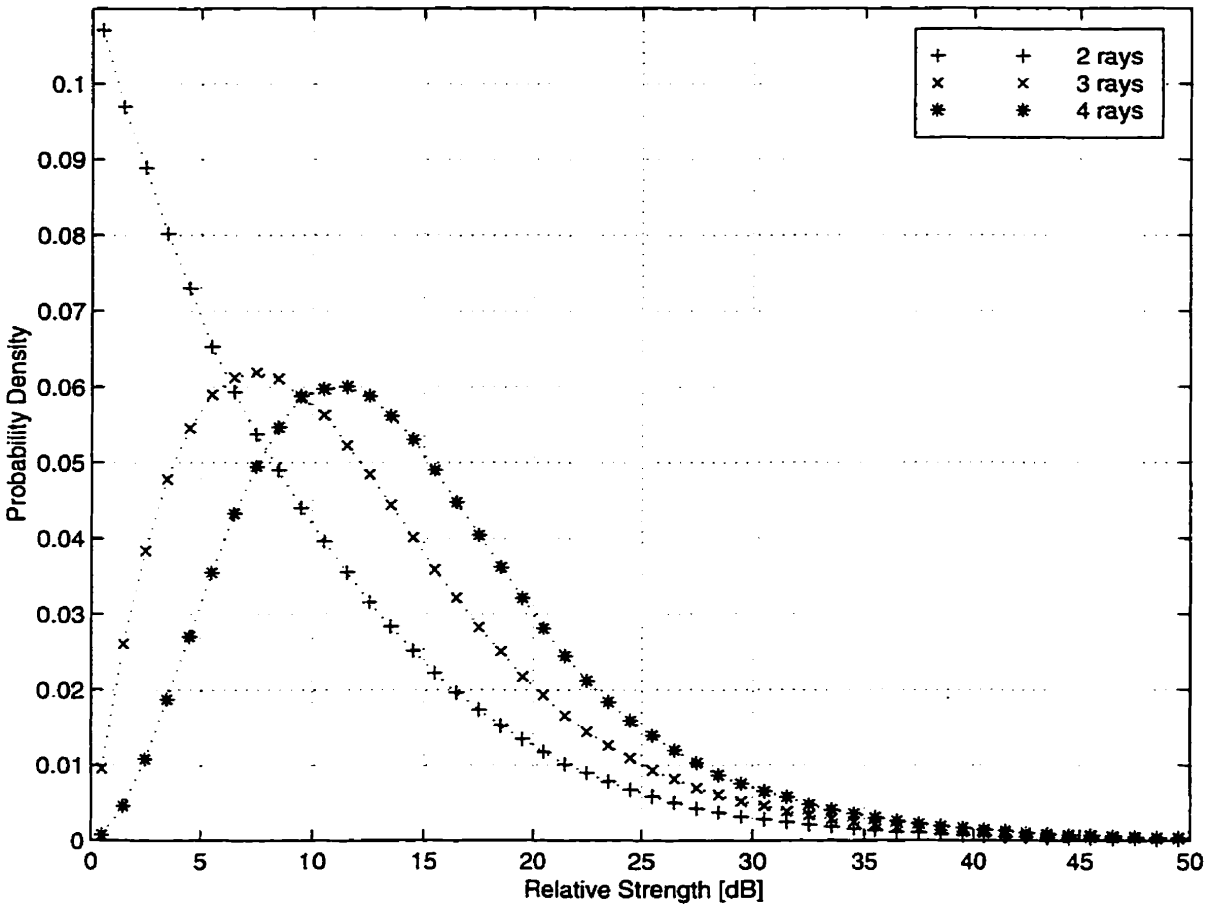


Figure 3.17: Simulated PDF of Relative Received Power Between Top 2, 3, and 4 Strongest Rays, Square Grid

covered by a given number of antennas.

## 3.7 Constraint on Differential Delay

Consider a free space environment in which a mobile station is receiving a signal from two simulcast transmitters. The differential delay between the two rays must be kept small relative to the symbol period in order to minimize the effect of intersymbol interference on the receiver performance. If the differential delay exceeds about a quarter of the symbol period then one ray must be stronger than the other ray by some minimum ratio in order to overcome the ISI introduced by the weaker signal. These two constraints define the region in the service area where communications is possible without the need for a channel equalizer at the receiver.

Let the position of the two transmitters be denoted by the vector $\mathbf{r}_1$ and $\mathbf{r}_2$. The coordinates of both transmitters and mobile receiver are restricted to two dimensions for simplicity. As noted earlier, the differential delay between the two rays observed at the mobile station must be shorter than the maximum delay $\tau_{\max}$ in order to avoid severe ISI.

$$|\|\mathbf{r} - \mathbf{r}_1\| - \|\mathbf{r} - \mathbf{r}_2\|| \leq \tau_{\max} c \tag{3.8}$$

In an environment free of multipath, the differential delay observed at the mobile station is less than or equal to the propagation delay that separates the two transmitters. For example, at a signaling rate of 48.6 kHz and a maximum tolerable differential delay of $\frac{1}{4}T_s$, the ideal maximum separation distance between two antennas is 1.54 km. Consequently, the spacing between the transmit antennas will have some bearing on the maximum signaling rate allowed on a simulcast channel.

When the antenna separation $d$ is greater than the propagation distance corresponding to $\tau_{\max}$, it is possible to delimit the service area into three regions. Figure 3.18 is a contour plot of the relation given by Eq. (3.8) where $\mathbf{r}_1 = \left(\frac{d}{2}, 0\right)$, $\mathbf{r}_2 = \left(-\frac{d}{2}, 0\right)$, and both axes are normalized by the antenna separation. A value of $d = 1.3\tau_{\max} c$ is assumed for illustration purposes only. On average, the differential delay exhibited in the inner (unshaded) region is within the required limit $\tau_{\max}$ whereas those corresponding to the two outer (shaded) regions are not. Note that the boundaries just described represent only an expectation in regards to predicting

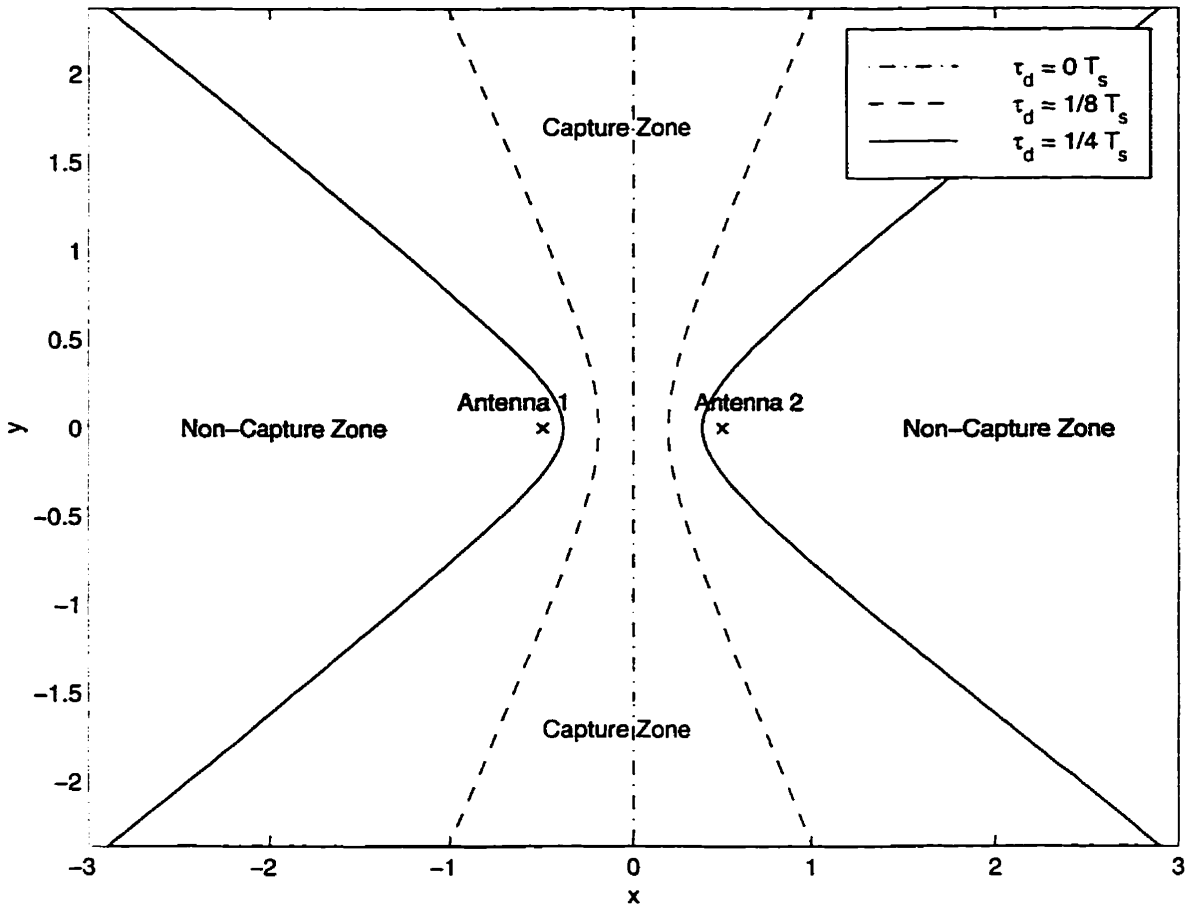


Figure 3.18: Contour Plot of Differential Delay Constraint, $\tau_{\max} = \frac{1}{4}T_s$, $d = 1.3\tau_{\max}c$

adequate receiver performance. The asymptotic angle between the demarcation lines satisfying Eq. (3.8) and the antenna bore-sight is

$$\theta(\tau_{\max}) = \pm \mathrm{Sin}^{-1}\left(\frac{\tau_{\max}c}{d}\right) \tag{3.9}$$

If the mobile station is situated in the outer (shaded) regions then it may be possible for the receiver to overcome the large differential delay provided that one ray is stronger than the other by at least the capture threshold $\rho_{\min}$. A free space propagation is assumed in which the power received from the $i^{th}$ transmitter is inversely proportional to the propagation distance raised to the path loss exponent $\alpha$. If the

relative power must be greater than or equal to $\rho_{\min}$ then

$$\begin{aligned} \frac{P_2}{P_1} &= \left\| \frac{\mathbf{r} - \mathbf{r}_1}{\mathbf{r} - \mathbf{r}_2} \right\|^{\alpha} \\ &\geq \rho_{\min} \end{aligned}$$

Substituting $\mathbf{r} = (x, y)$ in Eq. (3.10) yields

$$\left( x - \frac{\rho_{\min}^{2/\alpha} + 1}{\rho_{\min}^{2/\alpha} - 1} \right)^2 + y^2 \leq \frac{\rho_{\min}^{2/\alpha}}{(\rho_{\min}^{2/\alpha} - 1)^2} d^2 \tag{3.10}$$

Eq. (3.10) defines a region in the shape of a disk given the capture threshold and path loss exponent. Figure 3.19 is a plot of Eq. (3.10) with $\rho_{\min}$ and $\alpha = 3$. Note that when $\|\mathbf{r}\| \gg d$ the relative received power tends to unity. Thus, for transmit diversity at the base station where $d \approx 10\lambda$ and $\|\mathbf{r}\| > 100\lambda$, the mean power received from each antenna is approximately equal.

The region where communications is generally possible without the need for an equalizer is the union of the capture zones (ie. unshaded areas) shown in Figure 3.18 and Figure 3.19. In a real propagation environment, the presence of shadow fading distorts the position of the contour lines depicted in both figures.

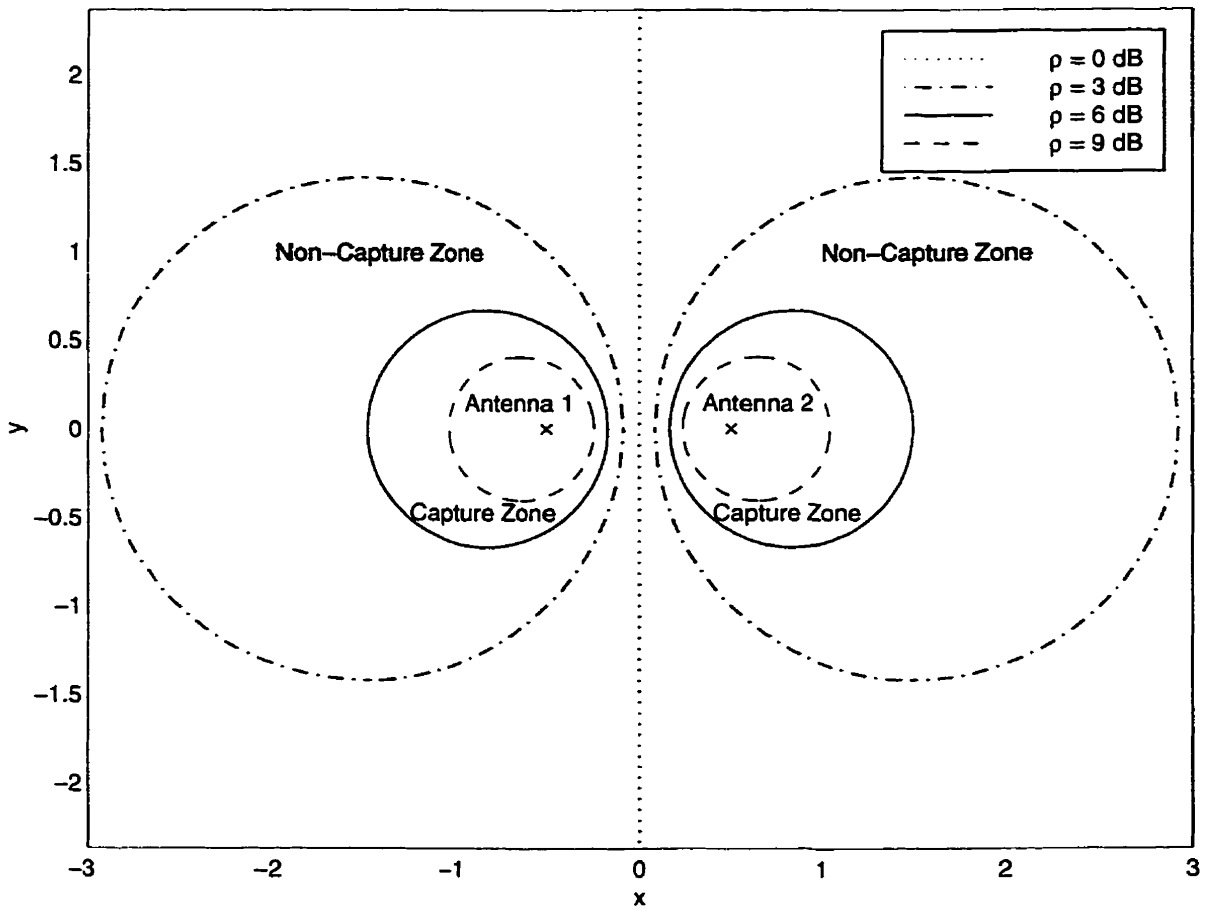


Figure 3.19: Contour Plot of Relative Power Constraint, $\rho_{\min} = 6$ dB, $\alpha = 3$

# Chapter 4

# Performance Analysis by Simulation

## 4.1 Motivation

In order to evaluate the performance of phase sweeping transmit diversity under time correlated fading conditions, it is necessary to resort to time domain simulations. This is because the coding gain provided by forward error correction coding depends highly on the autocorrelation properties of the fading envelope. Since the assumption of ideal interleaving is not applicable for a pseudo-stationary fading channel, the effect of finite interleaver memory is investigated. Three different coding systems are considered, the best of which is investigated further. The effect of various design parameters and channel conditions on system performance is determined via computer simulation. Wherever possible, the choice of specific system parameters is made based on existing standards for mobile communications.

## 4.2 System Description

The choice of channel coding, signaling rate, and frame format are borrowed from the Mobitex system from Ericsson [28][29] and/or the IS-54 standard [30] with some modification. In all cases, a differentially coherent receiver is assumed. The transmitted pulse shape is a square root raised cosine pulse with a roll-off factor of 0.35.

The sampling rate of the simulations is set at 16 times higher than the signaling rate. Time correlated Rayleigh fading and additive white Gaussian noise constitute the channel impairments. The maximum Doppler frequency is 0.93 Hz at 1 km/h, 9.3 Hz at 10 km/h, and 93 Hz at 100 km/h and is relative to a carrier frequency of 1 GHz. When multiple transmit antennas are used, it is assumed that independent fading envelopes apply to each antenna. Also, a differential delay of $\tau_d = \frac{1}{16}T_s$ separates the transmissions from different antennas for systems employing phase sweeping transmit diversity. At a signaling rate of 48.6 kHz, the differential delay corresponds to a path difference of 386 m. A finite non-zero value for $\tau_d$ accounts for the fact that propagation paths to the receiver may differ among the transmit antennas. One coded bit per signaling interval is transmitted using a rotated 4-QAM constellation with $\theta = 18.4°$ for $L = 2$ and a rotated 3-D hypercube constellation with $\theta = 28°$ for $L = 3$. The reader is referred to Chapter 3 for the architectural basis of the following schemes.

System A is patterned after the Mobitex standard. The signaling rate is 8 kHz. A frame consists of 56 header bits followed by 240 data bits. A shortened (12,8) Hamming block code is used to encode 160 information bits. The generator matrix is given by

$$\mathbf{G} = \begin{bmatrix} 1 & 1 & 1 & 0 & 1 & 1 & 0 & 0 \\ 1 & 1 & 0 & 1 & 0 & 0 & 1 & 1 \\ 1 & 0 & 1 & 1 & 1 & 0 & 1 & 0 \\ 0 & 1 & 1 & 1 & 0 & 1 & 0 & 1 \end{bmatrix} \tag{4.1}$$

The sequence of encoded bits is re-ordered at the *bit* level using a 20x12 block interleaver. The interleaved bits are grouped in pairs before being passed onto the symbol mapper. The coordinates of the selected points pass through a convolutional interleaver with an interleaving depth of 121. A frequency offset of 33 Hz is maintained between the two transmit antennas. A phase sweeping cycle occurs once for every 240 bits. Differential detection is employed by the receiver which makes hard decisions as to which constellation points were transmitted. After de-interleaving the bits, the block coded data is decoded with syndrome decoding.

System B employs a convolutional code rather than a block code. The signaling rate is set at 10.5 kHz in order to keep the information bit rate the same as in System A. A frame consists of 56 header bits followed by 320 data bits. A rate $\frac{1}{2}$ maximum

| System | Rate | Constraint length | Generators in octal | $d_{free}$ |
|---|---|---|---|---|
| B, C | 1/2 | 6 | 53 75 | 8 |
| D | 2/3 | 4 | 236 155 337 | 7 |

Table 4.1: Parameters of Convolutional Code for System B, C, and D

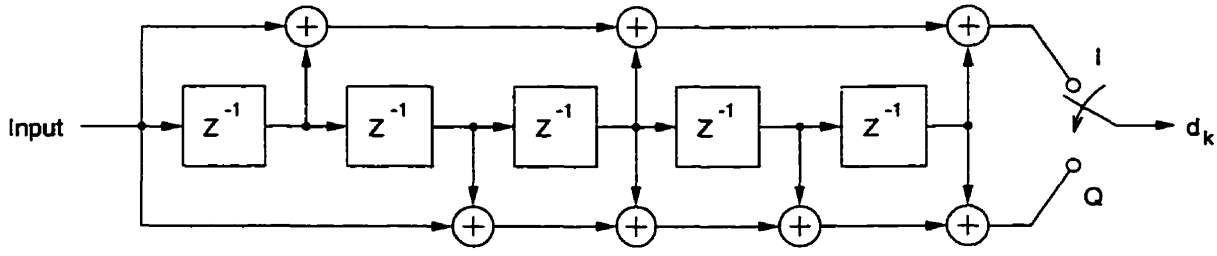


Figure 4.1: Encoder for Rate $\frac{1}{2}$ Maximum Free Distance Convolutional Code

free distance convolutional code with a constraint length of 6 is used to encode 155 information bits. The coefficients of the generator polynomials are listed in Table 4.1. There are 5 zero tail bits appended to the information bit stream at the end of each frame to reset the convolutional encoder to a zero state. The sequence of encoded bits is re-ordered at the *symbol* level using a 20x8 block interleaver. Each symbol consists of 2 coded bits which map to a point in a 2-D signal constellation. The coordinates of the selected points pass through a convolutional interleaver with an interleaving depth of 161. A frequency offset of 33 Hz is maintained between the two transmit antennas. A phase sweep cycle occurs once for every 320 bits. Symbol de-interleaving is performed on the soft decision output of the correlator. Soft decision decoding of the convolutional code is accomplished via the Viterbi algorithm. The path memory of the Viterbi decoder is 160.

System C is patterned after the IS-54 standard. It has a higher signaling rate of 48.6 kHz. A frame consists of 64 header bits followed by 260 data bits. A rate $\frac{1}{2}$ maximum free distance convolutional code with a constraint length of 6 is used to encode 125 information bits. There are 5 zero tail bits. The sequence of encoded bits is re-ordered at the *symbol* level using a 26x5 block interleaver where a symbol consists of 2 coded bits. The convolutional interleaver has an interleaving depth of

972. A frequency offset of 25 Hz is maintained between the two transmit antennas. A phase sweep cycle occurs once for every 1944 bits. That is, the interleaving spans 3 frames which is equal to 20 ms in duration. Symbol de-interleaving is performed on the soft decision output of the correlator. Soft decision decoding of the convolutional code is accomplished via the Viterbi algorithm [31]. The path memory of the Viterbi decoder is 130.

System D has a signaling rate of 37.1 kHz which is chosen so as to retain the same information bit rate as System C. A frame consists of 63 header bits followed by 234 data bits. A rate $\frac{2}{3}$ maximum free distance convolutional code with a constraint length of 4 is used to encode 150 information bits. The coefficients of the generator polynomials are listed in Table 4.1. There are 6 zero tail bits. The sequence of encoded bits is re-ordered at the *symbol* level using a 26x3 block interleaver. Each symbol consists of 3 coded bits which map to a point in a 3-D signal constellation. The convolutional interleaver has an interleaving depth of 891. A frequency offset of 14 Hz is maintained between the 3 transmit antennas. A phase sweep cycle occurs once for every 2673 bits. The interleaving spans 3 frames which is equal to 24 ms in duration. Symbol de-interleaving is performed on the soft decision output of the correlator. Soft decision decoding of the convolutional code is accomplished via the Viterbi algorithm. The path memory of the Viterbi decoder is 78.

A sample schematic view of the simulation program used to model the transmitter and receiver pair and to simulate the transmission of data at the physical layer is shown in Figure 4.2. The bit error rate for each system is determined as follows. The transmission of 1000 frames is simulated at a given level of SNR and mobile velocity. The SNR is incremented by 3 dB and another 1000 frames is simulated. This process is repeated for all SNR values of interest. The bit error rates are averaged over the 1000 frames, the value of which constitute the result of one simulation run. Furthermore, the results of 20 independent runs are averaged in order to span as many different channel conditions as possible. Though header bits and tail bits are inserted in the data stream, they are not included in the calculation of coded BER. In the following figures, the SNR scale denotes the total transmitted energy per information bit. The parameters $N$, $L$, and $\theta$ denote the number of transmit antennas, the dimension of the signal constellation, and the constellation rotation angle respectively.

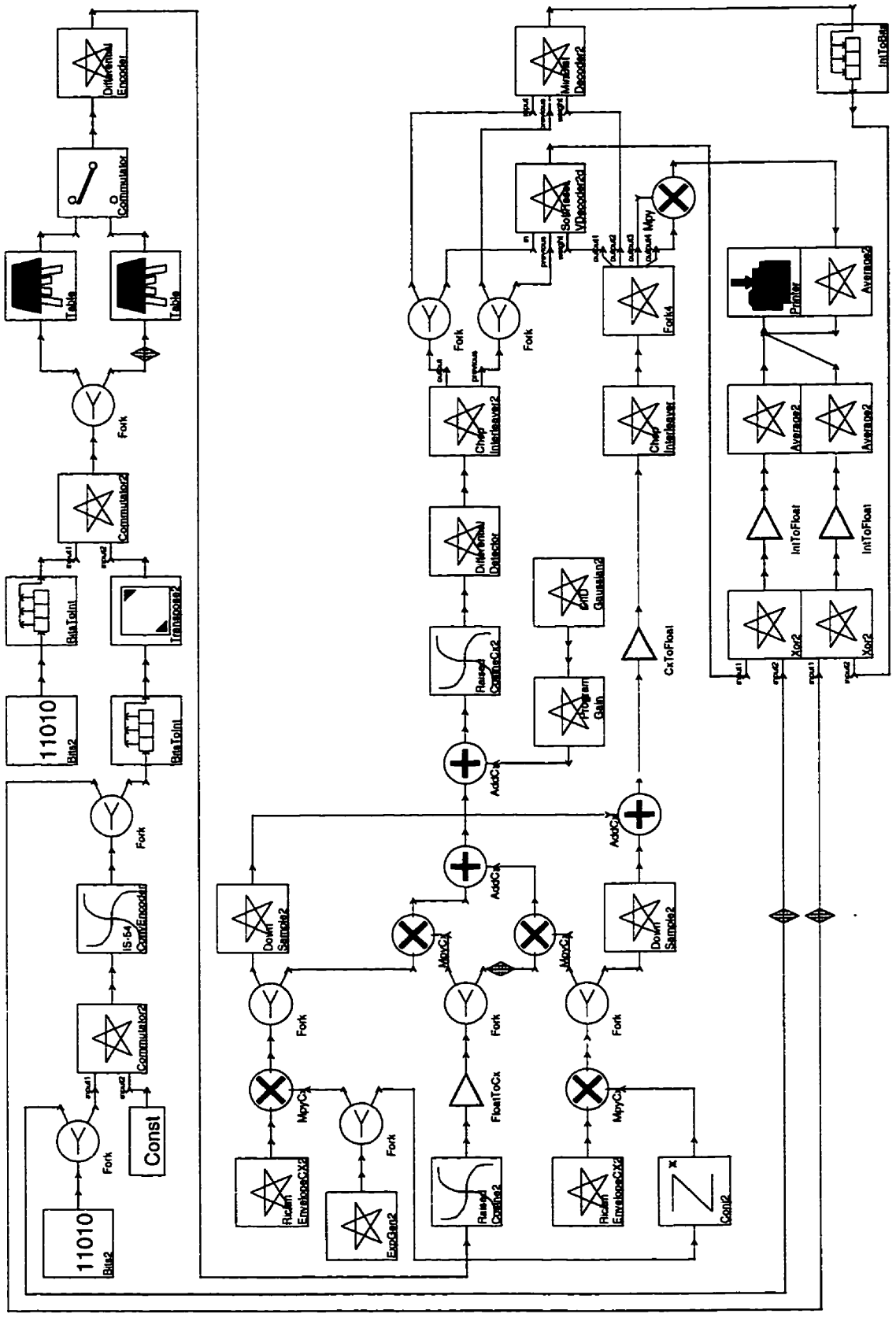


Figure 4.2: Schematic View of Ptolemy Simulation Program for System B and System C

## 4.3 Simulation Results

### 4.3.1 Coding Scheme

The coded bit error rates for System A, B, and C are shown in Figures 4.3-4.5 respectively. The simulations are carried out at a mobile speed of 1, 10, and 100 km/h. The baseline BER corresponds to the performance of single branch DPSK signaling over a Rayleigh fading channel.

At a speed of 1 km/h, the channel changes little over the time spanned by the interleaver memory. The coded BER varies approximately as $\frac{1}{\text{SNR}^2}$ for all the systems. The slope is indicative of the diversity order which is equal to 2, the number of antennas. Recall that the fading amplitudes affecting the two PAM signals which comprise the 4-QAM constellation are uncorrelated by design. Forward error control coding mitigates the simulcast interference but can not realize additional coding gain from time diversity because the underlying $a_i$ in Figure 3.4 exhibit slow fading.

At a speed of 10 km/h, the maximum Doppler frequency is increased 10 times over the previous example. This translates into a tenfold compression of the time axis for the autocorrelation of the slow fading envelope. Interleaving provides some improvement in time diversity for System A and even more for System B. Note that the there is still significant correlation between the fading amplitudes of adjacent coded symbols. There is little increase in coding gain for System C at this speed because the higher bit rate renders the normalized fading rate effectively lower than that of System A and B.

At a speed of 100 km/h, there is sufficient rapid de-correlation of the fading process to allow effective use of finite block interleaving. This results in sizable coding gain at a BER lower than $10^{-2}$ for System B and C which employ a convolutional code combined with soft decision decoding. However, System A (which utilizes a simple Hamming block code with hard decision syndrome decoding) does not perform well at 100 km/h. An error floor arises in the BER of System A at a high mobile velocity due to the complication of phase modulation that rapid fading brings about.

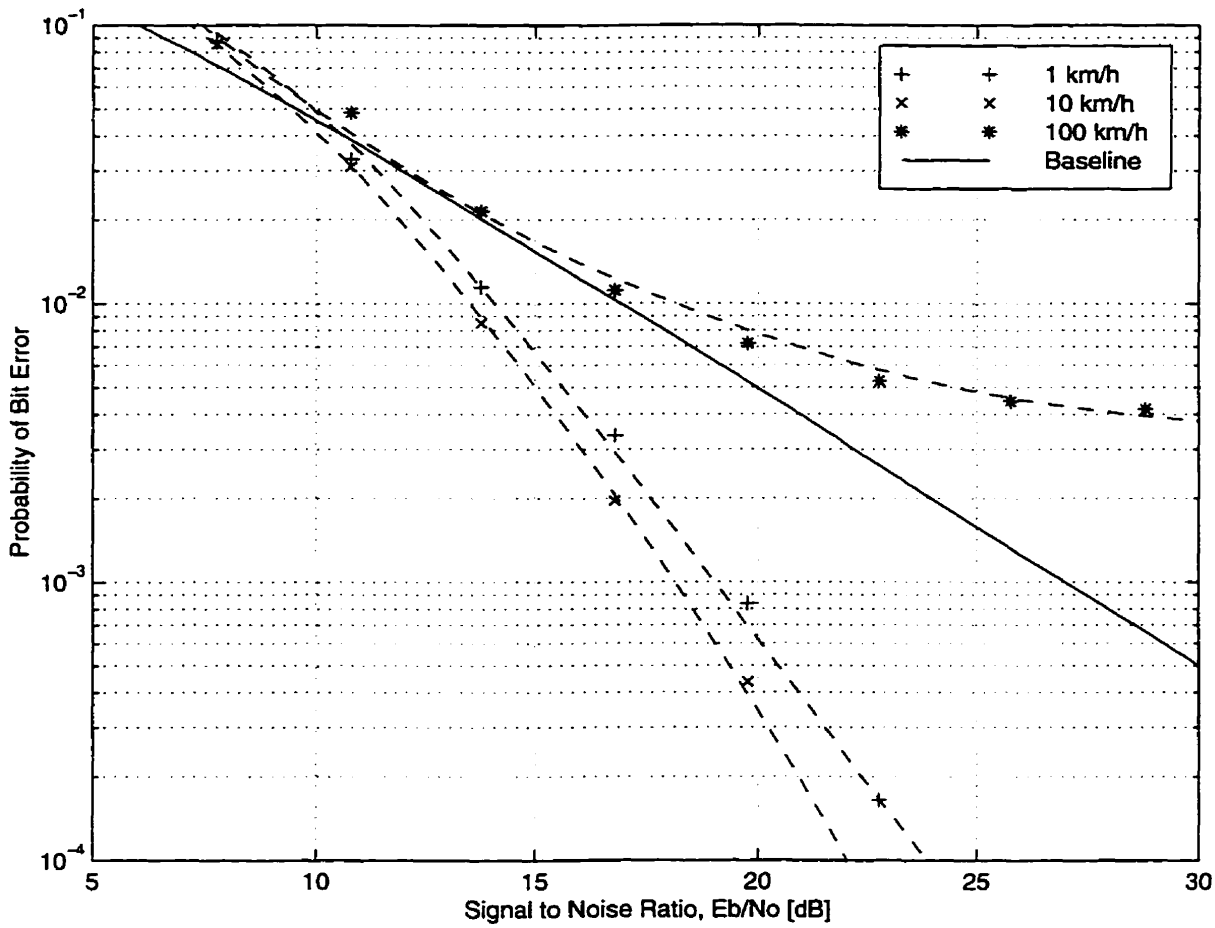


Figure 4.3: Bit Error Rate of System A, $N = 2$, $L = 2$, $\theta = 18.4°$

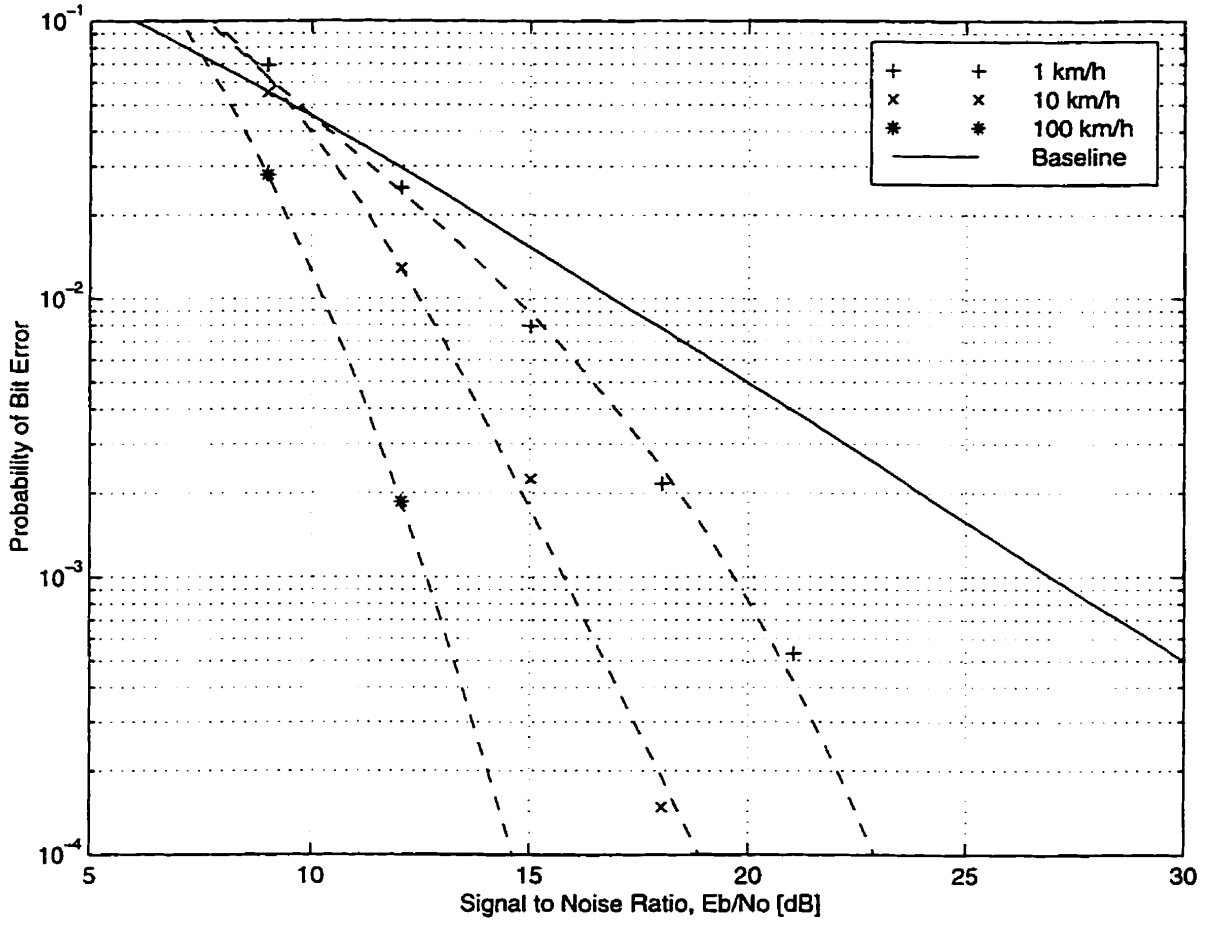


Figure 4.4: Bit Error Rate of System B, $N = 2$, $L = 2$, $\theta = 18.4°$

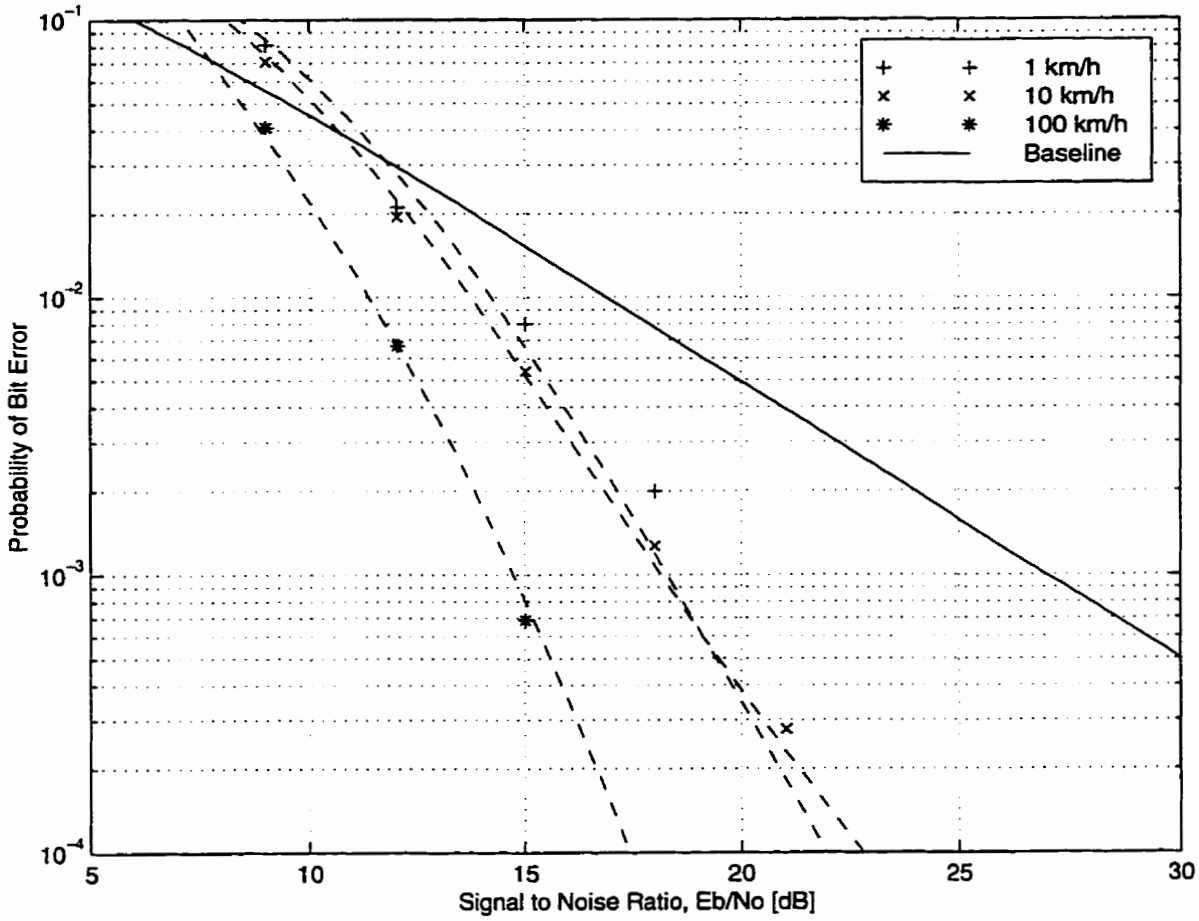


Figure 4.5: Bit Error Rate of System C, $N = 2$, $L = 2$, $\theta = 18.4°$

### 4.3.2 Single versus Dual Independent Branch Diversity

If only a single transmit antenna is used then the system degenerates into the simpler case proposed in [26] in which $L$ independent fading channels are created through interleaving in time. The key difference to note is that here a finite interleaver depth is assumed and the effect of channel coding is being considered. A configuration similar to System C is considered in the following where applicable.

Figure 4.6 shows a plot of the coded bit error rate for the case of a single transmit antenna (ie. $N = 1$). At 1 km/h, it is evident that the uncoded bit rate decreases roughly as $\frac{1}{\text{SNR}}$ compared to better than $\frac{1}{\text{SNR}^2}$ when ideal interleaving applies. Note that the coded bit error rate is actually worse than the baseline BER when the SNR is normalized by the number of information bits conveyed per symbol. The poor performance of both the block code and the convolutional code under slow fading conditions is attributed to a relatively large average duration of fade which spans longer than the available interleaver memory. The receiver is unable to randomize the effects of burst errors which degrades severely the coding gain provided by forward error correction codes. At 10 km/h, the coded BER improves dramatically by 7 dB at $P_e = 10^{-3}$. At 100 km/h, there is a further 6 dB in coding gain. Consequently, the performance of a single transmit antenna system (which relies strictly on time diversity for coding gain) is highly dependent on mobile velocity.

Rather than invoking phase sweeping, if the transmissions from the two antennas of System C are somehow orthogonal (eg. via TDM or FDM) then the two coordinates that comprise a symbol can be transmitted via separate independent fading channels. Figure 4.7 shows a plot of the coded bit error rate for the case of a dual independent branch diversity. Since the two coordinates that comprise a symbol are transmitted via two separate channels that undergo independent fading conditions, the diversity order of the system is at least equal to 2 regardless of the mobile velocity. This is illustrated in the comparable performance of the system at 1 km/h and at 10 km/h. At 100 km/h, there is additional coding gain from the use of block interleaving. Note how the BER curves here are similar to those of Figure 4.5. For the diversity system being considered, it is not necessary to make the two separate transmissions orthogonal in order to realize dual diversity branches.

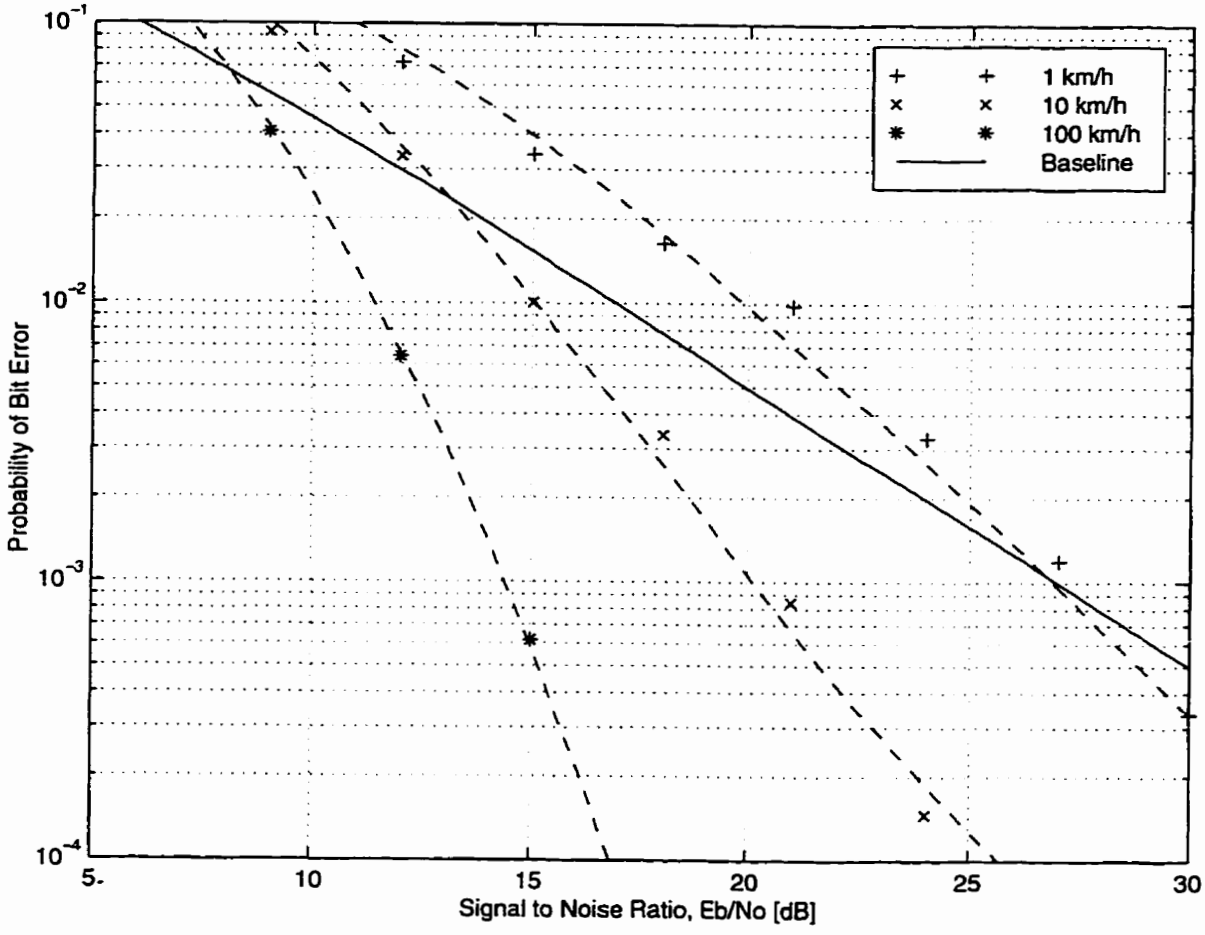


Figure 4.6: BER of Fading Resistant Transmission using Time Diversity, $N = 1$, $L = 2$, $\theta = 18.4°$

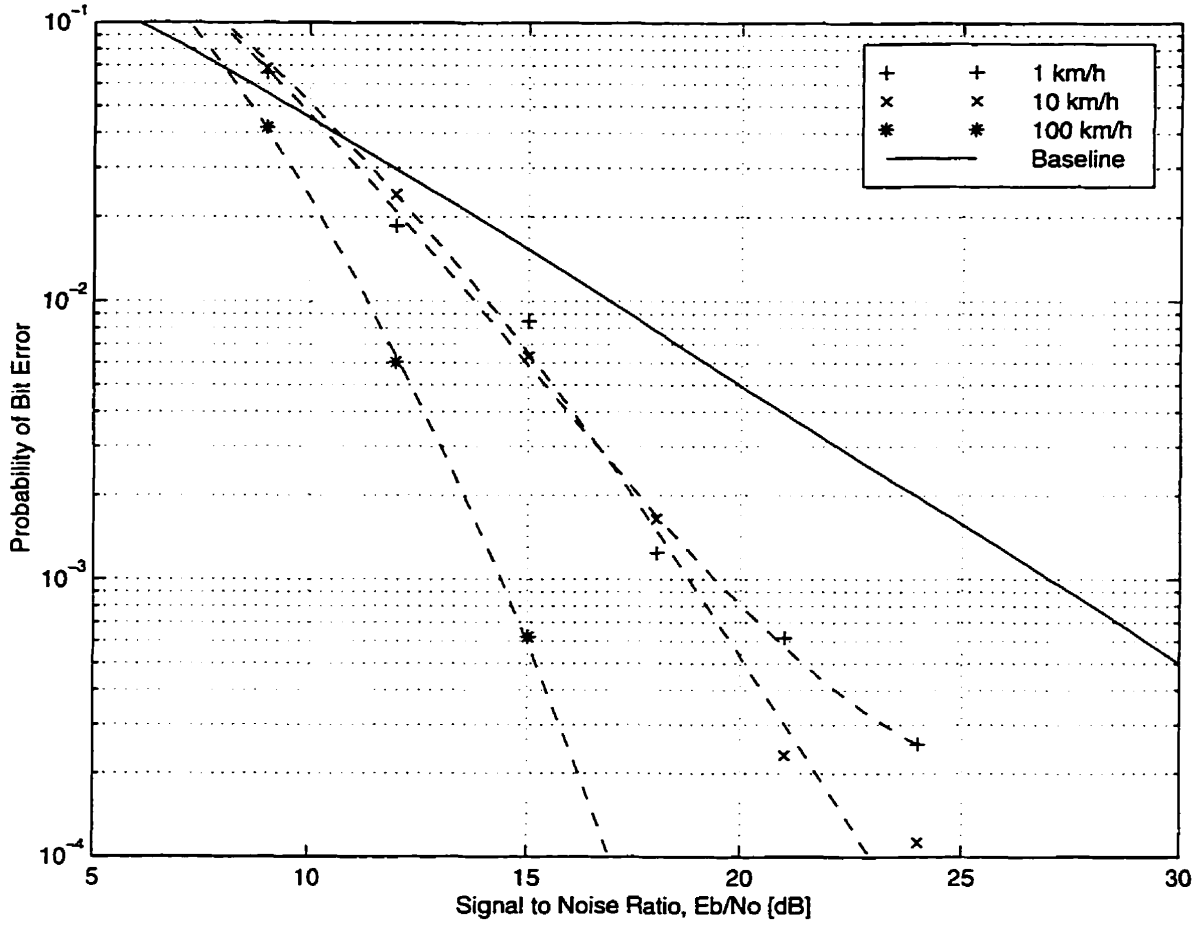


Figure 4.7: BER of Fading Resistant Transmission using 2 Independent Diversity Branches, $N = 2$, $L = 2$, $\theta = 18.4°$

### 4.3.3 2-D Constellations

Figure 4.8 shows a graph of the coded BER for System C as a function of the rotation angle of the 2-D constellation about the $x$-axis. A $\theta$ value of 31.7° and 18.4° correspond to the optimum constellations for a coherent and differentially coherent receiver in [26] respectively whereas $\theta = 26.6°$ is equivalent to the 2-D Kerpez constellation in [25]. The performance comparison is done at a mobile velocity of 10 km/h. The computer simulations carried out reveal that the $\theta = 18.4°$ constellation consistently outperforms that of $\theta = 26.6°$ and $\theta = 31.7°$ at both low and high velocity, for single and dual diversity branches. More over, the $\theta = 18.4°$ constellation continues to exhibit superior performance when applied to phase sweeping transmit diversity.

### 4.3.4 Differential Delay

The effect of increasing differential delay $\tau_d$ for System C is investigated here. It is assumed that the matched filter output of the receiver is synchronized to the sample time of the first incoming ray and that the second ray is delayed relative to the first by a fixed amount. The minimum resolution of the simulation is $\frac{1}{16}T_s$ where $T_s$ is the signaling period. Figure 4.9 shows that a differential delay of $\tau_d = \frac{1}{16}T_s$ has a negligible effect on of the coded BER relative to the ideal case of $\tau_d = 0$. For $\tau_d = \frac{1}{8}T_s$ and beyond, the probability of error is noticeably larger due to the presence of intersymbol interference. Note that a differential delay of $\tau_d = \frac{5}{16}T_s$ results in a markedly worse performance than $\tau_d = \frac{1}{4}T_s$. The sudden degradation in bit error rate is indicative of the sensitivity of PAM signals to ISI. Without the use of equalization, the superposition of the delayed signal with the first can cause the output of the correlator to lie in an incorrect decision region. Therefore, it is important to arrange simulcast transmitters in a manner such that the differential delay is kept less than or equal to $\frac{1}{4}T_s$.

### 4.3.5 3-D Constellations

The fourth channel coding scheme, denoted as System D, is an extension of System C to increase the dimensionality from two to three. The motivation is to evaluate the merits of employing three transmit antennas over two.

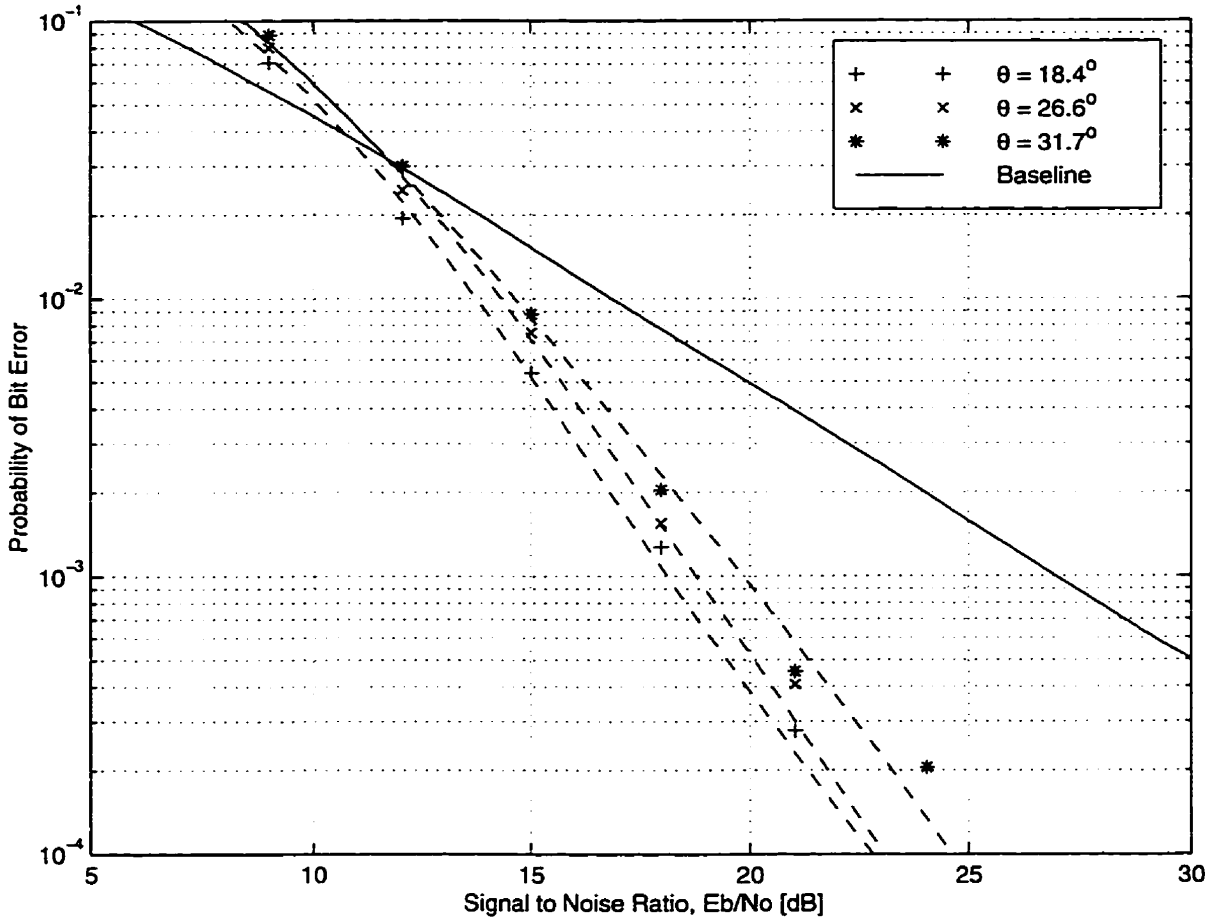


Figure 4.8: BER of Phase Sweeping Transmit Diversity for Various 2-D Constellations, $N = 2$, $L = 2$, $v = 10$ km/h

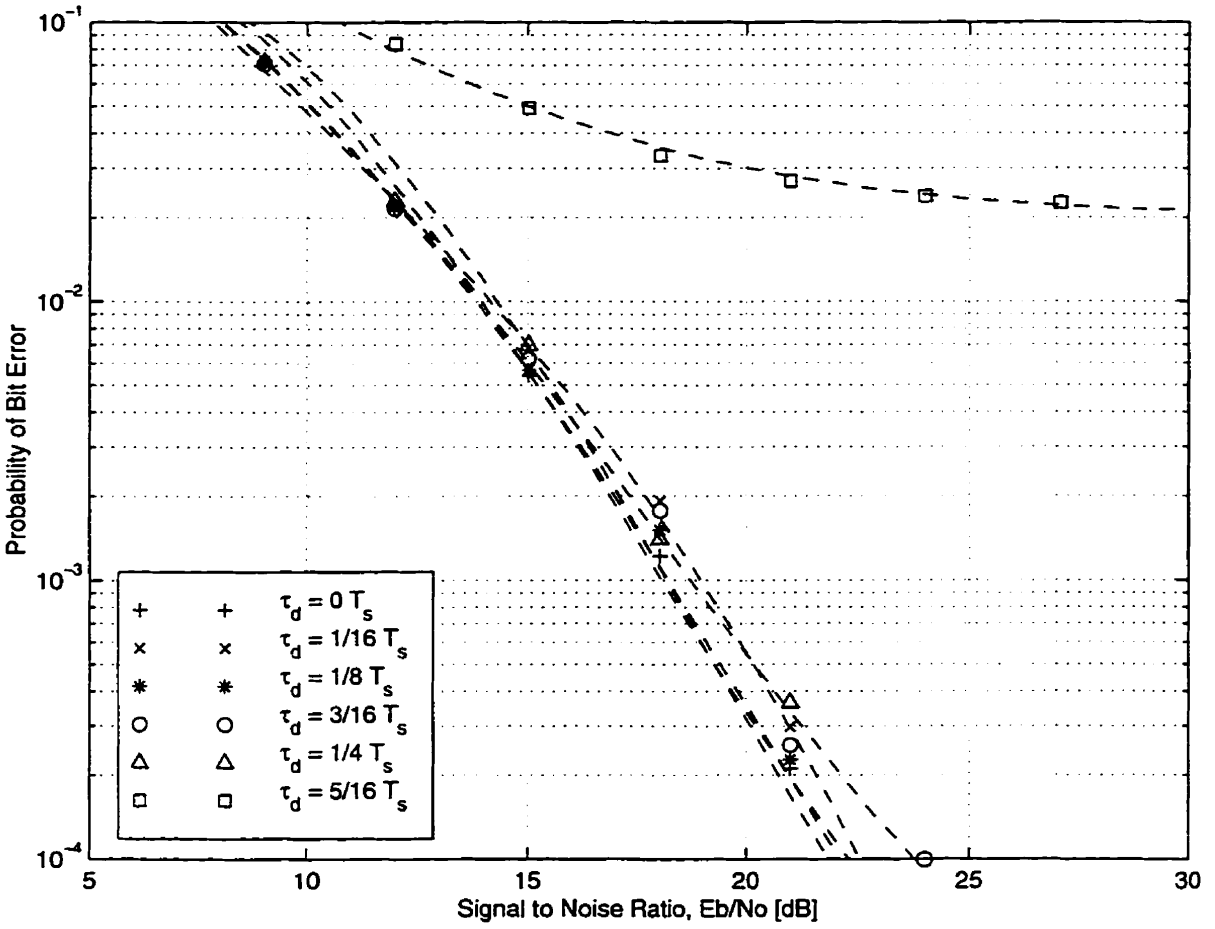


Figure 4.9: BER of Phase Sweeping Transmit Diversity versus Differential Delay, $N = 2$, $L = 2$, $\theta = 18.4°$, $v = 10$ km/h

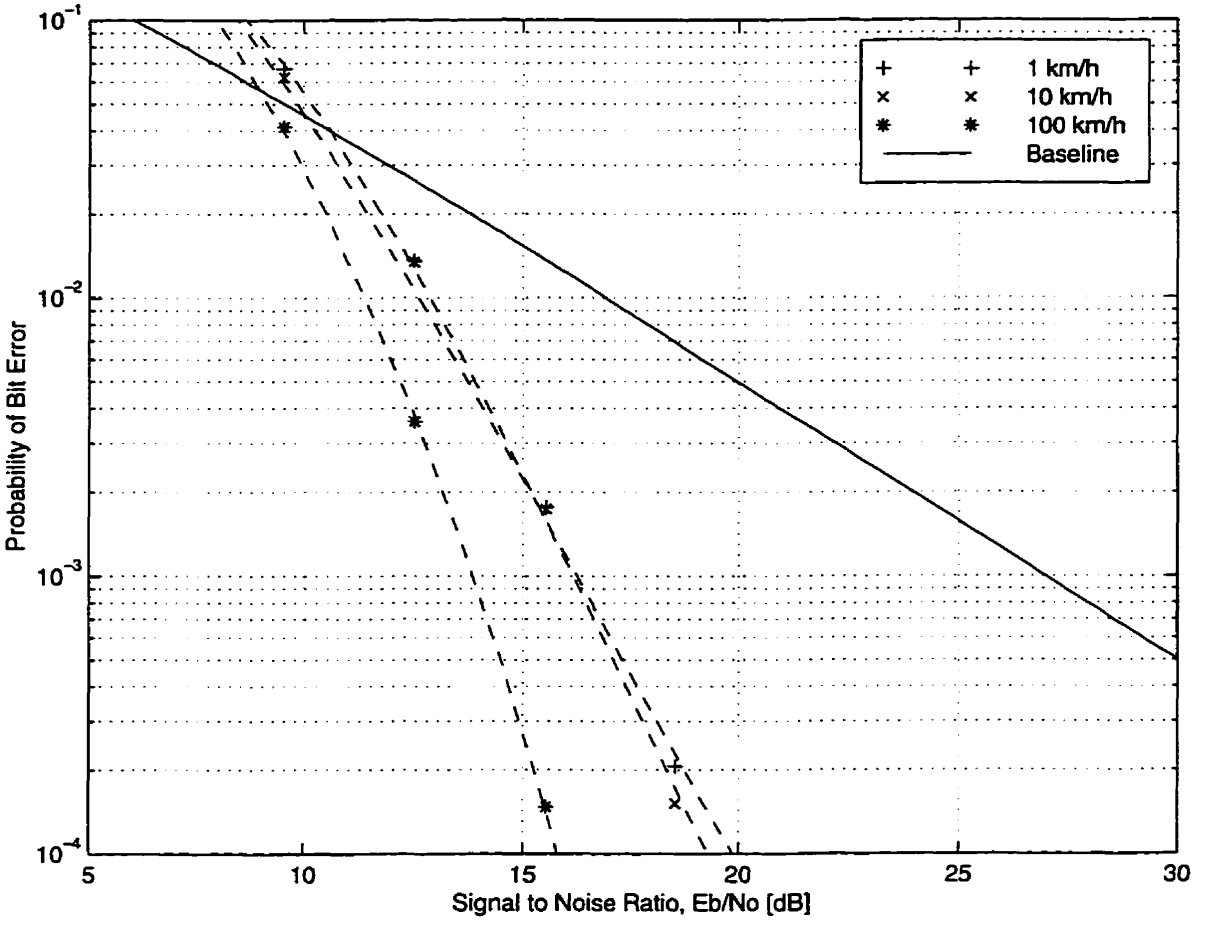


Figure 4.10: BER of Phase Sweeping Transmit Diversity with 3-D Fading Resistant Constellation (System D), $N = 3$, $L = 3$, $\theta = 28°$

The coded BER of phase sweeping transmit diversity with three antennas is shown in Figure 4.10. At 1 km/h, the probability of error varies slightly less than the expected $\frac{1}{\text{SNR}^3}$. The more gradual slope is attributed to the fact that a larger value for the differential delay (ie. $\tau_d = \frac{1}{8}T_s$) is assumed in the simulations when three transmit antennas prevail. This results in increased ISI relative to the other systems. Nevertheless, System D manages to realize a bit error rate of $10^{-4}$ at an SNR of 20 dB over a slow fading channel. The performance is comparable at a mobile velocity of 10 km/h. At 100 km/h, the coded BER decreases as $\frac{1}{\text{SNR}^4}$ yielding effectively a diversity order of 4.

The performance that arises from the use of only a single transmit antenna is

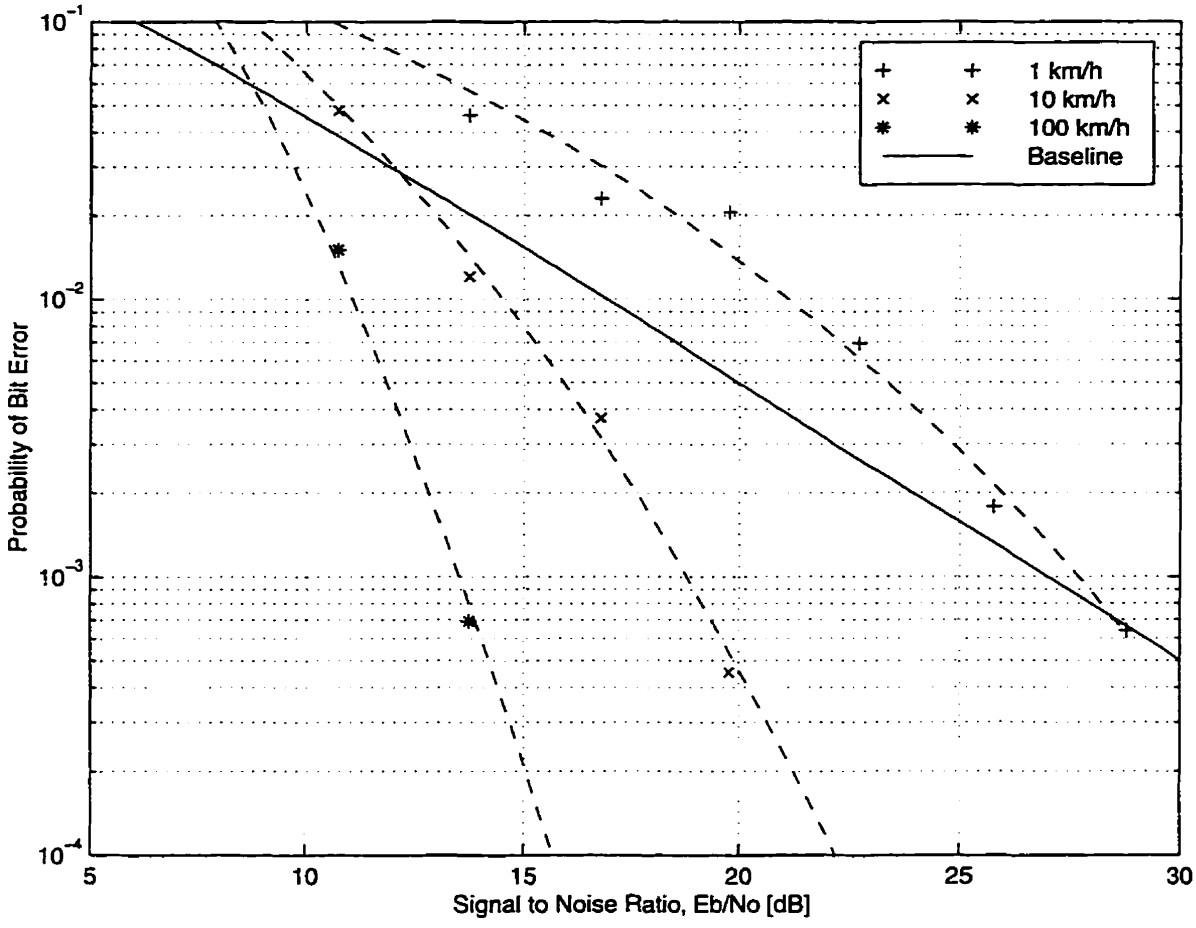


Figure 4.11: BER of Fading Resistant Transmission using Time Diversity, $N = 1$, $L = 3$, $\theta = 28°$

plotted in Figure 4.11. At 1 km/h, the coded BER is noticeably worst than the simpler baseline scheme. At 10 km/h, the coded BER improves dramatically by 8.5 dB at $P_e = 10^{-3}$. At 100 km/h, there is a further 5 dB in coding gain. It is noted that the performance at high mobile velocity is the same as in System D. The application of phase sweeping transmit diversity does not result in a degradation in the probability of error for this system.

Figure 4.12 shows the coded BER for a system with three independent diversity branches. Here, the superior performance under slow fading conditions emphasizes the importance of transmit diversity.

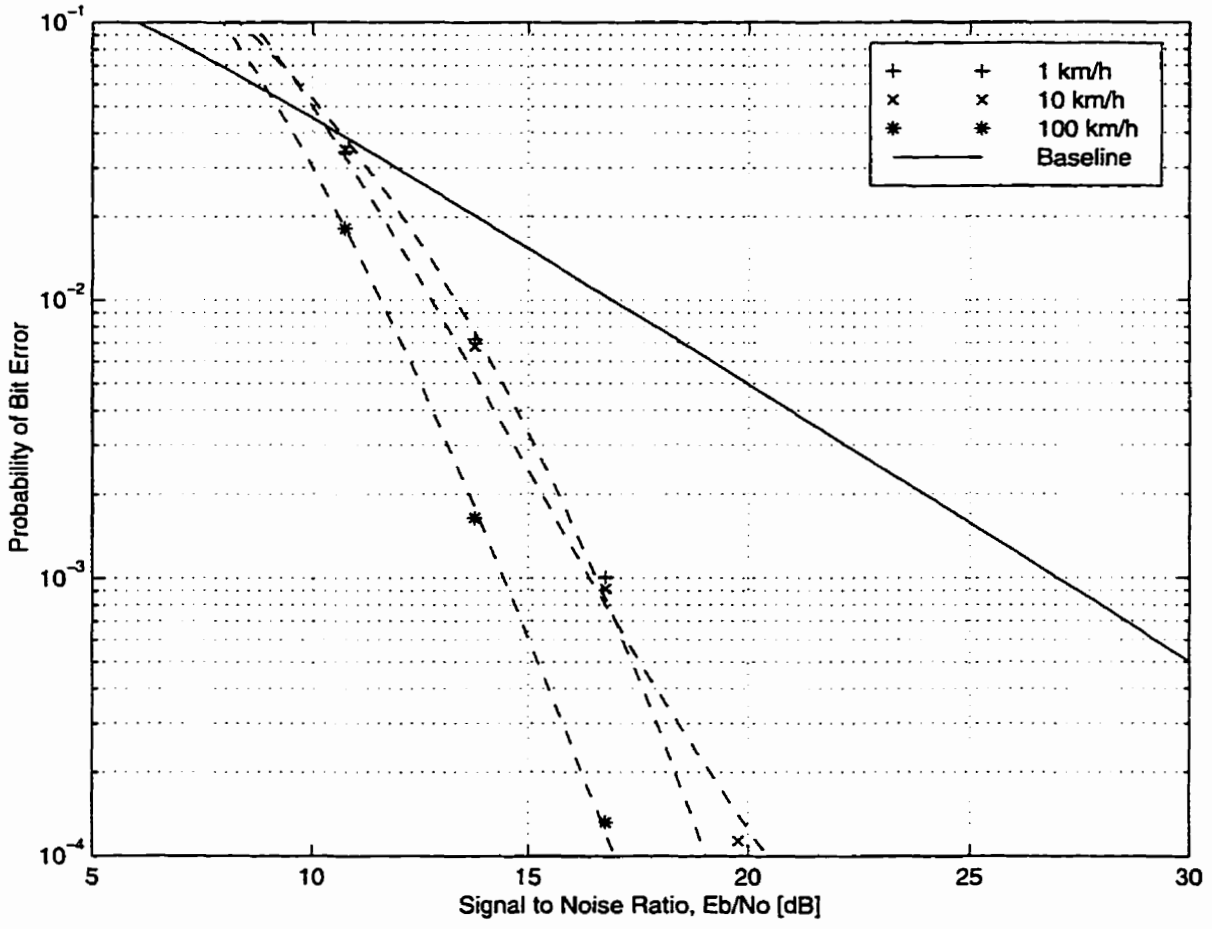


Figure 4.12: BER of Fading Resistant Transmission using 3 Independent Diversity Branches, $N = 3$, $L = 3$, $\theta = 28°$

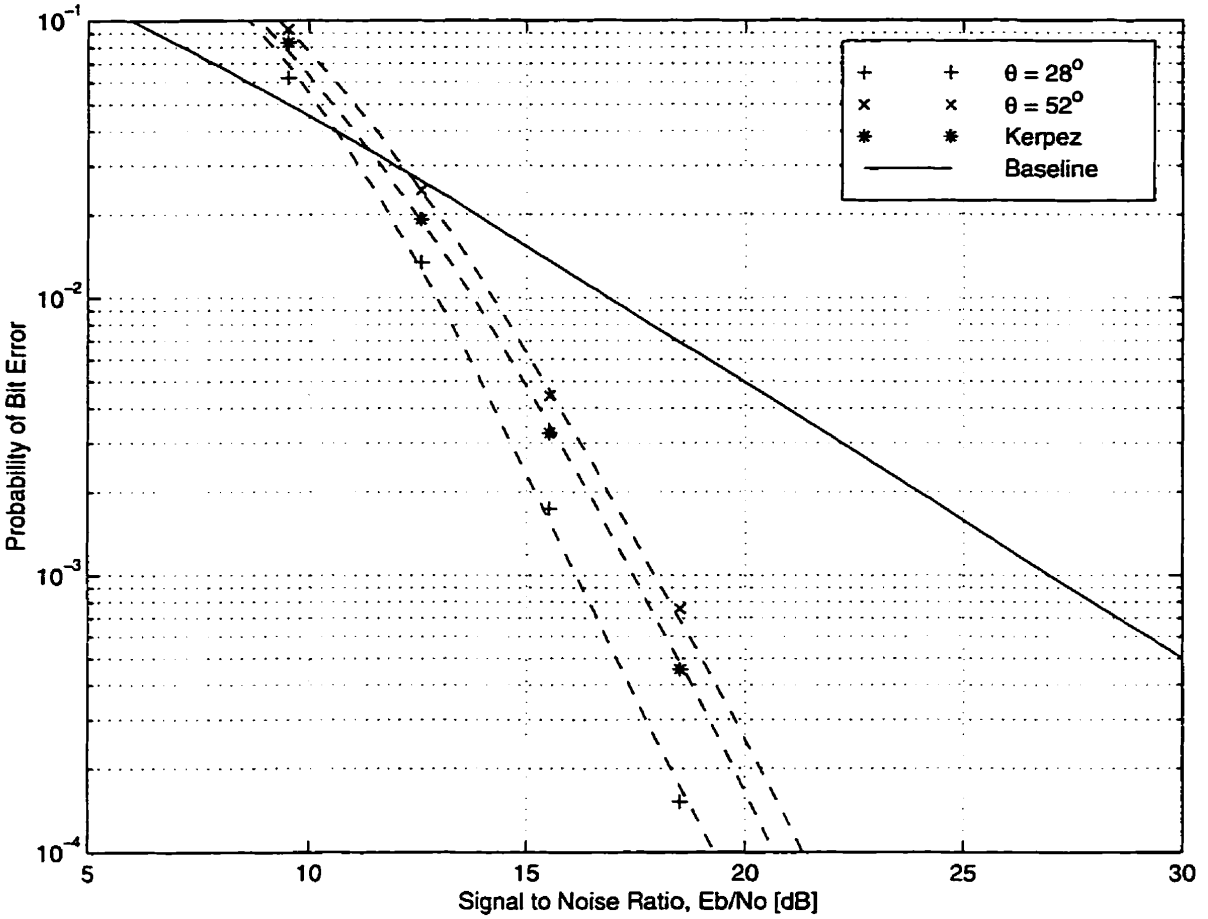


Figure 4.13: BER of Phase Sweeping Transmit Diversity for Various 3-D Constellations, $N = 3$, $L = 3$, $v = 10$ km/h

Figure 4.13 shows a graph of the coded BER for System D as a function of the rotation angle of the 3-D hypercube constellation about the vector (1,1,1). A rotation angle of 52° and 28° correspond to the optimum constellations for a coherent and differentially coherent receiver in [26]. The performance comparison is done at a mobile velocity of 10 km/h. The computer simulations carried out reveal that the $\theta = 28°$ constellation consistently outperforms the others at both low and high velocity, for single and triple diversity branches, with and without phase sweeping transmit diversity.

# Chapter 5

# Conclusions

## 5.1 Summary of Results

The mitigation of slow fading in the forward link of a mobile communications system is realized by employing multiple transmit antennas at the base station. Transmit diversity techniques are desirable because they are able to effect change on channel conditions, the design of a diversity receiver can be kept simple, and many users benefit from their application. A pseudo-stationary model to slow fading is adopted in which the coherence time of the fading process is much larger than the time spanned by the interleaver memory at the receiver.

In the study of simultaneous transmissions from multiple antennas, it is found that the case of three orthogonal carriers performs asymptotically better than co-phased transmission from two antennas. The autocorrelation of the fading envelope in the case of two and three antennas transmitting simultaneously is derived. By introducing a fixed frequency offset between the various transmissions, it is shown that the autocorrelation function could be forced to zero at a given time delay. Thus, it is possible to engineer uncorrelated fading amplitudes for two adjacent bits or symbols after de-interleaving has been applied.

Given a pseudo-stationary fading channel, another property of matching the frequency offset to the interleaving depth is that the average energy of an $L$-dimensional symbol transmitted as a sequence of $L$ 1-dimensional PAM signals is constant over one phase swept interval. The fact that the artificially induced fading amplitudes along

the $L$ signal dimensions are constrained by a constant energy relationship motivates the use of fading resistant constellations in the modulation.

A novel phase sweeping transmit diversity scheme is proposed for the forward link. By introducing artificial fast fading via multiple transmit antennas, there will be variations in the received signal envelope even when the mobile station remains stationary. A differentially coherent receiver is used to resolve the phase ambiguity that arises due to simulcast interference.

Minimizing an upper bound on the probability of symbol error for phase sweeping transmit diversity leads to an optimum constellation rotation angle for $L = 2$. It is found that the error curve of the simultaneous transmission scheme becomes steeper as the Rician fading channel approaches the characteristics of a Gaussian channel. Also, a block interleaver with an interleaving depth matched to the frequency offset parameter yields better performance than one which implements random interleaving.

The deployment of multiple transmit antennas over a wide area is suitable for overcoming shadow fading. A Monte Carlo analysis of a simulcast network of transmitters is performed to determine the probability distribution function of the average relative received power at a mobile terminal. In both hexagonal and square arrangement of transmitters, the likelihood of receiving two approximately equal strength rays is much more probable than receiving three approximately equal strength rays. Consequently, a diversity system with four or more antennas is not considered.

Time domain simulations of a phase sweeping transmit diversity system are carried out in order to determine the effects of time correlated Rayleigh fading and finite interleaver memory on a given coding and modulation scheme. A single transmit antenna system which relies strictly on time diversity to obtain coding gain results in the coded BER performance being highly dependent on the mobile velocity. Only the convolutional coded schemes with soft decision decoding are able to mitigate simulcast interference when it is complicated with high mobile velocity. The maximum tolerable differential delay between two simulcast transmissions before severe ISI occurs is $\tau_{\max} = \frac{1}{4}T_s$ for an $L = 2$ system. As a result of the phase sweeping transmit diversity technique, the coded BER curve for an $L = 2$ and $L = 3$ system varies as $\frac{1}{\mathrm{SNR}^2}$ and $\frac{1}{\mathrm{SNR}^3}$ respectively under pseudo-stationary Rayleigh fading channel conditions.

## 5.2 Future Research

It was shown that the performance of phase sweeping transmit diversity with dual antennas is poor when the differential delay separating the two rays is greater than a quarter of the signaling period. Channel equalization may help to mitigate the intersymbol interference that arises in an environment with a relatively large multipath delay spread. An equalizer can be used to realize diversity combining when the differential delay is sufficiently large. Given that condition, the simulcast channel resembles a two ray multipath fading channel.

A key assumption of the proposed transmit diversity scheme is that the autocorrelation function of the fading envelope is the same for the different transmit antennas but that their fading processes are uncorrelated. Field measurements of actual sites may be required to determine the degree to which the premise holds true. It should be emphasized that communications in the forward link is still possible even when the assumption is not valid.

The issue of hardware complexity has been overlooked in the research and warrants consideration if the system is to be implemented. In particular, the specification that transmitters maintain a fixed frequency offset between them may be a stringent requirement given technological constraints. If the multiple transmitters are common to one base station then it might be possible to derive the $L$ carriers from a common reference.

The choice of error correction coding employed in the simulations is based on existing standards for mobile communications which is not necessarily optimum for the phase sweeping transmit diversity proposed in this thesis. An investigation into other combinations of coding and interleaving may yield further improvement in diversity gain. In particular, a larger interleaver may better randomize the sequence of partial symbol erasures caused by phase sweeping transmit diversity.

The joint application of fading resistant constellations with coded modulation techniques for fading channels is a possibility that merits further study. In designing good codes for fading channels, it is typically the Hamming distance rather than Euclidean distance between codewords which is maximized. This reduces their susceptibility to erasures in symbol detection introduced by deep fades. Since fading

resistant constellations are already robust against complete symbol erasures, it is postulated that the optimization criterion for code design here might be different from the conventional case.

# Appendix A

# Constellations

## A.1 Baseline Constellations

The 4-QAM constellation and the 3-D hypercube constellation constitute the baseline constellations for $L = 2$ and $L = 3$ respectively.

$$C_{B2} = \begin{bmatrix} 1 & 1 \\ 1 & -1 \\ -1 & 1 \\ -1 & -1 \end{bmatrix} \tag{A.1}$$

$$C_{B3} = \begin{bmatrix} 1 & 1 & 1 \\ 1 & 1 & -1 \\ 1 & -1 & 1 \\ 1 & -1 & -1 \\ -1 & 1 & 1 \\ -1 & 1 & -1 \\ -1 & -1 & 1 \\ -1 & -1 & -1 \end{bmatrix} \tag{A.2}$$

## A.2 Optimally Rotated Constellations

The optimum rotated constellations for $L = 2$ and $L = 3$ for a coherent receiver were determined to be (see [26])

$$C_{R2,31.7^\circ} = \begin{bmatrix} 0.3249 & 1.3764 \\ 1.3764 & -0.3249 \\ 1.3764 & -0.3249 \\ -0.3249 & -1.3764 \end{bmatrix} \tag{A.3}$$

$$C_{R3,24^\circ,36^\circ,66^\circ} = \begin{bmatrix} -0.1778 & -0.4742 & 1.6564 \\ 0.9978 & 1.0039 & 0.9982 \\ 0.4803 & -1.6542 & 0.1817 \\ 1.6559 & -0.1760 & -0.4764 \\ -1.6559 & 0.1760 & 0.4764 \\ -0.4803 & 1.6542 & -0.1817 \\ -0.9978 & -1.0039 & -0.9982 \\ 0.1778 & 0.4742 & -1.6564 \end{bmatrix} \tag{A.4}$$

Similarly, the optimum rotated constellations for $L = 2$ and $L = 3$ for a differentially coherent receiver were found to be

$$C_{R2,18.4^\circ} = \begin{bmatrix} 0.6325 & 1.2649 \\ 1.2649 & -0.6325 \\ -1.2649 & 0.6325 \\ -0.6325 & -1.2649 \end{bmatrix} \tag{A.5}$$

$$C_{R3,76°,18°,14°} = \begin{bmatrix} -1.0017 & 1.0006 & 0.9977 \\ -0.3837 & 1.4607 & -0.8479 \\ 0.8439 & 0.3860 & 1.4625 \\ 1.4619 & 0.8462 & -0.3831 \\ -1.4619 & -0.8462 & 0.3831 \\ -0.8439 & -0.3860 & -1.4625 \\ 0.3837 & -1.4607 & 0.8479 \\ 1.0017 & -1.0006 & -0.9977 \end{bmatrix} \tag{A.6}$$

## A.3 Kerpez Constellations

The 2-D and 3-D Kerpez constellations are listed as follows (see [25]).

$$C_{K2} = \frac{1}{\sqrt{5}} \begin{bmatrix} -3 & -1 \\ -1 & -3 \\ 1 & 3 \\ 3 & 1 \end{bmatrix} \tag{A.7}$$

$$C_{K3} = \frac{1}{\sqrt{21}} \begin{bmatrix} -7 & 1 & 5 \\ -5 & -7 & 1 \\ -3 & 3 & -3 \\ -1 & -5 & -7 \\ 1 & 5 & 7 \\ 3 & -3 & 3 \\ 5 & 7 & -1 \\ 7 & -1 & -5 \end{bmatrix} \tag{A.8}$$

## A.4 Rotatation About Arbitrary Vector

Let $\mathbf{r} = (r_x, r_y, r_z)$ denote the vector about which the baseline 3-D hypercube constellation $C_{B3}$ is rotated. The rotation matrix which performs the desired transformation is given by

$$\mathbf{R} = \mathbf{R}_{xy}^T \mathbf{R}_{xz} \mathbf{R}_z \mathbf{R}_{xz}^T \mathbf{R}_{xy} \tag{A.9}$$

where

$$\theta_{xy} = \text{Tan}^{-1}\left(\frac{r_y}{r_x}\right) \tag{A.10}$$

$$\theta_{xz} = \text{Tan}^{-1}\left(\frac{\sqrt{r_x^2 + r_y^2}}{r_z}\right) \tag{A.11}$$

$$\mathbf{R}_{xy} = \begin{bmatrix} \cos\theta_{xy} & \sin\theta_{xy} & 0 \\ -\sin\theta_{xy} & \cos\theta_{xy} & 0 \\ 0 & 0 & 0 \end{bmatrix} \tag{A.12}$$

$$\mathbf{R}_{xz} = \begin{bmatrix} \cos\theta_{xz} & 0 & \sin\theta_{xz} \\ 0 & 0 & 0 \\ -\sin\theta_{xy} & 0 & \cos\theta_{xy} \end{bmatrix} \tag{A.13}$$

$$\mathbf{R}_z = \begin{bmatrix} \cos\theta & \sin\theta & 0 \\ -\sin\theta & \cos\theta & 0 \\ 0 & 0 & 0 \end{bmatrix} \tag{A.14}$$

The rotated 3-D constellations that result for $\mathbf{r} = (1, 1, 1)$ and $\theta \in \{28°, 52°\}$ are as follows.

$$C_{D3,28°} = \begin{bmatrix} 1.0000 & 1.0000 & 1.0000 \\ 0.3799 & 1.4641 & -0.8439 \\ 1.4641 & -0.8439 & 0.3799 \\ 0.8439 & -0.3799 & -1.4641 \\ -0.8439 & 0.3799 & 1.4641 \\ -1.4641 & 0.8439 & -0.3799 \\ -0.3799 & -1.4641 & 0.8439 \\ -1.0000 & -1.0000 & -1.0000 \end{bmatrix} \tag{A.15}$$

$$C_{D3,52^\circ} = \begin{bmatrix} 1.0000 & 1.0000 & 1.0000 \\ -0.1661 & 1.6537 & -0.4875 \\ 1.6537 & -0.4875 & -0.1661 \\ 0.4875 & 0.1661 & -1.6537 \\ -0.4875 & -0.1661 & 1.6537 \\ -1.6537 & 0.4875 & 0.1661 \\ 0.1661 & -1.6537 & 0.4875 \\ -1.0000 & -1.0000 & -1.0000 \end{bmatrix} \tag{A.16}$$

Note that by choosing $\mathbf{r} = (1, 1, 1)$, the coordinates along each dimension share a common set of discrete values. Although the constellations described by Eq. (A.4) and Eq. (A.6) are essentially equivalent to those of Eq. (A.16) and Eq. (A.15) respectively, the latter expressions are more elegant due to the symmetry of the coordinates.

# References


[1] G. C. Hess, *Land-Mobile Radio System Engineering.* Boston: Artech House, Inc., 1993.

[2] W. C. Jakes, Jr., *Microwave Mobile Communications.* New York: John Wiley & Sons, 1974.

[3] W. C. Y. Lee, *Mobile Communications Design Fundamentals.* New York: Wiley, 1993.

[4] J. H. Winters, "Switched Diversity with Feedback for DPSK Mobile Radio Systems," *IEEE Trans. Vehic. Technol.*, vol. VT-32, pp. 134–150, Feb. 1983.

[5] Y. K. Hahm, G. Y. Jung, Y. S. Kim, and H. K. Park, "TCM with Preswitching Diversity in Slow Rayleigh Fading Forward Link," *Electron. Lett.*, vol. 32, pp. 2153–2154, Dec. 1995.

[6] S. Ogose and T. Hattori, "Spectrum Efficiency for Multitransmitter Simulcasting in Land Mobile Radio," *Electron. Lett.*, vol. 25, no. 9, pp. 612–613, 1989.

[7] J. H. Winters, "The Diversity Gain of Transmit Diversity in Wireless Systems with Rayleigh Fading," in *Proc. IEEE International Conf. on Commun.*, pp. 1121–1125, 1994.

[8] P. E. Mogensen, "GSM Base-Station Antenna Diversity Using Soft Decision Combining on Up-link and Delayed-Signal Transmission on Down-link," in *Proc. 43rd IEEE Vehic. Technol. Conf.*, pp. 611–616, 1993.

[9] C. S. Bontu, D. D. Falconer, and L. Strawczynski, "Delayed Diversity Transmission for Indoor Wireless Applications," in *Proc. PIMRC'94*, pp. 75–79, 1994.

[10] N. Seshadri and J. H. Winters, "Two Signaling Schems for Improving the Error Performance of Frequency-Division-Duplex (FDD) Transmission System using Transmitter Antenna Diversity," in *Proc. 43rd IEEE Vehic. Technol. Conf.*, pp. 508–511, 1993.

[11] Y. Kondo and K. Suwa, "Linear Predictive Transmitter Diversity for Microcellular TDMA/TDD Mobile Radio System," in *Proc. 43rd IEEE Vehic. Technol. Conf.*, pp. 602–606, 1993.

[12] R. D. Koilpillai, S. Chennakeshu, and R. L. Toy, "Low Complexity Equalizers for the U.S. Digital Cellular System," in *Proc. 42nd IEEE Vehic. Technol. Conf.*, pp. 744–747, 1992.

[13] O. Nørklit, P. C. F. Eggers, and J. B. Andersen, "Jitter Diversity in Multipath Environments," in *Proc. 45th IEEE Vehic. Technol. Conf.*, pp. 853–857, 1995.

[14] O. Nørklit and J. B. Andersen, "Mobile Radio Environments and Adaptive Arrays," in *Proc. PIMRC'94*, pp. 725–728, 1994.

[15] A. Hiroike, F. Adachi, and N. Nakajima, "Combined effects of Phase Sweeping Transmitter Diversity and Channel Coding," *IEEE Trans. Vehic. Technol.*, vol. 41, pp. 170–176, May 1992.

[16] V. Weerackody, "Characteristics of a Simulated Fast Fading Indoor Radio Channel," in *Proc. 43rd IEEE Vehic. Technol. Conf.*, pp. 231–235, 1993.

[17] R. Petrovic, W. Roehr, and D. Cameron, "Simulcast in Narrowband PCS," in *Proc. 1995 IEEE MTT-S Symposium on Technologies for Wireless Applications*, pp. 65–69, 1995.

[18] P.-E. Östling, "Performance of MMSE Linear Equalizer and Decision Feedbvack Equalizer in Single-Frequency Simulcast Environment," in *Proc. 43rd IEEE Vehic. Technol. Conf.*, pp. 629–632, 1993.

[19] P.-E. Östling, "Handover with Simulcasting," in *Proc. 42nd IEEE Vehic. Technol. Conf.*, pp. 823–826, 1992.

[20] S. Harbin, C. Palmer, and B. K. Rainer, "Measured Propagation Characteristics of Simulcast Signals in an Indoor Microcellular Environment," in *Proc. 42nd IEEE Vehic. Technol. Conf.*, pp. 604–608, 1992.

[21] Y. P. Zhang, Y. Hwang, and J. H. Sheng, "Propagation Characteristics of UHF Simulcast Signals in Tunnel Environments," in *Proc. International Conf. on Commun. Tech.*, pp. 457–460, 1996.

[22] F. Ling, "Matched Filter Bound for Time Discrete Multipath Rayleigh Fading Channel," *IEEE Trans. on Commun.*, vol. 43, pp. 710–713, Feb./Mar./Apr. 1995.

[23] J. E. Mazo, "Exact Matched Filter Bound for Two-Beam Rayleigh Fading," *IEEE Trans. on Commun.*, vol. 39, pp. 1027–1030, July 1991.

[24] V. M. DaSilva and E. S. Sousa, "Fading-resistant transmission from several antennas," in *Proc. PIMRC'95*, pp. 1218–1222, 1995.

[25] K. J. Kerpez, "Constellations for Good Diversity Performance," *IEEE Trans. on Commun.*, vol. 41, pp. 1412–1421, Sept. 1993.

[26] V. M. DaSilva, *Transmitter Diversity and Fading-Resistant Modulation for Wireless Communication Sytems.* PhD Thesis, University of Toronto, 1996.

[27] V. M. DaSilva and E. S. Sousa, "Differentially coherent fading-resistant transmission from several antennas," in *Proc. 46th IEEE Vehic. Technol. Conf.*, 1996.

[28] Ericsson, *Mobitex System Overview.* June 1992.

[29] D. Kim, G. L. Stüber, and N. Hightower, "Performance of Simulcast Systems in Mobile Radio Environments," in *Proc. IEEE Vehic. Technol. Conf.*, pp. 495–499, 1997.

[30] EIA/TIA/IS-54, *Dual Mode Mobile Station Base Station Compatibility Standard.* Oct. 1990.

[31] E. A. Lee and D. G. Messerschmitt, *Digital Communication.* Norwell, MA.: Artech House, Inc., second ed., 1996.

# IMAGE EVALUATION
# TEST TARGET (QA–3)

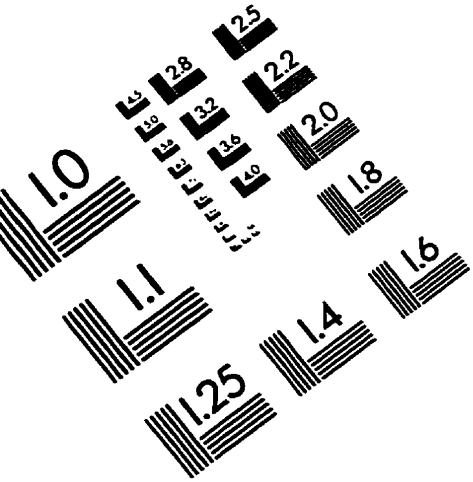


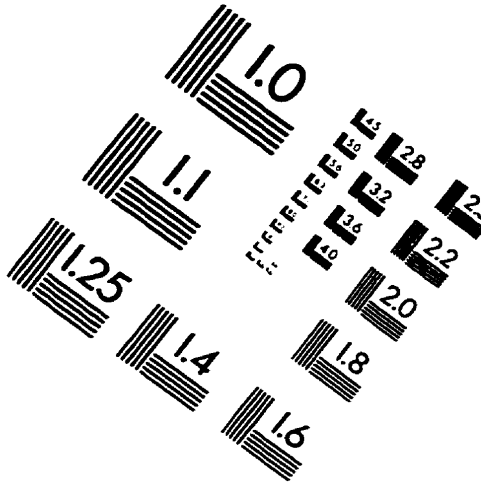


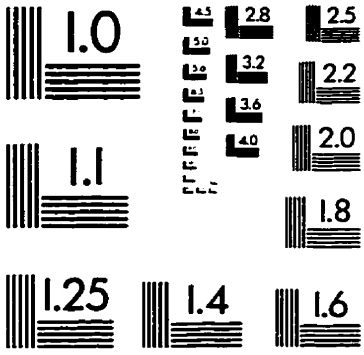


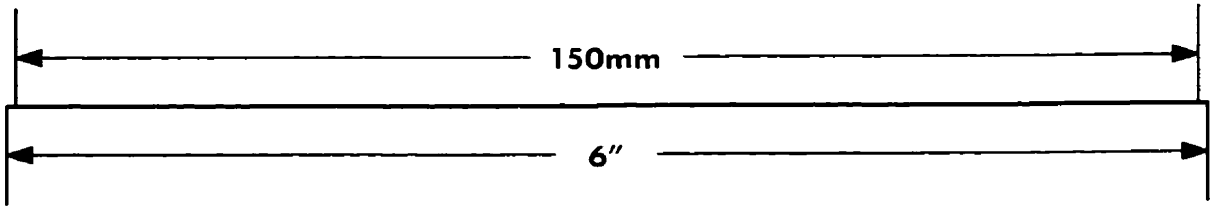


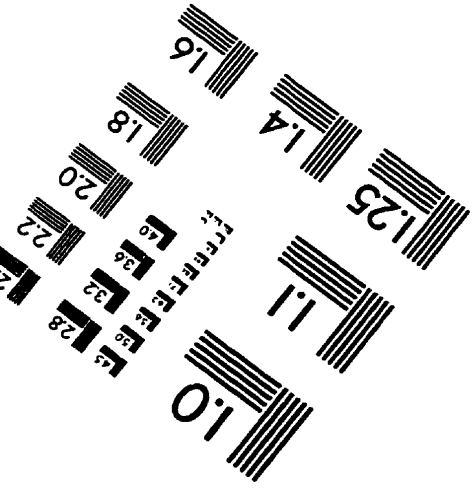


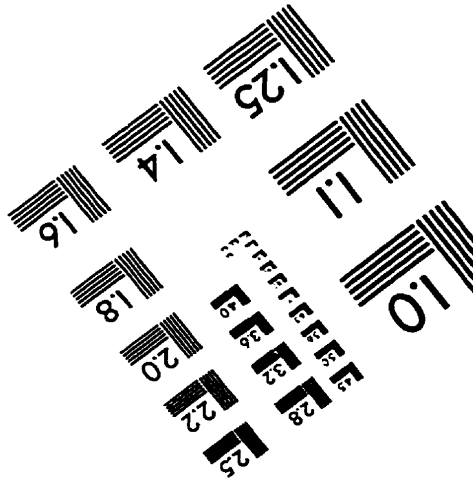


APPLIED IMAGE, Inc
1653 East Main Street
Rochester, NY 14609 USA
Phone: 716/482-0300
Fax: 716/288-5989